UNIVERSITÀ DEGLI STUDI “MEDITERRANEA” DI REGGIO CALABRIA
DIPARTIMENTO DI AGRARIA
Dottorato di Ricerca in
Scienze Agrarie, Alimentari e Forestali
Curriculum Scienze Forestali
Ciclo XXXVI, 2020/23 - SSD: AGR/10- Costruzioni Rurali e Territorio Agroforestale

Giovanni Lumia

An innovative proposal to implement Multispecies Ecological Networks in the framework of sustainable landscape planning. An application in the Reggio Calabria metropolitan area.

PH.D. THESIS

Tutor
Prof. Giuseppe Modica

Co-Tutor
Dott. Samuel Cushman

Ph.D. Coordinator
Prof. Leonardo Schena

Reggio Calabria 21/02/2024

Index

Abstract

It is now well known throughout the world that the well-being of a society is strongly linked to the environment in which it develops and grows. The environment is no longer seen as a container of resources to be drawn upon in times of need but rather as a system capable of providing a range of services (ecosystem services) only if it is preserved in its naturalness. The animal and plant species that inhabit the land are the result of a slow evolution that has been going on for millions of years, and for that reason, they need time to adapt to changes. Human activities such as urban expansion, agriculture or reclamation of various kinds tend to upset these balances rapidly. This trend in the last century has led to increasing degradation of natural environments and consequent loss of biodiversity. In this regard, the scholarly community has particularly emphasised the importance of protecting the planet's natural areas in the last century. It was further seen that merely protecting individual areas is insufficient; rather, protection measures are effective if protected areas are placed in an ecological network, canonically consisting of core areas, corridors, and stepping stones. To create efficient ecological networks, it is necessary to have a good knowledge of the territory on which one is working, and in this context, the recent work on the production of the Nature Map of the National Territory is an added value, making available to the planner a Habitat Map for each region. This Ph.D. thesis focused on ecological networks, paying attention to the mechanisms that generate them, those that damage them, and the most modern strategies for identifying and restoring them. The goal was to create an ecological network over a part of the Calabrian territory, knowing that it was necessary to find a balance between the natural and artificial components of the land. It started by analysing free and freely available cartographic data, particularly land use maps of the study area. Then it moved on to the creation and use of a habitat map. The present doctoral work actively contributed to the creation of the latter. Subsequently, simulations were conducted, and ecological network modelling was put in place, with free and open-source software support, to identify the most reliable strategy for realising the ecological network over the survey area. In particular, graph theory, circuit theory, resistant kernels approach and Pathwalker simulations were explored. The results obtained indicated the resistant kernels approach and Pathwalker simulations as the most reliable strategies in predicting the movement of animal species over the area. The results also suggest that using a habitat map instead of a land use map increases the robustness and reliability of the ecological network.

Riassunto

È ormai risaputa in tutto il mondo che il benessere di una società è fortemente legato all'ambiente in cui questa si sviluppa e cresce. L'ambiente non è più visto come un contenitore di risorse a cui attingere al momento del bisogno ma piuttosto come un sistema in grado di dare una serie di servizi (servizi ecosistemici), solo se preservato nella sua naturalità. Le specie animali e vegetali che popolano il territorio sono frutto di una lenta evoluzione che va avanti da milioni di anni e per tale ragione necessitano di tempo per adattarsi ai cambiamenti. Le attività umane come espansione urbana, agricola o bonifiche di varia natura tendono a sconvolgere rapidamente questi equilibri. Questo trend nell'ultimo secolo ha portato ad un degrado sempre maggiore degli ambienti naturali e alla conseguente perdita di biodiversità. A tal proposito nell'ultimo secolo la comunità scientifica ha spinto particolarmente sull'importanza di tutelare le aree naturali del pianeta. Si è visto inoltre come limitarsi a proteggere delle singole aree non sia sufficiente ma, piuttosto, le misure di protezione risultano efficaci se le aree protette vengono inserite nel contesto di una rete ecologica, canonicamente costituita da core areas, corridoi e stepping stones. Per realizzare reti ecologiche efficienti è necessario avere una buona conoscenza del territorio su cui si opera e, in questo contesto, il recente lavoro sulla produzione della Carta della Natura del territorio Nazionale risulta un valore aggiunto, mettendo a disposizione del pianificatore una Carta degli Habitat per ogni regione. La presente tesi di Dottorato ha focalizzato la sua attenzione proprio sulle reti ecologiche, ponendo attenzione ai meccanismi che la generano, a quelli che la danneggiano, e alle più moderne strategie che permettono di individuarle e ripristinarle. L'obbiettivo è stato quello realizzare una rete ecologica su una parte del territorio calabrese sapendo che è necessario trovare un equilibrio fra componente naturale e artificiale del territorio. Si è partito analizzando i dati cartografici gratuiti e liberi disponibili, in particolare mappe di uso del suolo dell'area studio, per poi passare alla realizzazione e utilizzo di una carta degli habitat. Il presente lavoro di dottorato ha contribuito attivamente alla realizzazione di quest'ultima. Successivamente sono state condotte simulazioni e messe in atto modellazioni di reti ecologiche, con il supporto di software gratuiti e liberi, al fine di individuare la strategia più affidabile in termini predittivi, per la realizzazione della rete ecologica sull'area d'indagine. In particolare, sono state esplorate: teoria dei grafi, teoria dei circuiti, approccio delle resistant kernels e simulazioni Pathwalker. I risultati ottenuti hanno permesso di indicare l'approccio delle resistant kernels e le simulazioni di Pathwalker come le strategie più affidabili nel predire il movimento delle specie animali sul territorio. I risultati suggeriscono oltretutto che l'utilizzo di una carta degli habitat al posto di una carta degli usi del suolo aumenta la solidità e l'affidabilità della rete ecologica.

1 General Introduction

Over the past century, the sharp and rapid increase in the human population, which has grown dramatically from around 2.6 billion to 7.8 billion in 2021, has been a significant cause of biodiversity loss (Cafaro et al., 2022). The emergence of large cities, new and numerous villages, road networks, railways, power grids, water networks, and numerous other man-made interventions have resulted in the fragmentation, isolation, and loss of natural habitats (Diniz et al., 2020; Hudson, 1991a; Sauter et al., 2019). Habitat fragmentation refers to the reduction in the area of natural surfaces, the progressive spacing between residual fragments, and the consequent loss of habitat quality (Li et al., 2022).

There has been increasing awareness of this issue in recent years, so how landscape planning is conceived has changed rapidly. Europe has taken a stand on this issue, starting with the "Environmental Ecological Network" (EECONET) project in the Netherlands (Bennet, 1991.). Subsequently, the initiatives of the Institute for European Environmental Policy (IEEP), the "European Landscape Convention" (CoE, 2000), the "EU Biodiversity Strategy for 2030," the 'Natura 2000' project (EU), which has as its ultimate goal sustainable land management toward planning interventions that promote ecological restoration and, the emergence of new protected areas that go to form an Ecological network on European territory. Not to be forgotten was Italy, which, with the 'Carta della Natura' project (of the 'Istituto Superiore per la Protezione e la Ricerca Ambientale', ISPRA (https://www.isprambiente.gov.it/en/projects/biodiversity/ecological-network-and-terrritorial-planning, ISPRA website, last access on 10 November 2023:), took part in the Natura 2000 project and thus built a nationwide ecological network. Governments and the scientific community then began to think about the importance of planning land interventions sustainably and the best strategies to implement them, starting precisely from the planning of the Ecological Networks themselves (Balbi et al., 2019; Mateo-Sánchez et al., 2015; Rudnick et al., 2012; Tiang et al., 2021).

1.1. Ecological Networks (ENs) overview

The first time the Ecological Network was discussed was at EECONET, and here, the characteristics that its main components, namely patches, ecological corridors and stepping stones have been discussed:

- A patch, as per the original definition in EECONET, is defined as a cover type providing habitat value which differs from its surroundings, for which it is possible to delineate a perimeter. A more recent definition of a patch can be given by saying that it is defined as an area of variable extent predominantly occupied by features of natural origin whose level of quality can be defined by its biodiversity content (Keeley et al., 2021). A patch may be a distinct habitat for certain species, have varying degrees of conservation, or be included among protected areas (Hilty et al., 2020). For example, areas protected by the Natura 2000 programme, such as Birds Directive sites (BDS) or Habitats Directive sites (Sites of Community Importance, Special Areas of Conservation) (European Commission website, last access 30 October 2023: https://environment.ec. europa.eu/topics/nature- and-biodiversity/habitats-directive_en).

- An ecological corridor is defined as a portion of land that connects two patches, habitats or ecosystems and allows the movement of a species between EN elements (Clark, 2010). It can, therefore, actively contribute to the maintenance of biodiversity by fostering genetic exchange among patches and itself occupying an area of land with distinctly natural features.
- Stepping stones are other connecting elements. They are essential transit points between patches, which may fall within a corridor; they are also crucial for ecological processes such as carrying material and energy flows (Luo et al., 2021a). Unlike ecological corridors, which are elements that develop linearly and maintain spatial continuity between patches, stepping stones (an example of stepping stones may be ponds or lakes useful as stopovers for migrating birds or for moving amphibian species) are a series of non-contiguous natural areas that serve as a resource for animals moving over the landscape that stop within them (Hilty et al., 2020).

Starting from the elements described above, the planner who intends to build an ecological network is required to put together the minimum set of patches, corridors, and stepping stones needed to protect the most biological diversity of a given area (Margules & Pressey, 2000). Building on this very general consideration, there are numerous other factors to consider when constructing an ecological network, depending on the goal for which it is created. One of them can be to have Ecological Networks aimed at protecting single species, particular areas rich in biodiversity, entire habitats, or species groups (Elsen et al., 2018; Erwin, 2007). In general, for modelling ENs there are three dominant approaches (S. A. Cushman, Lewis, et al., 2013), based, respectively, on (1) single-species, (2) multi-species, and (3) coarse-filters or ecological systems. In single-species modelling, the analysis considers the needs of only one species of interest (Bourdouxhe et al., 2020; Cushman et al., 2009; S. A. Cushman et al., 2016; Hardion et al., 2019). In contrast, multi-species modelling considers the needs of a set of species, called focal species, considered representative of all species present in the examined context (S. A. Cushman & Landguth, 2012; Diniz et al., 2020; Guimarães, 2020; Lechner & Lefroy, 2014a). Finally, the coarse-filter approach assesses the connectivity of intact or natural ecosystems irrespective of any focal species (Cushman et al., 2012a; Diniz et al., 2018).

In the case of the multi-species approach, the most widely used conservation strategy is to identify focal species, i.e., a set of species whose characteristics are such that they can summarise the needs of all other species that inhabit their area (Beier et al., 2011; Lambeck, 2002). In order to implement this strategy, a set of species that are very similar in terms of autecology will then be identified; among them, one will be chosen to be used as a representative species of the whole group; subsequently, this procedure will be repeated for all groups of species with similar characteristics until all focal species in the area are obtained. In most works dealing with ecological network modelling, numerous variables regarding the target species' autecology are considered (Fricke & Svenning, 2020; Xing & Fayle, 2021).

Specifically, the most commonly used data (Boitani et al., 2003; Poisot et al., 2021; Saura & de la Fuente, 2017) are those referring to dispersal ability during migration, dispersal ability during resource search, home range of the species, species habitat affinity, risk elements, disturbance elements, or elements impeding species movement in the territory (McGarigal, 2005; Modica et al., 2021; Tarabon et al., 2022). Dispersal distance (either migration or search for resources) refers to the distance (minimum, average, maximum, etc.) that an animal needs to travel in order to carry out activities that are essential to the fulfilment of its life cycle, such as migrating to find a partner, nest, food, etc. (Boitani et al., 2007a; Nevřelová & Novota, 2020; Sáez et al., 2023; Xu et al., 2019). Home range, with reference to either a single species or a collection of species, refers to the portion of land large enough to contain resources necessary for the fulfilment of the vital functions of the individuals that populate it (Boitani et al., 2003; Dugatkin, 2020; Formica et al., 2010; Zheng et al., 2018). Risk, impediment, or disturbance are factors that can endanger the animal's life or disturb or even prevent its normal activities. These elements are most often anthropogenic in origin and are divided into material elements such as cities, roads, railways, dams, or various infrastructures, which physically hinder the activities of animals, or polluting factors such as noise or light disturbance (Beyer et al., 2016; W. Xu et al., 2021; Yavartanoo et al., 2023).

Once the autecological information of the species to be protected has been obtained, it is necessary to combine this knowledge with a study of the area on which interventions are to be planned. Indeed, it is well known that not all protected areas enjoy good quality and capacity to conserve biodiversity (Jones et al., 2018; Venter et al., 2018). This is very often due to the incorrect distribution of protected areas, which are then isolated from the rest of the territory, increasing the risk of species extinction (Newmark, 1995, 2008; Prugh et al., 2008). This phenomenon has been studied and demonstrated in the theory of metapopulation and island biogeography (Hanski, 1999; MacArthur & Wilson, 1963; McCullough, 1996). Metapopulation theory shows that the possibility of species living in an area to explore new territories promotes genetic exchange and reduces the risk of extinction. In the island biogeography theory, on the other hand, it is shown that the possibility of extension of one or more species in a protected area is directly related to the distance from other natural areas. The greater the isolation, the greater the probability of extinction. Both of these theories thus confirm that protected areas are much more helpful when placed within an ecological network (Hilty et al., 2020). In addition, the theory of island biogeography shows that the quality of a patch, or protected area, also depends on its size and shape.

The main causes of the change in patch shape and size are attributed to landscape fragmentation, which reduces the average area of patches and changes their shape, causing a negative effect that is called edge effect (Dunn & Loehle, 1988; Ewers et al., 2007; Fletcher, Jr. et al., 2007; Gustafson & Gardner, 1996). It has been shown that the properties of patches also change in relation to shape and size, in particular we will have a greater amount of interior habitat in a patch that tends to be circular and larger in size, while we will have an increasing quote of edge habitat in a patch with a stretched shape and smaller size (Diaz & Apostol, 1992; Murcia, 1995; Ries et al., 2004). An interior habitat is characterised by greater stability, the species that inhabit it have achieved an equilibrium in species-to-species and species-to-territory relationships, this allows the interior habitat to maintain its biodiversity content more stable and lasting over time (Bender et al., 1998; Ries et al., 2004). Biodiversity levels that remain high over time further increase habitat stability (Zurita et al., 2012). Indeed, it is well known that greater biodiversity leads to greater ecosystem resilience and a reduced chance of extinction(Isaac et al., 2018). An edge habitat, on the other hand, is characterised by greater instability (Gascon et al., 2000; Gignac & Dale, 2007). This is populated by species that live on the edge, with greater proximity to unfavourable areas and from which variables can come into play that very quickly upset the balance (Harper et al., 2005).

Together, all of these considerations support the need for larger, well-connected ecological networks to ensure biodiversity conservation over time, and it has been these considerations that have led governments and researchers around the world to work to identify innovative strategies that enable the modelling of effective ecological networks on the ground.

1.2. Ecological networks implementation, state of the art summary

The functioning of an ecological network is based on the assumption that landscape structure influences and is influenced by flows, considered as movements of resources or species (Franco, 2004; Levins, 1969). Over the years, various schools of thought have arisen, proposing different theories but this basic principle unites them all. Among the most popular strategies created for the purpose of identifying, weighing and spatialising network elements are:

- Circuit theory is one of the most widely used strategies that build on these foundations. This theory assimilates the movement of animal species, within complex territories, to the flow of electric current moving on a matrix composed of elements of different conductivity. Several software programmes have emerged to perform simulations based on these principles, several software programmes have emerged, capable of exploiting data such as raster images vector elements, typically used for mappings in GIS software. In order to apply circuit theory to landscape ecology, the planner need to make a number of evaluations on previously acquired data related to land and species. First, a level of resistance to habitat-species movement needs to be identified. At this stage you need to have a matrix, typically a raster, that virtually represents specific properties of the land over which you intend to plan. The properties may refer to land use, habitat, elevation, slope, etc., the pixels in the raster will therefore have resistance values assigned considering the level of affinity of the animal to that particular attribute. The next step is to determine which pixels are to be considered as patches, i.e., source of initiation of the animal's movement, and next, it is necessary to identify a maximum dispersal distance and an energy cap available to the walker. The simulation starts from the pixels classified as patches, from which the movement continues following the principle of minimum cost path. This implies that the walker in the movement follows adjacent pixels with the lowest resistance value. At each step from one pixel to another, depending on the resistance cost of that pixel, the walker consumes energy, and the movement stops when the energy is exhausted or when a patch is reached (Foltête et al., 2021a).
- Among the most commonly used strategies is the graph theory. This approach, when applied to ecological networks, allows patches to be taken as nodes and corridors as links in a graph, allowing ecology-related properties to be quantified through a series of metrics and connectivity indices (Foltête, 2019; Foltête, Clauzel, et al., 2012; Ruiz et al., 2014; Urban, J. D., Keitt, 2001). Graph nodes and links are nothing more than a simplification, represented in mathematical form, of complex ecosystems in a way that makes their dynamics easier for the planner to understand and evaluate (Gross & Yellen, 2005). Several software programmes have emerged that exploit the principle of graph theory to make these complex operations faster to perform, considering that the network may contain thousands of nodes and links. Among these, Graphab (Foltête et al., 2021a) is the only tool able to include the construction and visualisation of graphs, connectivity

analyses and links with external data and is easily compatible with Geographical Information Systems (GIS) software. The Graph construction begins by assigning a node to each patch, while the links are later identified by exploiting circuit theory. To achieve this, it is necessary to assign resistance values to each pixel in the matrix, the simulation starts from the pixels classified as patches and, if the walker in the simulation does not exhaust its energy and manages to reach another patch, a link between the nodes of the two respective patches is created. The potential of graph theory is it allows a series of numbers of connectivity metrics to be calculated. First, it allows the calculation of a number of nodes, links, and components, which give the planner a first view of how elements are distributed in the ecological network and on the state of fragmentation of the network. Second, it allows the identification of a number of indices of connectivity for the qualitative assessment of the different elements. Among the most widely used is the Integral Index of Connectivity (Freeman, 1977), which is capable of evidencing the robustness of an ecological network. This index is in addition very sensitive to variation, allowing for the evaluation of factors such as change in patch number, links, partial loss of patch area, and loss of entire components. This makes it an ideal index for the planner who wants to assess changes in an ecological network caused by fragmentation over time, or if assumptions are to be made about future changes (such as defragmentation scenarios). Another important index widely used in the field of ecological connectivity is the Betweenness Centrality Index (Freeman, 1978). It expresses the importance of nodes (and thus patches) as a source of connection for other parts of the ecological network. This means that a node with BC of value 0 has importance as a connector for no other node in the network, BC of increasing value means increasing connections for other elements (Newman, 2004). There are also a number of other widely used indices such as the Harary Index (H) (Ricotta, 2000), Flux (F) (Foltête et al., 2012) and Probability of Connectivity (PC) (Pascual-Hortal & Saura, 2008), all indices capable of making quality assessments about a network. This diversification of metrics and indices shows all its potential and usefulness when action is to be taken to protect the environment.

Another strategy widely used in the literature to implement ecological networks is based on resistant kernels (Compton et al., 2007). This model is based on the combination of two models used in the past, the kernel estimator (Silverman, 2018) and least-cost paths with resistant surfaces (Worton, 1989). The kernel estimators are typically used when needed to obtain valuations on home ranges. Having a two-dimensional datum x, y of points, it produces a three-dimensional surface representing (a raster image representation) an estimate of the underlying probability distribution by summing across bivariate curves centred on each sampled point (Compton et al., 2007). This approach, which, like the others of Circuit theory, is based on resistant surfaces, has now surpassed the old approaches based on binary habitat/nonhabitat classifications of island biogeography and classic metapopulation models (Ricketts, 2001). As we have already explained, minimum path analysis indicates the shortest functional distance between two points, but this minimum path approach can be extended to a multidirectional approach. In this case, the functional distance between a focal cell and every other cell in the landscape within a maximum scattering or migration distance will be measured (Compton et al., 2007). In this case, we will obtain a kind of minimum-cost "kernel," a surface that can be scaled to represent the dispersal probability of an individual from the focal cell to any other location in the pixel array. To obtain the robust kernel estimator, it will be necessary to create a minimum-cost kernel for each focal cell that represents a source of dispersal (i.e., a location in the landscape where the animal is assumed to initiate movement) and sum all the kernels in each cell.

These above-mentioned strategies, which account for a large part of the literature, gave rise to a new approach based on movement simulations (Cushman et al. 2023; Kumar et al., 2024). This model, which was created accompanied by the Pathwalker software to simplify its application, is partly based on the already established strategies (theory of resistant kernels and circuits), and partly on new strategies that take new variables into account. Whereas the old models only took into account the energy mechanism (known as the virtual budget available to the animal that stops its movement when energy is exhausted) this new approach includes three other new mechanisms: attraction, risk and the autocorrelation factor. Attraction is a factor that simulates the movement of an animal that knows the territory, and therefore always chooses the most suitable routes to move. Risk, on the other hand, simulates the animal moving through a hostile territory, and therefore with each step the animal has an increasing probability (directly proportional to the amount of unfavourable or dangerous environments it encounters) of suddenly stopping its movement. The autocorrelation factor makes it possible to simulate the movement of an animal in an unfamiliar territory, and thus also to take paths that are not necessarily the best ones.

Furthermore, the rapidly advancing development of satellite systems carrying multispectral sensors, capable of collecting data on a daily basis, has given rise to new opportunities for studying the landscape and thus its connectivity. Indices of vegetative vigour have emerged that are now used in studies for modelling ecological networks such as the VFC (Yu et al, 2021;

Lumia et al., 2023; Liu et al., 2022) and NDVI (Hu et al., 2021; Prăvălie et al., 2022; Zelený et al., 2021).

1.3 Objectives and organisation of the thesis

In the framework of this Ph.D. thesis, partly carried out abroad in collaboration with the School of Forestry department, Northern Arizona University (United States of America), the research activity aims to implement through cartographic representation an ecological network within a Mediterranean climate's - ecosystem's metropolitan area in Calabria region (southern Italy). and to the realisation of a habitat map in the context of the European Natura 2000 programme (Natura 2000 project, link: https://environment.ec.europa.eu/topics/nature-and-biodiversity/natura-2000_en; last access 31 January 2024).

The aim of the PhD thesis work in its first phase (Chapter 1) was to (by studying recent literature and its evolution over time) identify among the most common connectivity modelling strategies those most suitable for creating an ecological network in the study area and to hypothesise a defragmentation scenario on it. In this phase, the theory of graphs, circuits and related connectivity indices were exploited, and some of the most modern techniques were used to assess vegetation qualities using multispectral satellite images.

In the second phase of the work (Chapter 2), new strategies found in the literature, born during the PhD thesis period, were explored. In particular, a new connectivity model based on movement simulations performed in the Pathwalker software environment was focused (discussed in the previous section). At this phase, what has been done is to take the network that was constructed in Chapter 1, in particular the corridors, and assess its quality using Pathwalker's motion simulation model. In fact, unlike graph theory which can only identify corridors as simple lines (least cost paths, line data type), the movement simulation model allows three-dimensional surfaces (two dimensions for the X and Y coordinates, and one dimension for the pixel value of which each pair of coordinates in the matrix, raster data type) of the corridors.

In a third phase (Chapter 3), the performance of two different connectivity models, resistant kernel and graph theory, was tested. Specifically, it was observed what the differences are in terms of prediction when comparing different parameters; source point distribution (referring to the place from which the animal starts its movement in the simulations), dispersal distance (the maximum distance the animal can travel in the simulation) and method used (graph theory or resistant kernel). Next (Chapter 5), motion simulations (Pathwalker) were used to test the performance of the first two approaches (graph theory and resistance kernels). What was done is to create 3 networks, 1 for each of the models, and also calculating the respective connectivity indices, and comparing everything to assess how these values deviate from the predictions made by Pathwalker. The reason for using Pathwalker as a validator is related to its being more versatile, as it can take into account a greater number of parameters ignored by the other two models. (Kumar et al, 2022; Cushman et al., 2023; Lumia et al., 2024).

In the last phase (Chapter 6), all the strengths of the various methods studied in the previous chapters were identified and put together to create a definitive ecological network for the study area and also hypothesise defragmentation interventions on it. Specifically, the network patches were identified with the help of Graphab and Sentinel-2 satellite images,while the corridors with the Pathwalker movement simulation model.

The first steps of our work, chapters 2 – 5, were carried out using free and open base map data obtained from the European Copernicus Project Database. The final step (chapter 6) was carried out using an habitat map specifically constructed for this purpose. In fact, part of the work of this PhD thesis involved the construction of a habitat map for the Calabria region in the context of the European Natura 2000 programme and Habitat Map project (https://www.isprambiente.gov.it/it/servizi/sistema-carta-della-natura last access 20 February 2024).

2 Ecological network implementations based on Copernicus free datasets.

Adapted from

Lumia G., Praticò S., Di Fazio S., Cushman S., Modica G.: **Combined use of urban Atlas and Corine land cover datasets for the implementation of an ecological network using graph theory within a multi-species approach.**
https://doi.org/10.1016/j.ecolind.2023.110150.

Ecological Indicators 148 (2023) 110150

Contents lists available at ScienceDirect

Ecological Indicators

journal homepage: www.elsevier.com/locate/ecolind

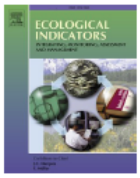

Combined use of urban Atlas and Corine land cover datasets for the implementation of an ecological network using graph theory within a multi-species approach

Giovanni Lumia [a], Salvatore Praticò [a,*], Salvatore Di Fazio [a], Samuel Cushman [b], Giuseppe Modica [c]

[a] *Dipartimento di Agraria, Università degli studi 'Mediterranea' di Reggio Calabria, loc. Feo di Vito s.n.c, 89122 Reggio Calabria, Italy*
[b] *US Forest Service, Rocky Mountain Research Station, 2500 S. Pine Koll Dr., Flagstaff, AZ 86001, United States*
[c] *Dipartimento di Scienze Veterinarie, Università degli studi di Messina, Viale G. Palatucci s.n., I-98168 Messina, Italy*

A R T I C L E I N F O

Keywords:
Remote sensing (RS)
Vegetation Fractional Coverage (VFC)
Sentinel-2
Google Earth Engine (GEE)
Graphab
Landscape connectivity

A B S T R A C T

Ecological sustainability has recently risen to prominence in scientific research and management applications. Approaches to measuring ecological connectivity and their application to optimize ecological network (EN) design are powerful tools against landscape fragmentation and biodiversity loss.

We focused on building an EN by identifying the most sensitive areas for ecological connectivity within the Reggio Calabria (Italy) metropolitan area. We also proposed a defragmentation scenario to improve the obtained EN.

The CORINE Land Cover and the Urban Atlas 2018 were used to obtain a fine-scale representation of the study area. Ten terrestrial mammal species were used to model connectivity following a multi-species approach. Dispersal distance, patch size, and resistance to species movement were used to identify patches and corridors. Vegetational fractional coverage based on three years time series of Sentinel-2 red-edge normalized difference vegetation index was used to discriminate areas with higher naturalness. We used graph theory and connectivity metrics to test the EN's robustness and identify locations for restoration in a defragmentation scenario.

The obtained EN, formed by three separate components, was composed of 724 arcs and 300 nodes with an average patch area of 27.04 ha. After the defragmentation hypothesis, the EN, formed by only one component, was composed of 771 arcs and 328 nodes with an average patch area of 26.82 ha.

It was possible to analyze an EN's connectivity and evaluate the impact of a scenario intended to enhance multi-species connectivity. By comparing several connectivity metrics, we highlighted the potential of land interventions as a planning tool to enhance future ecological sustainability and biodiversity conservation.

Over most of the Earth's biomes, contiguous natural landscapes have been fragmented into a mosaic of residual patches divided by barriers dispersing animal species across the landscape (Diniz et al., 2018; Hudson, 1991b). Species have evolved, and populations were previously sustained in often dramatically different environments than the one in which human-driven perturbations have produced; moreover, the reduction of areas of residual natural ecosystems inevitably has effects on the life cycles of the species themselves (Hanski, 1999).

In this scenario, for sustainable spatial planning, ecological networks are themselves the object of spatial planning (Balbi et al., 2019b; Mateo-Sánchez et al., 2015b; Tarabon et al., 2020; Tiang et al., 2021b, 2021c) and their implementation can counteract landscape fragmentation (Liccari et al., 2022), create and strengthen relationships, and promote exchanges between otherwise isolated elements (De Montis et al., 2016; Fichera et al., 2015). Moreover, landscape improvement policies and actions are widely recommended as tools for combating climate change (Heller & Zavaleta, 2009).

Given urban sprawl affecting many regions worldwide and the conflict between urbanisation and ecological planning, assessing landscape connectivity in peri-urban areas is crucial (Dong et al., 2020). Rural fringe areas are characterised by specific dynamics and patterns of contiguity, inclusion with the urban environment and its sprawling, and the natural contexts and their connectivity elements. Such dynamics often underline alterations affecting the ecosystem functionality, reducing the provision of ecosystem services, and jeopardising the quality of life of many animal and vegetal species and human settlements. Rivers and riparian zones are the most threatened ecosystems and should be protected adequately (Samways & Pryke, 2016). Moreover, it was recently recognised that riparian zones can be essential in improving landscape ecological connectivity (Ribeiro et al., 2022).

For this work, we chose a multi-species approach based on the needs of 10 focal species, identified exclusively among medium and small mammals. A widespread practice for modelling an EN is to anchor the ecological network in nodes defined by protected areas (Bonnin, 2007; Kheirkhah Ghehi et al., 2020). The approach adopted in this first step of the Ph.D. thesis is novel in employing two different land use maps for the network modelling: Urban Atlas (UA2018) and Corine Land Cover (CLC2018). These datasets, provided by the European Union Copernicus programme, were created to meet different needs. CLC provides a representation of the land uses of 39 countries and contains information that can support the European Union's Environmental Action Programmes. UA was created to provide a very detailed representation of urbanised areas, covering 788 FUAs (Functional Urban Areas) of 39 European countries in the 2018 release. A Digital Terrain Model (DTM) and multispectral

satellite images were used to support the UA and CLC, which together allowed a high degree of detail set for the representation of natural and artificial elements of the study area. Our model proposes an accurate choice of faunal species, considering the adopted large spatial scale (1:10,000) and the heterogeneous landscapes with the significant and increasing occupation of urbanised areas. Moreover, we optimised our model of EN using a high-resolution DTM and a multi-temporal Vegetation Fractional Coverage (VFC) capable of better-discriminating areas with higher naturalness and based on a three-year (2016-2019) time series of Sentinel-2 red-edge Normalised Difference Vegetation Index ($NDVI_{\_4re}$). Finally, the proposed EN and the current landscape configuration were assessed and compared with a defragmentation scenario proposed, reconnecting isolated patches and improving riparian zones in specific areas. A set of landscape indicators was defined to this end. Reconnecting isolated patches, especially in rural-urban fringe areas, is crucial in promoting climate-resilient defragmentation measures in heterogeneous landscapes. The proposed method was developed using free and open-source software (FOSS).
The main objectives of the work presented here are: (i) to identify the most important areas for wildlife connectivity based on a multi-species approach; (ii) to develop a defragmentation scenario within a heavily anthropised area to improve network connectivity; (iii) to compare the pre- and post-defragmentation networks to assess their effectiveness.

2.1. Materials and Methods

The method (Fig. 2.1) is structured in 4 phases: (i) collection and organisation of the database to accurately describe the geomorphological characteristics of the area, as well as the ecological characteristics of the area and the autecological characteristics of the considered species (habitat, home range, dispersal distance, level of affinity to various land uses); (ii) data processing using FOSS and remote sensing techniques, to create the structure of the EN of the entire examined area; (iii) Analysis of the implemented EN through connectivity metrics and indices; (iv) defragmentation intervention scenario development to improve the current network and comparison of pre- and post-intervention network connectivity metrics and indices.

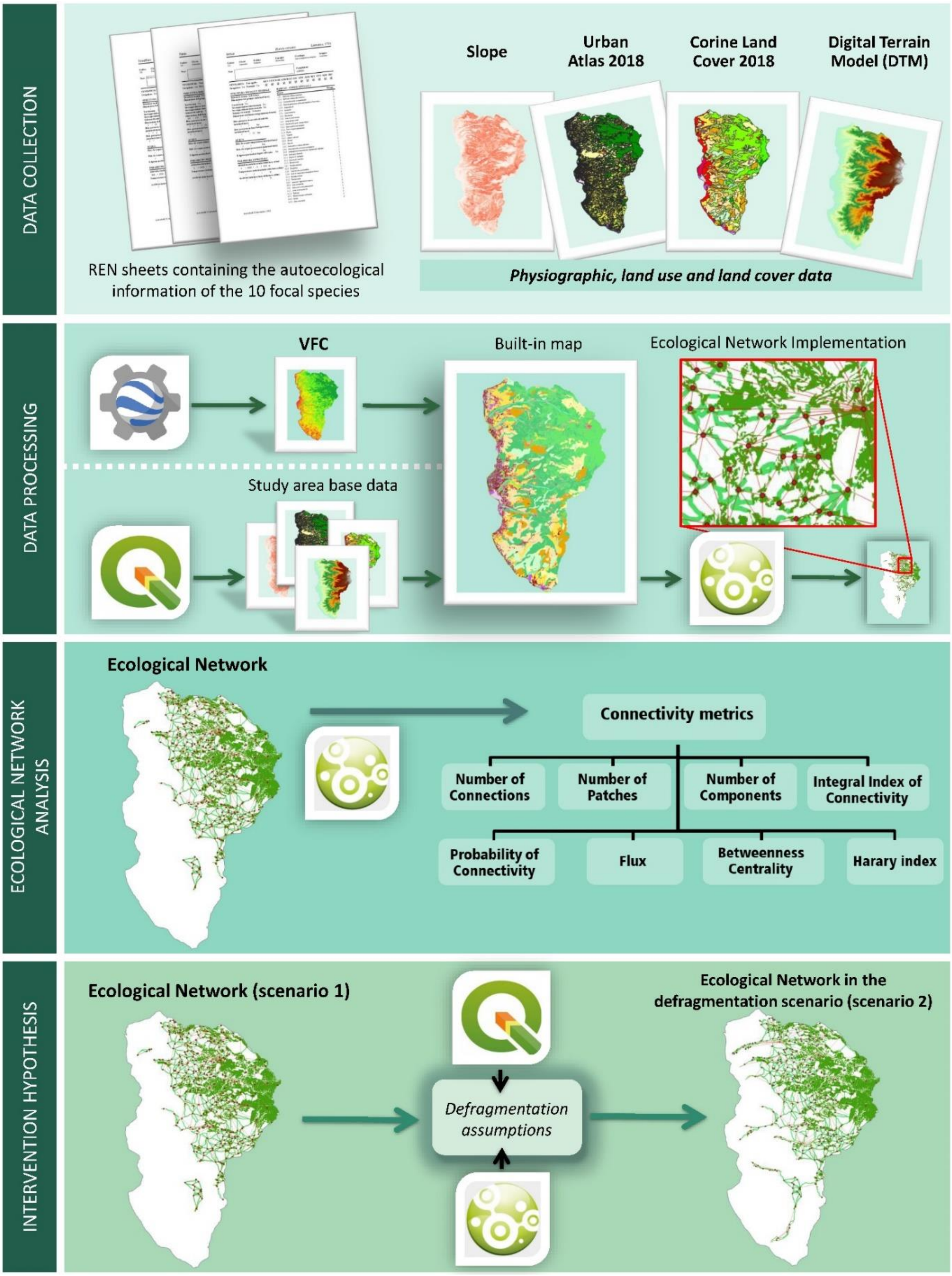

Figure 2.1 - Workflow of the proposed method, entirely developed in free and open-source software (FOSS) environments (QGIS, Google Earth Engine, and Graphab).

2.1.1. Study area

The analysis was applied in the metropolitan area of Reggio Calabria, which has an extension of 47,822.63 ha and is located in the southernmost part of the Calabria Region (Italy) (Fig. 2.2). According to the Urban Atlas 2018 data, the urbanised areas and the road system cover an area of 6773.25 ha (14.16% of the investigated area).

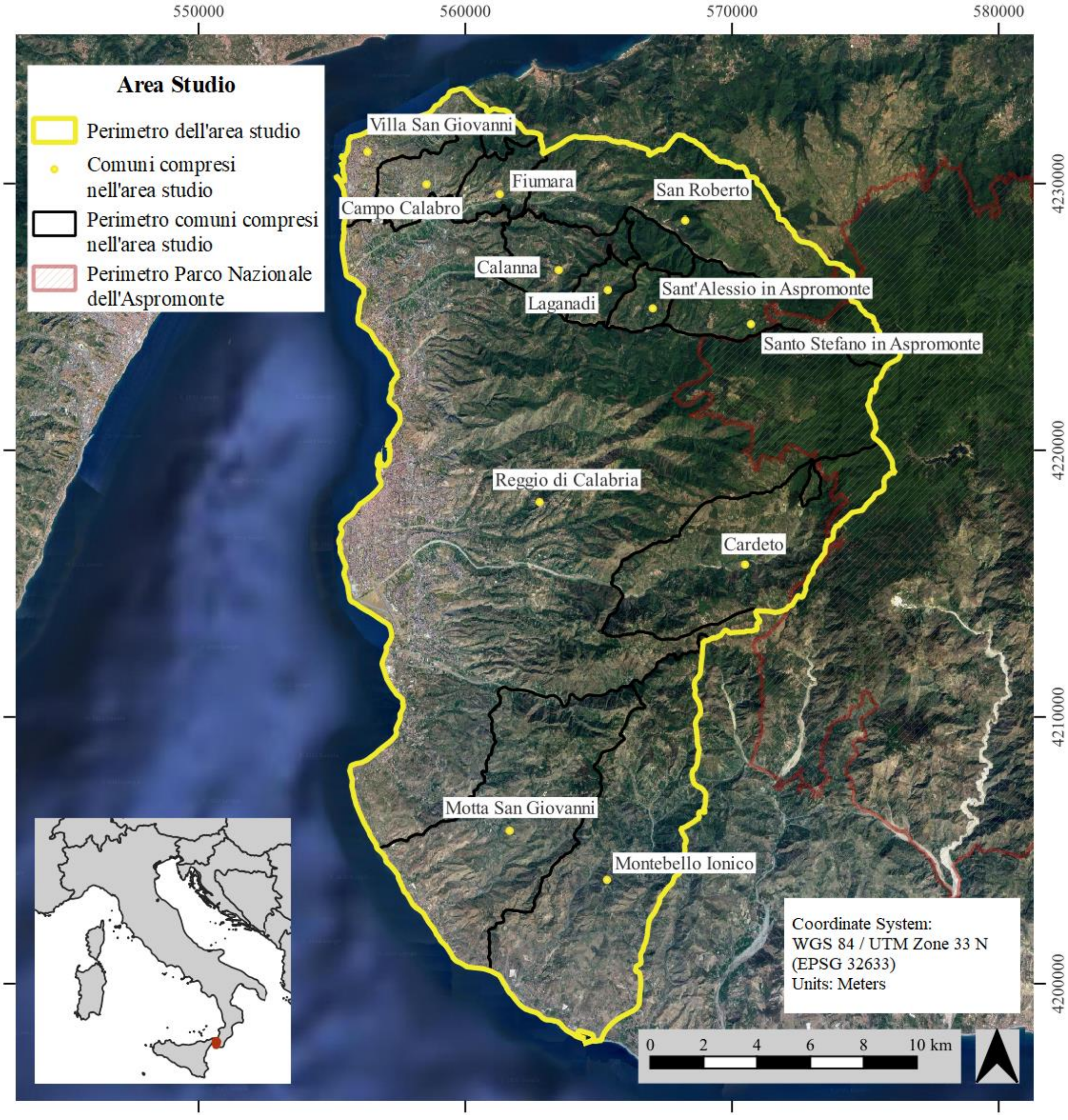

Figure 2.2 - Study area. In yellow is the perimeter of the Urban Atlas Reggio Calabria data for 2018, including 12 municipalities (black line) in the province of Reggio Calabria. In red is the boundary of the Aspromonte National Park, which partially crosses the study area.

The region is characterised by a typical Mediterranean climate (Pellicone et al., 2018), with a rainy winter and dry summers. The study area includes twelve municipalities between Villa San Giovanni and Montebello Ionico, with a 68.9 km coastal strip facing the sea at the Stretto di

Messina. The investigated territory extends to the highest peaks of Aspromonte, including part of the Aspromonte National Park.

2.1.2. Base data collection and organisation

All data used for building the EN are synthesised in Table 2.1. Two vector data layers provided by the European Union Copernicus programme were used (https://land.copernicus.eu/ - last access 30 June 2022). The CLC data was characterised by a minimum mapping unit (MMU) of 25 ha and 25 different land use classes grouped into 5 categories. The UA dataset has very high geometric and thematic detail of man-made elements (buildings, infrastructure, etc.), including 27 different land use classes with an MMU of 0.25 ha for category 1 and 1ha for categories 2 to 5. The legend used by UA and CLC has a hierarchical structure on several levels. The first level is the most general and consists of 5 categories: 1, highly artificial areas; 2, agricultural areas; 3, natural areas; 4, wetlands; 5, water elements. In the present study, the 2018 UA and CLC 2018 datasets were integrated using the UA for land use classes of the first category, which goes up to the fourth hierarchical level by highlighting important infrastructural elements such as secondary roads (Bourgeois & Sahraoui, 2020), which are missing in CLC. For the remaining categories, we used the CLC dataset (Fig 2.4). Although it has a lower spatial resolution, it shows greater thematic detail in the differentiation of agricultural and forest land, going up to the third hierarchical level, unlike the UA datum, which remains at the second level. Through the code editor of the Google Earth Engine (GEE) (Gorelick et al., 2017), multispectral images of Sentinel-2 in a time series from 2016 to 2019 were processed. A cloud masking operation was performed, removing images with cloud coverage of 70 % or more in the first instance. This was done to exclude cloud-covered pixels from the analysis and, secondly, in images with high cloud cover, even pixels not covered by clouds may have noise, cirrus, or georeferencing problems(Xu M. et al., 2019). At this point, further filtering was performed, masking all pixels with a probability of being covered by clouds greater than 20% (this value is referred to as the band named “probability” in the S2_Cloud_Probability dataset). Finally, Sentinel-2 multispectral images were used to obtain vegetation vigour and naturalness information through specific spectral indices (§ 2.4).

A 5 x 5m resolution raster DTM and the derived slope raster were used to characterise the topographic conditions of the study area, highlighting those areas not suitable because of their slope or elevation.

2.1.3. Animal species identification

For the construction of the EN, ten medium and small mammal species, summarised in figure 2.3, were identified and selected as focal species, which we considered representative, in terms of ecological requirements, of other mammal species with which they share the ecosystem. They act as umbrella species, i.e., at the top of the trophic chain and of particular conservation interest, and their protection implies the conservation of the underlying trophic levels. The method is based on actual data collected by Boitani (Boitani et al., 2003) on the behavioural and auto-ecological properties of the selected species. This information gives values that refer to optimal minimum/maximum thresholds, such as the distance an animal can travel in a hostile environment to reach resources, the size of the surface area it needs to carry out its life cycle, and the affinity of the species to a given environment.

Table 2.1 - Spatial dataset used in this research work.

Data description	Reference year	Data source
Land use - CORINE Land Cover (CLC) at the third level of representation	2018	Copernicus, Land Monitoring Service (https://land.copernicus.eu/ -last access 17 February 2022)
Land use - Urban Atlas (UA) at the fourth level of representation	2018	
Digital Terrain Model (DTM) 5 x 5m geometric resolution	2008	Calabria Region Cartographic Centre (CCR) (http://geoportale.regione.calabria.it/opendata - last accessed 06 March 2022)
Multispectral imaging - Sentinel-2 MultiSpectral Instrument (MSI), Level-1C	From 2016 to 2019	European Space Agency (ESA) (https://sentinel.esa.int/web/sentinel/user-guides/sentinel-2-msi/product-types/level-1c - last accessed 07 March 2022)
Cloudiness - Sentinel-2 Cloud Probability		

Different types of territory present a diverse permeability depending on the mobility of the various species passing through it (Battisti, 2004), so the ten focal species were selected, taking this factor into account as well. For instance, some reptiles' perception of a vertical wall - in terms of a barrier or impediment to free mobility - differs from that of some mammals and birds. The decision to not consider large species such as the wolf is linked to the objective of planning at a detailed urban scale. Small and medium-sized species searching for resources have considerably less mobility (10 km on average) than the wolf's 90 km travel capacity. Considering the size of the study area (35 km at the two furthest extremes), it would be more appropriate to conduct evaluations over larger areas for a species with high space requirements, such as the wolf. The assumption is that when studying the landscape and designing planning interventions within it, it is necessary to consider the scale of analysis and thus check whether the needs of the reference species are compatible with that level of detail (Beier et al., 2011; Compton et al., 2007). To capture the details and needs of certain species, it is, therefore, sometimes necessary to reduce the observation scale of the landscape (or vice versa to increase it) (Nie et al., 2021).

The species selection was based on existing literature for the same study area (Modica et al., 2021), prioritising species protected by national and international legislation (https:// www. mite.gov.it/ pagina / repertorio - della-fauna – italiana - protetta - last accessed 16 February 2022).

Species	L. 157/92 art. 2 (1)	L. 157/92 (2)	BERNA Ap.2 (3)	BERNA Ap.3 (4)	CITES All. A (5)	CITES All. B (6)	HABITAT Ap.4 (7)	HABITAT Ap.5 (8)	IUCN (9)
Martes martes L.	X			X				X	
Martes foina Erxleben		X		X					
Felis silvestris Schreber	X		X			X			
Hystric cristata L.		X	X				X		X
Sciurus vulgaris L.		X			X				X
Eliomys quercinus L.		X		X					X
Glis glis L.		X		X					X
Erinaceus europaeus L.		X		X					
Mustela nivalis L.		X		X					
Muscardinus avellanarius L.		X		X			X		X

(1) Standards for the protection of homeothermic wildlife and hunting harvest, species protected explicitly in Article 2 of the Law of February 11, 1992
(2) Standards for the protection of homeothermic wildlife and hunting, species protected by the law of February 11, 1992
(3) Annex 2 of the Convention on the Conservation of European Wildlife Habitats, adopted in Bern on September 19, 1979
(4) Annex 3 of the Convention on the Conservation of European Wildlife Habitats, adopted in Bern on September 19, 1979
(5) Regulation on protecting wild fauna and flora species by regulating trade therein. Species listed in Annex A of Regulation (EC) No. 2307/97
(6) Regulation on protecting wild fauna and flora species by regulating trade therein. Species listed in Annex B of Regulation (EC) No. 2307/97
(7) Annex 4 to Habitats Directive 43/92/EEC called Animal and Plant Species of Community Interest Requiring Strict Protection. Updated with Council Directive 97/62/EC of October 27, 1997.
(8) Annex 5 to Directive 43/92/EEC "Habitats" named Animal and plant species of Community interest whose taking in the wild and exploitation could be subject to management measures. Updated with Council Directive 97/62/EC of October 27, 1997.
(9) Belonging to one of the categories assigned by the International Union for Conservation of Nature (IUCN), which identifies the conservation status of animal and plant species by giving categories listed on the so-called Red List: extinct; extinct in the wild; critically endangered; endangered; vulnerable; lower risk; protection dependent; near risk; relative risk; insufficient data; not assessed.

Figure 2.3 - National and international legislation protecting identified focal species.

2.1.4. Data processing

UA and CLC data layers were integrated into QGIS 3.22 (http://www.qgis.org - Last accessed 05 June 2022). All class 1 geometries of the Urban Atlas were saved separately and overlaid with the CLC vector, obtaining the comprehensive vector data of the study area (Fig. 2.4). A topological check of the data obtained was then carried out, and the errors detected (points, broken lines, redundant features, etc.) were corrected using the GRASS toolset 'v.clean'. In addition, all polygons with a surface area smaller than the MMU were merged with those neighboring them. The MMU for UA was retained as it was lower than that of CLC. The vector data was then converted to a raster to allow subsequent processing. Considering that the UA datum was produced by interpretation from satellite images with a resolution of 2 or 4 m (e.g., Pléiades, KOMPSAT, Planet, SPOT6, SuperView, etc.), the rasterization process was fixed at 2.5 m x 2.5 m of spatial resolution.

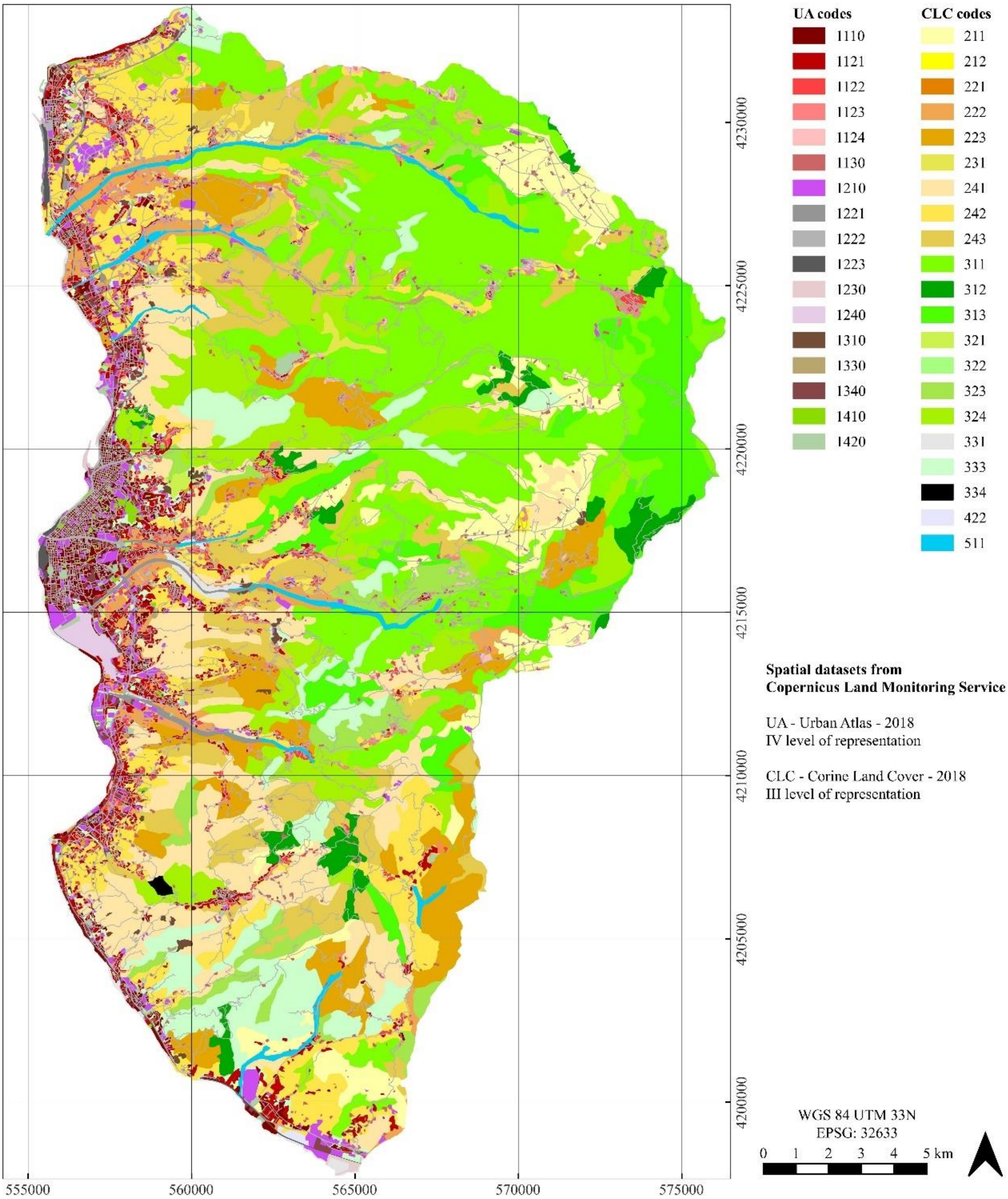

Figure 2.4: Map of the implemented dataset using Corine Land Cover (CLC) 2018 for classes 2 (Agricultural areas), 3 (Forest and seminatural areas), 4 (Wetlands) and 5 (Water bodies), and Urban Atlas (UA) 2018 for class 1 (Artificial Surfaces).

Using the FOSS Graphab 2.6 (Foltête et al., 2012; 2021), for each raster pixel, we assigned a value expressing the resistance that a given land use opposes to the movement of species in an interval ranging from 1 (lowest resistance) to 100 (highest resistance). Pixels with increasing values refer to increasingly artificial areas, while pixels with low values refer to highly natural areas. These values express the difficulty a species has in crossing the different landscape elements according to the autecological needs of the focal species, identified by Boitani et al. (2003). Slope, derived from the 5 m DTM, was considered in identifying patches and corridors. In Graphab 2.6 environment, the importance of slope (p) was weighed through a coefficient (c) as in the following equation (Eq.1) (Tarabon et al., 2022a):

$$r_{final} = r * (1 + c \cdot p) \quad \text{(eq. 1)}$$

Where r is the pixel resistance and r_{final} is the pixel resistance weighted by the slope (p). When c=1, the resistance value is doubled for a slope of 10%, while if c=10, the resistance is doubled for a slope of 100% (p=1). Since in this work, we considered the value of the coefficient c to be 1, as the slope increases, the permeability decreases.

Through the Code Editor of GEE, we implemented a function to calculate the area's average Vegetation Fractional Coverage (VFC) index over 3 years, from 2016 to 2019, using Sentinel-2 L1C satellite images. This indicator is widely used in remote sensing to monitor the condition of plant communities (Shobairi et al., 2018), making it possible to discriminate areas of higher naturalness falling within the study area (Shobairi et al., 2018; Yu et al., 2021). Before calculating the VFC index, we processed the time series, masking all pixels with a probability of cloud coverage. The latter operation was developed in the GEE environment by exploiting the S2 Cloud:probability dataset produced by the European Commission in collaboration with the European Spatial Agency (ESA) and the SentinelHub service. For the production of the S2 Cloud:probability dataset, in particular, ESA used the Sentinel2-cloud-detector (whose library is available in the s2cloudless python package), an algorithm based on machine learning for the automatic detection of clouds in Sentinel-2 images. Once processed the images of the time series, we calculated the average 4-band red-edge Normalized Difference Vegetation Index ($NDVI_{4re}$) (Eq. 2) using the formula proposed by Liu et al. (2022). It has been shown that the red edge indices can correct the underestimation of vegetation vigour when vegetation cover is high and mitigate its overestimation when levels of vegetation cover are low (Liu et al., 2022):

$$NDVI_{4RE} = \frac{(\alpha * R_{RE3} + (1-\alpha) * R_{RE2}) - (\beta * R_{red} + (1-\beta) * R_{RE1}}{(\alpha * R_{RE3} + (1-\alpha) * R_{RE2}) + (\beta * R_{red} + (1-\beta) * R_{RE1}} \quad \text{(eq. 2)}$$

where R_{RE1}, R_{RE2}, R_{RE3}, and R_{red} are the four Red-Edge bands of Sentinel-2 imagery; α and β are weighting coefficients representing the proportion of RE3 and Red reflectance, respectively (Liu et al., 2022). In our proposed method, the value of both coefficients was fixed at 0.7.

The average VFC value was then calculated (Eq. 3):

$$VFC = \frac{NDVI_{4RE} - NDVI_{4REmin}}{NDVI_{4REmax} - NDVI_{4REmin}} \quad \text{(eq. 3)}$$

VFC value ranges between 0 and 1. For our purpose, we considered only those with a VFC value greater than 0.6 as suitable areas.

2.1.5. Construction of the multi-species ecological network (EN)

Graphab 2.6 was used to construct the multi-species ecological network of the entire study area, using the principles of graph theory (Ersoy et al., 2019a; Foltête, 2019; Foltête, Clauzel, et al., 2012; Godet & Clauzel, 2021).

The maximum affinity of a species to a particular land use has been considered as a possible habitat. The home range was used to set a lower area threshold for habitat patches. Only habitats with a surface of at least 2 hectares were considered possible patches. This choice is consistent with Boitani's finding that 2 hectares is the minimum home range size for each focal species we selected. Considering the above variables (slope less than 100%, home range $\geq$ 2 ha, VFC $\geq$ 0.6, and excellent affinity to land use), we finally identified the EN patches.

For the identification of ecological corridors, a crossing threshold was established to be valid for all focal species, understood as the maximum distance an animal can travel in a hostile environment to reach resources. The threshold was set at 2 km because literature and empirical evidence obtained through interviews with local experts indicate it as the maximum distance that focal species can travel with less mobility. This value will, therefore, be more than sufficient for species capable of spanning greater distances.

2.1.6. Building network components: patches and ecological corridors

The modelling process in Graphab 2.6 returns a series of nodes and arcs as graphic representation of patches and ecological corridors, respectively. The arcs were identified by considering two topological and weighting parameters of the arcs themselves. The Graphab 2.6 software allows for two different alternatives, 'planar topology', in which only the links forming a 'planar graph' are considered (i.e., in the construction of the graph, only the arcs that connect the nodes in the planar representation of the graph itself, and never intersect, would be considered), and 'complete topology' in which all the arcs between patches are potentially taken into account. In our case, the latter method was used, as it does not exclude any possible pathways and provides an initial linear representation of displacements, allowing for a realistic representation of ecological corridors (Godet & Clauzel, 2021). Taking into account the patches, the maximum crossing threshold, and the strength value assigned to each pixel of the raster relating to the land uses of the study area, it was possible to identify ecological corridors and Least Cost Paths (LCPs). Ecological corridors represent potential pathways for species movement within patches best suited to connectivity due to their ecological characteristics. They are in raster in which each pixel has a value indicating the resistance to animal movement. These values tend to increase as one approaches the edges of the ecological corridor. Conversely, they decrease as one approaches the centre of the ecological corridor, in the area that coincides with the identified LCP. The areas where the ecological corridor shows the least resistance to animal movement correspond to those of maximum connectivity near LCPs (Theobald, 2006; Zeller et al., 2012). For this reason, to have an adequate representation of the most suitable ecological corridors, we defined a 100 m buffer around the LCPs and retained only those ecological corridors branching off within the limits of this buffer. The patches, i.e., surfaces elements identified by nodes, and the ecological corridors, i.e., surface elements identified by arcs, represent the component of the obtained EN.

2.1.7. Network connectivity metrics and indices analysis

Several connectivity parameters and indices were calculated to analyse the obtained EN. The selection of these indices is related to their ability to characterise the network, quantify its connectivity, and identify its elements of centrality. This was possible by calculating the following metrics (Tab. 2.2): Integral Index of Connectivity (IIC), Number of Components (NC), Harary Index (H), Betweenness Centrality (BC), Flux (F), and Probability of Connectivity (PC) (Saura & Pascual-Hortal, 2007). The indices described in the table were calculated on the entire network.

The last phase involved a defragmentation scenario proposed to improve the connectivity of the areas identified at the end of the previous phase. The defragmentation scenario was developed considering a peculiar element of the Calabrian region, the so-called ‘fiumare’. These torrential watercourses were identified as crucial elements connecting the urban fabric’s green spaces with the rest of the network. In fact, these rivers cross the entire Calabrian territory from upstream to downstream, also passing through the core of the urban centre of Reggio Calabria. The Calabrian rivers are considered fragile and delicate elements, and hydrogeological constraints are imposed on them.

Table 2.2 - Ecological network connectivity metrics calculated in this work.

Connectivity metrics	Ecological meaning	Definition	Formula	References

Integral Index of Connectivity (IIC)	The probability that individuals randomly located in the landscape within a patch can access each other. A higher value indicates greater connectivity.	For the entire graph: product of the capacities of the patches divided by the number of links between them, the sum is divided by the square of the area of the study area.	$\frac{\sum_{i=1}^{n}\sum_{j=1}^{n}\frac{a_i * a_j}{1+nl_{ij}}}{A_L^2}$	(Freeman, 1977)
Number of Components (NC)	Measure describing the number of isolated areas in the landscape. A high number of components in relation to the total number of patches indicates that the landscape is highly fragmented.	Helpful in describing the level of isolation between groups of landscape patches.	//	(Urban, J. D., Keitt, 2001)
Harary Index(H)	The number of patches that help connect other patches across the landscape. A high value indicates a highly connected landscape.	Sum of the inverse of the number of connections between all patch pairs.	$H = \frac{1}{2}\sum_{i=1}^{n}\sum_{j=1}^{n}\frac{1}{nl_{ij}}$ j≠ i	(Ricotta, 2000)
Betweennes Centrality (BC)	The sum of the shortest paths through the focal patch i, each path being weighted by the product of the capacities of the connected patches and their probability of interaction. P_jk represents all patches traversed by the shortest path between patches j and k.	//	$BC_i = \sum_i \sum_k a_j^{\beta}\, a_k^{\beta}\, e^{-ad_{jk}}$ $j, k \in \{1..n\}, k < j, i \in P_{jk}$	(Orjan Bodin & Santiago Saura, 2010)
Flux (F)	For the entire graph: sum of the potential dispersions of all patches.	//	$F = \sum_{i=1}^{n}\sum_{j=1}^{n} a_j^{\beta} e^{-ad_{ij}}$ j≠i	(Foltête, Céline Clauzel, et al., 2012a)
Probability of Connectivity (PC)	The probability that two random points in the landscape fall within interconnected habitat areas (i.e., reachable to each other). Values are between 0 and 1.	Sum of the products of the capacities of all pairs of patches weighted by their interaction probability, divided by the square of the area of the study zone. This ratio is the equivalent of the probability that two points. randomly placed in the study area are connected.	$PC = \frac{\sum_{j=1}^{n} a_i a_j p_{ij}^{*}}{A_L^2}$	(Saura & Pascual-Hortal, 2007)

2.1.8. Hypothesis of ecological defragmentation scenario

On the one hand, the rivers are considered efficient natural ecological corridors (Bishop-Taylor et al., 2015; Guo & Liu, 2017a; May, 2006). These characteristics are the ideal place to focus an urban defragmentation scenario (Wang et al., 2022; Wang et al., 2021). On the other hand, it is difficult and expensive to expropriate urbanised public or private property areas to build and enhance EN. For this reason, the characteristics of the rivers as environments protected by regional legislation and their natural tendency to connect the landscape elements offer the opportunity to efficiently design conservation designed around the river network (Tarabon et al., 2021).

This phase of analysis aimed to connect isolated environments within the urban context through the re-naturalisation of the torrents, which inappropriate agricultural uses have often degraded. Significant portions of these riparian areas, especially in the mid-valley and valley sections, are characterised by no or little vegetation cover. Therefore, we proposed restoration by planting suitable shrubs and tree species typical of Calabrian woods with a prevalence of hygrophilous species.

Starting from the vectorial data of the study area obtained from the previous operations, resistance values were reassigned in a buffer strip of 100 m around the river rod in the stretches that fall within land-use classes of category 2. Areas belonging to classes of category 1 were excluded from the reassignment for the reasons specified in section 1. The resistance values of these areas were assigned, assuming the natural vegetation of poplars, willows, and alders, which are commonly found in rivers affected by human activity. Once the new resistance values had been assigned to the areas affected by the defragmentation intervention, a new EN was constructed to consider the assumed improvements. Finally, the connectivity indices were recalculated, highlighting their quantitative and qualitative variation.

2.2. Results

2.2.1. Vegetation Fractional Coverage (VFC)

The VFC index can take values from 0 to 1, extremes included and reflects the size of the plants' photosynthetic area and the vegetation's growth density. The closer it gets to zero, the more the stand is devoid of vegetative activity (S. Zhang et al., 2019). Four different vegetation categories were identified based on the VFC values: (i) high naturalness VFC > 0.7; (ii) medium naturalness VFC between 0.4 and 0.7; (iii) low naturalness, VFC between 0.1 and 0.4; (iv) zero naturalness VFC < 0.1 (Fig. 2.5). The threshold of VFC values ≥ 0.6 was used to improve the process of identifying possible patches, as this threshold only includes areas of medium and high naturalness. Overall, VFC values greater than 0.6 were found in hilly and mountainous areas, while progressively lower values were found as one approached sea level, falling below 0.1 along the entire coastal strip (Fig. 2.5).

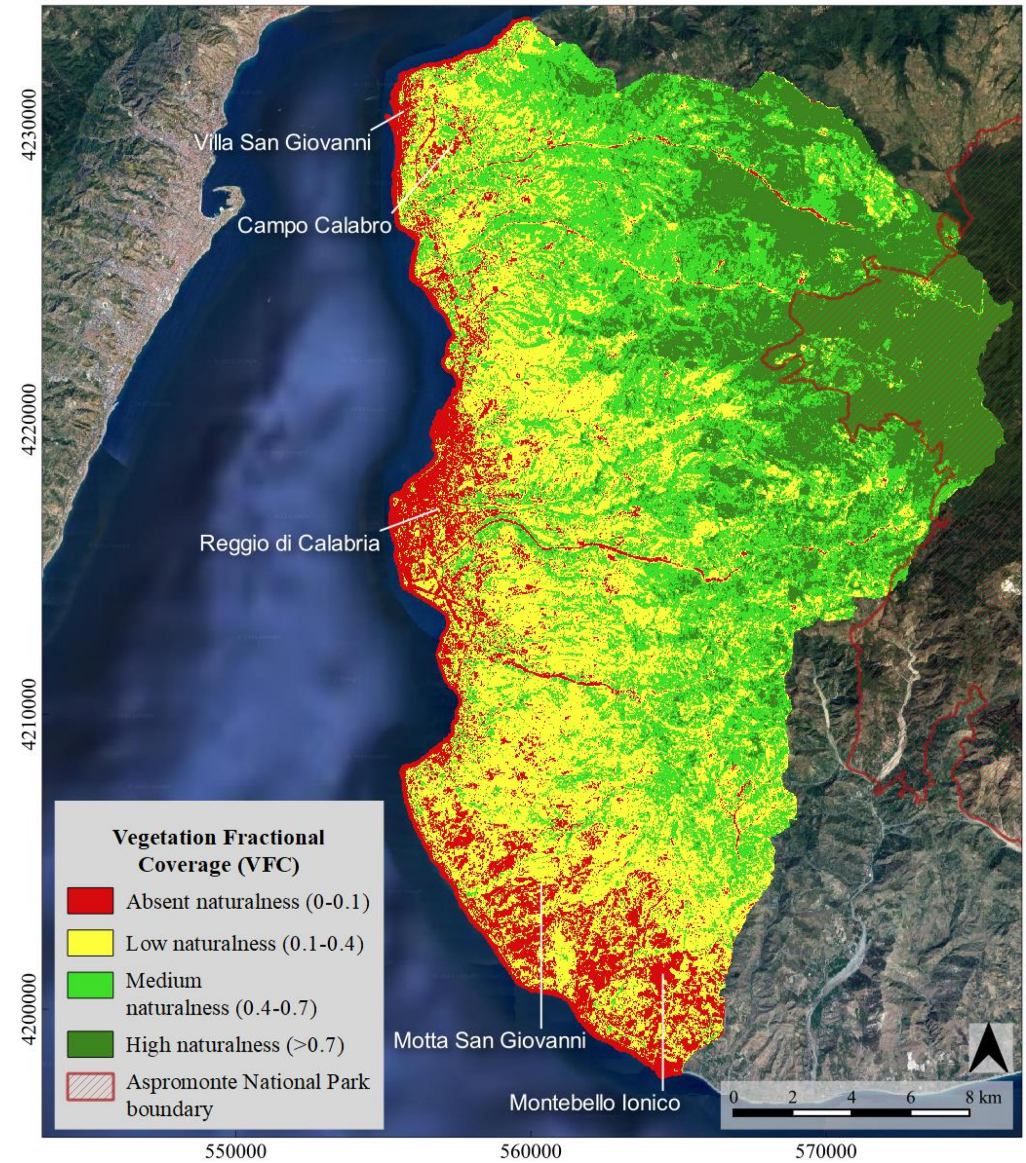

Figure 2.5 - Vegetation Fractional Coverage (VFC) of the study area for the period 2016-2019, reclassified according to four classes: high naturalness, medium naturalness, low naturalness, and absent naturalness.

2.2.2. Ecological network (EN) spatial configuration

We present the design of the ecological network in the study area and describe its connectivity indices that characterise its quality and robustness in two different situations: the one using the UA and CLC datasets and the other based on the defragmentation scenario. In figure 2.6, the two ENs are shown according to their canonical components (patches, nodes, arcs, and ecological corridors) in the two scenarios analysed, pre- (scenario 1, Sc1) and post- (scenario 2, Sc2) improvement proposal.

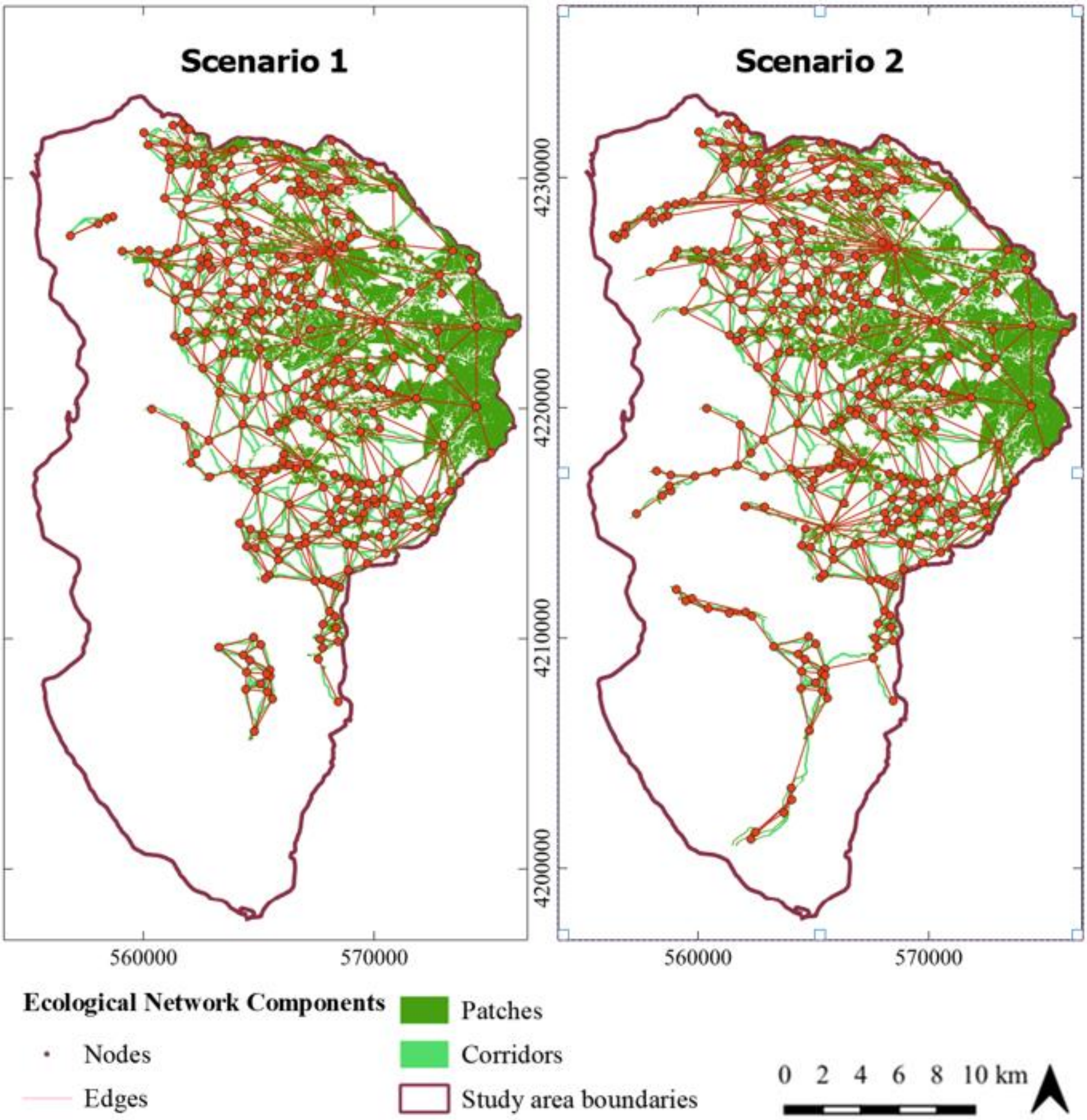

Figure 2.6 - Spatial configuration of the Ecological Networks, represented according to the canonical components: nodes, arcs (edges), ecological corridors and patches based on 2018 data (Scenario 1) and the defragmentation scenario (Scenario 2).

For the first scenario (Sc1), 724 arcs and 300 nodes were identified. The 300 patches range in size from 2 ha to 856 ha, with an average area of 27.04 ha. The total area occupied by the network (patches, ecological corridors) is 10776.93 ha (22.28 % of the surveyed area), of which 8114.93 ha are occupied by the patches and 2662 ha by the ecological corridors. A total of 58.71% of the ecological corridors fall within the areas occupied by wooded areas and natural environments (class 3), 36.86% within agricultural areas (class 2), 2.67% within the class of water bodies (class 5) and finally only 1.77% fall within artificial areas (class 1, mainly distributed on secondary roads and railways). Concerning the patches, on the other hand, 93.11% are occupied by wooded areas and natural environments (class 3), and 5.6% by agricultural areas (class 2). Figure 2.7 shows the network distribution data concerning land uses summarised at the first level for class 1, and the third level for classes 2, 3 and 5.

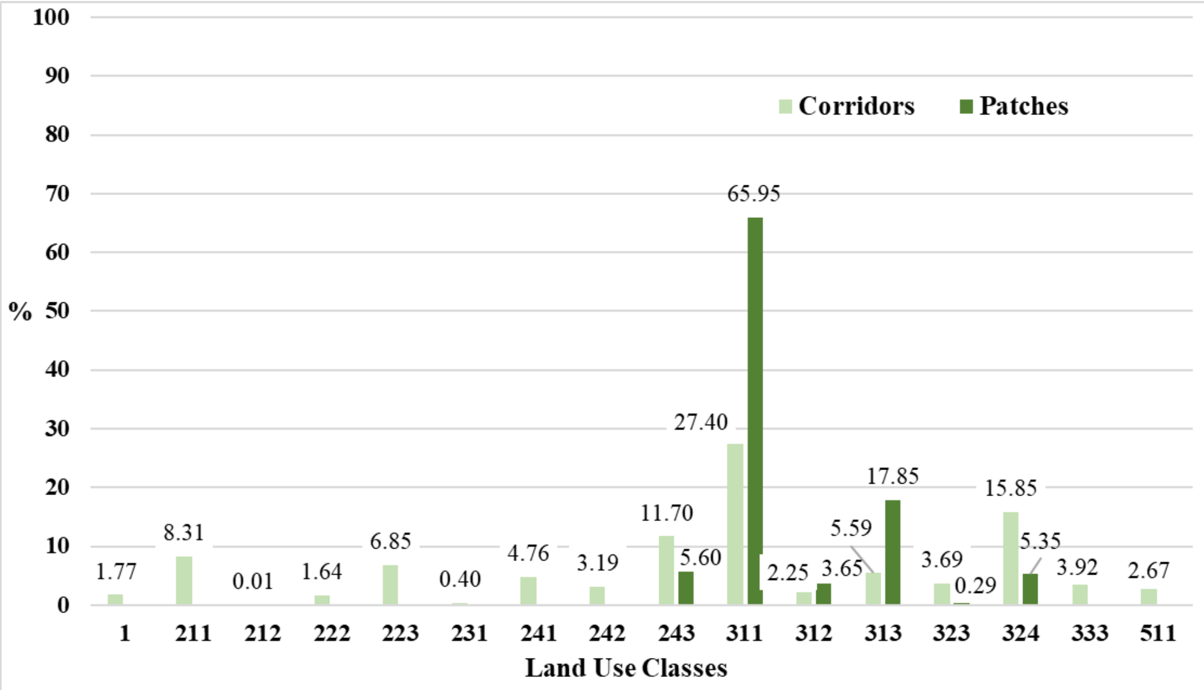

Figure 2.7 - Area occupied (expressed as a percentage) by land uses in the study area of Scenario 1 concerning patches (dark green) and ecological corridors (light green). Due to the low presence of corridors and patches within class 1, this was summarised at level 1, and classes 2, 3, and 5 were kept at level 3.

For the second scenario (Sc2), 771 arcs and 328 nodes were identified. The patches range in size from 2 ha to 936 ha, with an average area of 26.82 ha. The total area occupied by the network (patches, ecological corridors) is 11237.2 ha (23.49 % of the surveyed area), of which patches occupy 8549.91ha and 2687.28 ha by ecological corridors (Fig. 2.8). The majority of the corridors is concentrated in natural land cover types, with 65.44 % in the areas occupied by woodlands and natural environments (class 3), 30.37 % in the areas occupied by agricultural land (class 2), 1.29 % in the areas occupied by artificial surfaces (class 1, of which 0.51% on sports green areas, and the remaining 0.78% on secondary roads and railways) and 2.67 % in the class referring to water bodies (class 5). 97.89% of the patches are identified in class 3, 2.05% in class 2 and the remaining 0.06% in class 1. The increase in the area of the patches of + 434.98 ha is due for 257.05 ha to the direct effect of the greening interventions and the remaining 177.93 ha to the incorporation of many natural areas bordering the interventions that were of less than 2ha in the area, and therefore not considered patches previously.

Regarding the indices analysed (Tab. 2.3), the NC went from 3 in Sc1 to 1 in Sc2. A general value increase was seen in the defragmentation scenario for the connectivity indices IIC, H, F, and PC. The IIC and BC indices were calculated at the level of individual nodes (Figg. 2.9 and 2.10); the highest indices' values were found in mountainous areas, far from the coast, and areas with predominantly forest land use.

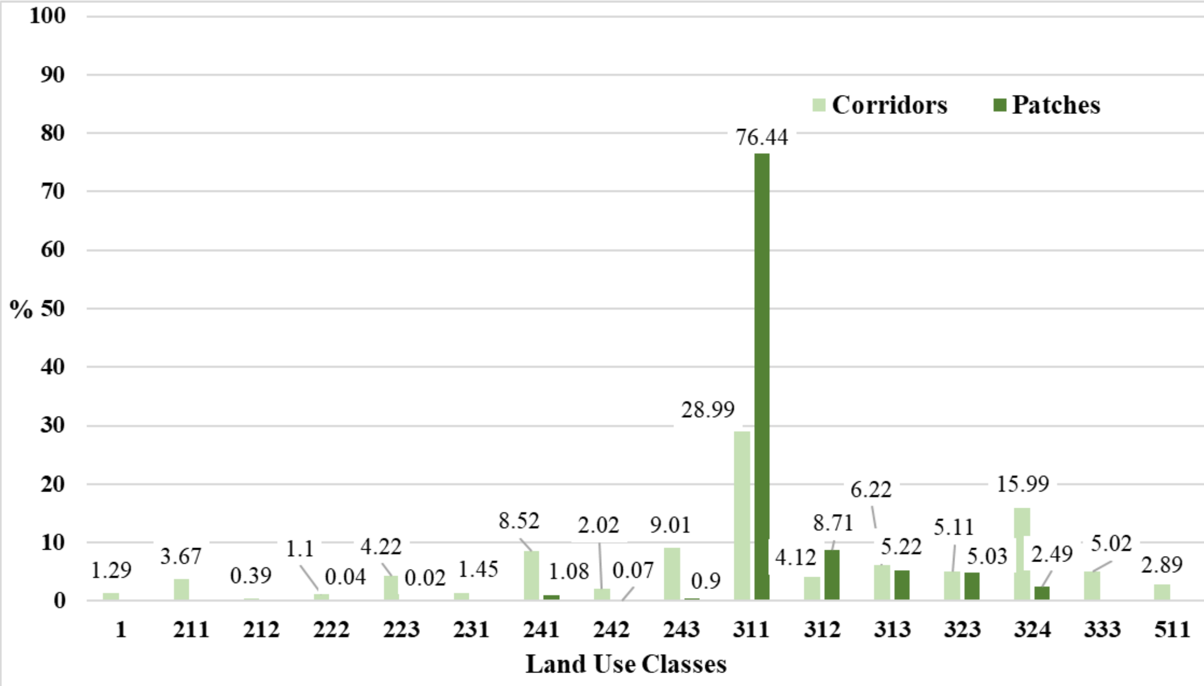

Figure 2.8 - Area occupied (expressed as a percentage) by land uses in the Scenario 2 study area concerning patches (dark green) and ecological corridors (light green). Due to the scarce presence of corridors and patches within class 1, this has been summarised at the first level and classes 2, 3, and 5 have been maintained at the third level.

The average values of both indices increased in the defragmentation scenario compared to the 2018 scenario (Tab. 2.3). In correspondence with the urban centre of Reggio Calabria, we identified patches disconnected from the rest of the network with values of the indices calculated at the node level (IIC and BC) lower than the average of the entire network.

Table 2.3 - Overall connectivity indices calculated on ecological networks in the two scenarios, data as of 2018 (Scenario 1) and defragmentation (Scenario 2).

Connectivity Indices	Scenario 1	Scenario 2
Number of Patches (NP)	300	328
Number of Connections (NL)	724	771
Number of Components (NC)	3	1
Integral Index of Connectivity (IIC)	0.029	0,032
Probability of Connectivity (PC)	0.031	0,033
Flux (F)	2.23	2.95

Betweenness Centrality (BC)	0.20	0.25
Harary Index (H)	8200.50	9704.03

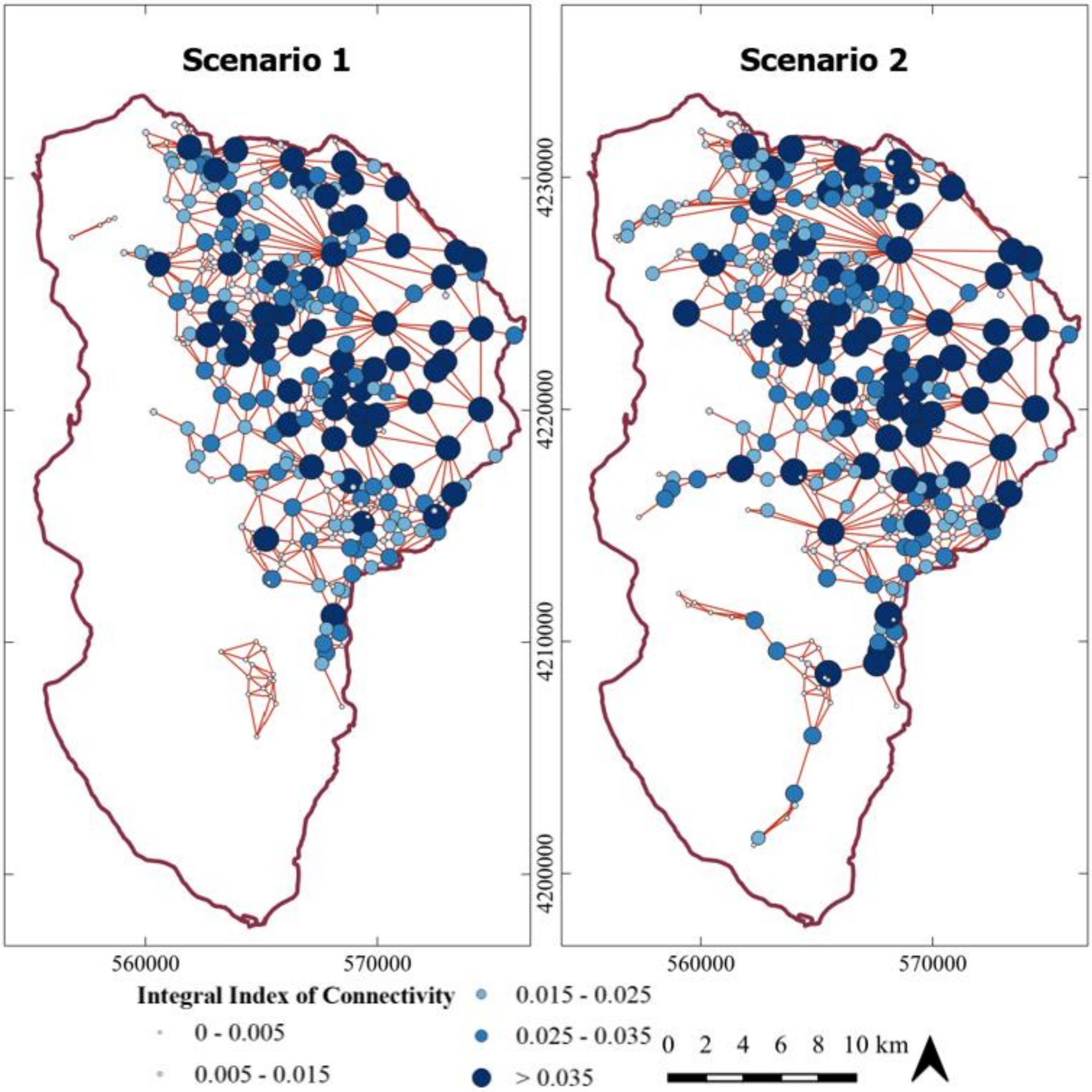

Figure 2.9 - Integral index of connectivity (IIC) calculated at node level for the two scenarios analysed: scenario 1 (data as of 2018) and scenario 2 (defragmentation hypothesis).

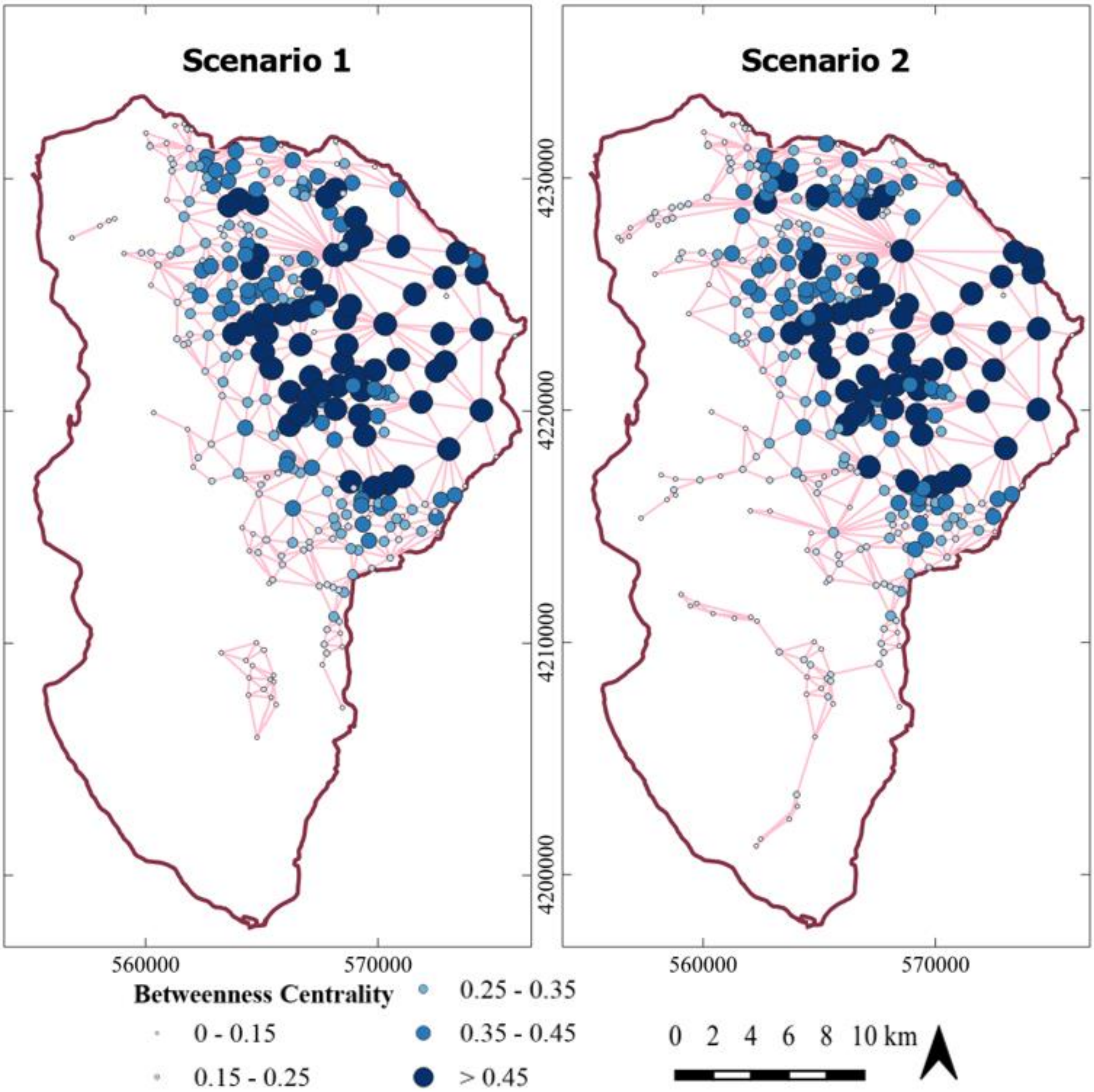

Figure 2.10 – Betweenness Centrality (BC) calculated at node level for the two scenarios analysed: scenario 1 (data as of 2018) and scenario 2 (defragmentation hypothesis).

2.3. Discussion

The analysis of the existing landscape shows that the area with the most well-connected patches, corresponding to the strongest point of the ecological network, is located between 500 m and 1300 m a.s.l., in the municipalities of Sant'Alessio in Aspromonte, Laganadi, and Santo Stefano in Aspromonte, within and close to the Aspromonte National Park boundaries, in the central-eastern and north-eastern part of the study area. The analysis of VFC values confirms this. In these locations, areas of solid naturalness stretch broadly around built-up areas, and even near them, mean VFC values were high (VFC > 0.6), with values consistent with strictly forest stands (Shobairi et al., 2018). On the other hand, the most significant fragmentation problems were seen in the coastal municipalities, especially in correspondence with the most human-modified centres, such as the municipalities of Reggio Calabria, Motta San Giovanni and Montebello Ionico. The territory is mainly occupied by cultivated fields, buildings, and human infrastructure in these places. The VFC values are consistent with this trend, averaging less than 0.4. Analysing the results referring to both Sc1 and Sc2 scenarios, it emerges that the suggested defragmentation interventions showed the best results in the most altered locations.

The proposed interventions led to an increase in the indices' values in the area occupied by patches; an increase in NP from Sc1 (300) to Sc2 (328) was observed, which is consistent with the increase in NL from 724 (Sc1) to 771 (Sc2). The increase in NP and NL generated a partial change in the spatial configuration of the post-intervention network. Here, additional connections branch off into the degraded areas to the south and west of the study area. In particular, the increase in ecological corridors made it possible to connect a group of 18 patches that were isolated in Sc1 to the rest of the network, thus having in Sc2 only one component after the intervention proposal, as opposed to the 3 identified for Sc1. Recent studies have shown that increased node connectivity leads to higher species richness at the local scale (α-diversity) (Liccari et al., 2022). The increase in the number of patches (+28) is related to the re-greening interventions. These have made it possible to increase the eligible area of those areas bordering watercourses with fewer than 2 hectares and had therefore been considered unsuitable as patches in Sc1. This reveals the capacity of the interventions to restore habitat fragments that were excluded from connectivity even outside the intervention area itself.

The analysis suggests that the proposed ecological corridors could create a bridge between the coastal and mountainous areas, leading to greater accessibility by the rest of the network to these patches, which, in some cases (5 patches in the municipality of Reggio Calabria), were dead ends of the network route, connected by a single connection and therefore at greater risk of disappearance. This led to an increase in the number of connections of the isolated areas and created new connections in Sc2, which is confirmed by the rise in the Harary Index (+1503.53 in Sc2), where higher values of this index, such as those found in Sc2, indicate a more connected landscape (Harary, 1969; Pascual-Hortal & Saura, 2006; Ricotta, 2000). This evidence is confirmed by the variation in BC values at the node level in Sc2. Nodes with a higher BC value are considered stepping-stones (small areas that allow animals, which exploit their resources, to move from one patch to another) that increase the robustness of the network (Urban et al., 2009). In particular, 18 nodes isolated in Sc1 had their BC value increased, contributing to a rise in the mean BC value of the entire network. This is due to both the rise in the number of connections between isolated nodes and the increase in the average area of the nodes. The emergence of stepping-stones allowed the connection of previously isolated urban areas, confirming the findings of recent studies demonstrating the ability of these elements to provide favourable habitats for urban ecosystems (An et al., 2021a; Luo et al., 2021b).

Overall, connectivity index values are higher in upland, highly naturalised areas and lower in coastal, highly humanised areas; these results are in line with the trend found in recent pieces of research (Lechner & Lefroy, 2014a; Meza-Joya et al., 2019; Mu et al., 2020; Tiang et al., 2021b).

The increased potential for animals to exploit stepping-stones to move from one patch to another in Sc2 is confirmed by increases in the F-index, which expresses the probability that animals can move between patches (Saura & Pascual-Hortal, 2007). An increase in this value is highly correlated with the rise in the PC index, which expresses the probability that two individuals placed at a random point in the network can access each other by moving.

The changes in the IIC index further confirm the improved network quality in Sc2. The increase in IIC values measured in the entire network and the area of the 18 patches isolated in Sc1 expresses an increase in the probability of the patches accessing each other (Pascual-Hortal & Saura, 2006, 2008).

Concerning the distribution of patches and ecological corridors in the two different scenarios, it was found that the general trend remained unchanged; thus, the most occupied class, considering the adopted CLC legend, remains the third, followed by the second. There was, however, a redistribution of values within the classes. In particular, in Sc2, we find an increase in the concentration of patches and ecological corridors (+5% and + 6.7%, respectively) compared to class 3 in Sc1. This has resulted in the second scenario in a network developed more on natural areas, where the fauna movements involve the crossing of smaller portions of land altered by human activity. Furthermore, the slight change in the distribution of corridors in class 1 of Sc2, compared to Sc1, shows how the interventions allowed urban green areas to enter the network while they were previously excluded. The presence of corridors crossing secondary roads gives rise to hints about the possibility of making interventions (e.g., elevated green bridges, green underpasses) that allow animals to pass through while reducing the number of road kills (Girardet et al., 2015). On the other hand, the absence of corridors on highways makes it clear how these elements are barriers to species movement, making interventions on them valuable possibilities. This type of consideration on roads is made possible by the use of Urban Atlas roads elements are absent on Corine Land Cover.

Another element of relevance is the reduction of the NC from Sc1 (3) to Sc2 (1), an indicator that the level of isolation between patch groups has been reduced. In Sc2, there are no longer any isolated patch groups and the interventions in river areas have reduced the degree of fragmentation of the network. This shows differences from other research, where no improvement interventions were planned (i.e., Modica et al., 2021; Tarabon, et al., 2021). In general, what emerges from the trend in the values of the metrics analysed is that expanding green areas along river courses would benefit the whole EN. We have shown how these metrics offer information regarding the network's robustness, which can greatly support planning (Foltête et al., 2014; Rayfield et al., 2011).

2.4. Conclusions

With the present work, it was possible to analyse the connectivity of an ecological network built on land use data in 2018 and to evaluate the impact of a scenario intended to enhance multi-species connectivity. We demonstrated how the level of spatial detail achieved through the integrated use of highly accurate data, such as CLC and UA, in conjunction with VFC index analyses, allows for constructing a robust EN. The defragmentation scenario focused on the restoration of green vegetation in the areas surrounding the torrents and demonstrated how incorporating small fragments of land into the constructed network improved the connectivity of the entire network. The high naturalness component identified in these fragments, underlined by the VFC analyses, demonstrated their potential in ecological terms. These isolated elements are, in fact, not used for anthropogenic productive activities and are too small to be considered patches, remaining confined to disconnected islands in the landscape. Our analysis shows the high value of interventions that enhance these fragments of high naturalness in their contribution to multi-species landscape connectivity. The proposed interventions have also shown how to create new corridors and patches on the edges of urban areas.

There are limits to our analysis deriving from its development of an EN based only on land use maps. These could be overcome by having future empirically optimised habitat and resistance maps availability (Cushman, 2006; Cushman & Lewis, 2010; Mateo-Sánchez et al., 2014, 2015b). In addition, more species could be included, adding bigger mammals, amphibians, reptiles, birds, and insects. Another limitation is the lack of specific studies of certain behavioural characteristics of species. Numerous errors are still made when evaluating an individual’s behaviour in the face of a land alteration, and the responses of animals to a man-made element are not always linear (A. Rudnick et al., 2012). Some species tend to avoid agricultural areas, others are attracted to and even benefit from them, and others may be attracted or repelled by light or noise pollution.

In terms of prospects, the use of indices calculated from multispectral satellite data shows promise for studying variations in connectivity. Variations in plant populations could be related to the phenomena that may be causing them, urban and agricultural expansion, global warming, and pollution.

Our multi-species approach does not require long lead times for data collection and would be suitable for short- and medium-term planning (Lechner et al., 2015). Restoring connectivity requires financial actions based on concrete interventions on the ground, with the need to spatially identify patches and ecological corridors. This type of planning approach could be considered to identify areas where attention should be focused.

3 Combining Pathwalker simulations and Graphab graphs

Adapted from

Lumia G., Cushman S., Praticò S., Modica G.: **Intra-network analysis based on comparison between graph theory approach and Pathwalker**. Doi: 10.1007/978-3-031-37114-1_20

Intra-network analysis based on comparison between graph theory approach and Pathwalker

Giovanni Lumia[1[0000-0003-0745-4497]], Samuel Cushman[2], Salvatore Praticò[1[0000-0003-1684-178X]], Giuseppe Modica[3[0000-0002-0388-0256]]

[1] Dipartimento di Agraria, Università degli studi 'Mediterranea' di Reggio Calabria, Reggio Calabria, Italy

[2] Wildlife Conservation Research Unit, Department of Biology, University of Oxford, The Recanati-Kaplan Centre, Tubney House, Oxon, Tubney, OX13 5QL, United Kingdom

[3] Dipartimento di Scienze Veterinarie, Università degli studi di Messina, Messina, Italy

giovanni.lumia@unirc.it

Abstract

Today there is increasing investigation of how to succeed in land operations without damaging delicate natural ecosystems. Over the past century, the planning of land interventions operated without following a guideline has led to fragmentation of ecosystems and progressive biodiversity loss. Several strategies have emerged in this regard to identify corridors and protected areas on the territory. It is important to compare the many strategies in the scientific landscape to assess the levels of correlation present among them and to understand how to exploit the products of the analyses in our favour in the planning sphere on a territory threatened by pressing anthropi sation. The present work compared movement simulations produced by Pathwalker software and corridors identified on the territory by Graphab software. We took advantage of Pathwalker's ability to evaluate movement predictions by taking into account factors such as mortality risk, attraction and energy in the simulation. This work was important because it allowed to classify predictions according to scales of reliability. In particular, we classified the connectivity indices obtained from the elaborations in Graphab according to 4 levels of reliability ranging from a high degree of consistency to a low degree of consistency. Pathwalker simulations were compared to the above indices to assess similarities and differences. This work is important as it allows to give exploit the combination between different connectivity prediction models provide concrete tool to the planner at decision making time.

Understanding what techniques and approaches should be followed to protect the environment and habitat loss is one of the hottest topics of scholarly debate in the last century (Casas et al., 2021; Guo & Liu, 2017b; Tarabon et al., 2022b). The importance of proper planning of land interventions to avoid fragmentation and loss of biodiversity is now well known. Scientists are questioning what strategies should be followed to give the planner a tool. A promising and recent new strategy for simulating movement patterns is Pathwalker (An et al., 2021b; Foltête, Céline Clauzel, et al., 2012b; Kaszta et al., 2018b; G. Wang et al., 2022b). In this work we decided to combine graph theory and Pathwalker simulations to evaluate the reliability of the predictions. Initially, we identified patches, nodes, and edges through graph theory and calculated several connectivity indices commonly used in the literature for evaluating network elements. In the second step, we divided according to four levels of consistency values of 3 connectivity indices calculated in the Graphab environment. Finally, we divided each connectivity index into 4 consistency levels and used Pathwalker movement simulations to evaluate the response of each of the 4 levels.

3.1. Materials and Methods

3.1.1. Base data

As for previous chapters, the work was carried out on the Reggio Calabria metropolitan area. The data used in the connectivity simulations come from databases produced in the European context of the Copernicus project (https://land.copernicus.eu/ - last access 30 June 2022). In particular, we used the same strategy as for Chapter 2 to jointly used Corine land Cover data as of 2018 (CLC 2018, which has a high level of thematic detail for natural and semi-natural areas) and Urban Atlas as of 2018 (UA 2018, which has a high level of thematic and geometric detail for man-made areas).

The simulations were performed taking into consideration the requirements of 10 selected focal species considering the works in the same area. Autecological information on the species (dispersal distance, home range, habitat suitability) was retrieved from the database on Italic fauna produced by Boitani et al. (2003).

3.1.2. Data processing

For the first processing done in Graphab, we used the combined map of CLC and UA as the basis on which to perform the simulations. The subsequent considerations that we will list below regarding resistance to movement, home range and dispersal threshold were made based on the autecological data collected by Boitani listed in the National Ecological Network (REN) sheets (Boitani et al., 2002b).

In the simulation, we assigned a value indicating the resistance these environments offer to animal movement for each of the different land use codes. Specifically, the land use map was rasterised and resistance values were assigned to each pixel corresponding to the respective land use. The raster was initially at a resolution of 2.5 m x 2.5 m and later resampled to 10 m x 10 m by a bilinear interpolation function. This operation allowed lightning processing without losing information about smaller elements in the map (streets and isolated buildings). The assigned values range from 1 (least resistance to movement) to 100 (greatest resistance to movement). The dispersal threshold was set at 2 km, whereas 2 km is a value that allows each of the 10 focal species to move from patch to patch, as seen in previous work on the same area (Modica et al., 2021). The minimum home range extension was set at 2 ha following the same assumption made for the dispersal threshold. Patches inferior to 2 ha were still considered suitable areas (stepping stones) for animal movement over the territory (Gurrutxaga & Saura, 2014). Having set all these parameters within the Graphab software, we obtained a graphical visualisation of the network, composed of nodes, patches, edges, and links, and on it we calculated the Integral Index of Connectivity, Betweenness Centrality index (BC), and Probability of Connectivity (PC) using the Graphab 2.8 software functions.

Starting from the raster land use data and using the graph nodes obtained in the previous elaborations in Graphab as source points, we formed the basis for launching the following operations in Pathwalker. In particular, Pathwalker allows the simulation of the movement considering three parameters, which are energy (mechanism 1), risk (mechanism 2) and attraction (mechanism 3) and four different combinations of them (mechanisms 4,5,6 and 7). For this work, we decided to operate with mechanism 7, which combines all three: energy, risk, and attraction. In addition, we used a parameter to consider in the simulation the tendency of a moving animal to continue the same path or to change direction. This parameter ranges from 0 (minimum tendency to change direction) to 1 (maximum tendency to change direction); we set it at 0.25. Operations were produced by setting all of these parameters within the Pathwalker environment and launched through Anaconda's Powershell Prompt.

We then went on to categorise the values of the connectivity indices calculated in Graphab into four levels of consistency for each of IIC, PC and BC. Subsequently, the level of correlation (using the Pearson correlation coefficient) with Pathwalker simulations was evaluated for each level using the RStudio environment.

3.2. Results

Here, we present results regarding the network created by graph theory, obtaining predictions of movement patterns by Pathwalker simulations and comparing the two methods to identify points of affinity or disagreement.

The network obtained by Graphab consists of 328 nodes that resulted in the same number of patches with an average area of 26 ha. The patches cover 8549.91ha, and the areas most represented are the environments classified as forested (76% of the total number of patches). Generally, the largest patches are located in areas far from population centres, hilly and mountainous areas. In contrast, the smaller patches with greater distance between each other are near population centres and closer to the coast.

Table 3.1. Overall connectivity indices are calculated on the implemented ecological network.

Connectivity Indices	Overall
Integral Index of Connectivity (IIC)	0.032
Probability of Connectivity (PC)	0.033
Betweenness Centrality (BC)	0.25

The connectivity indices analysed tended to have higher values in mountainous and hilly areas than in flat areas and closer to the coast. The values of the connectivity indices IIC, BC and PC (summarised their overall values in Tab. 3.1) were divided into 4 levels ranging from lower to higher values (Fig. 3.1, top right, top centre and top left) and correlated with the values and of the Pathwalker simulation (Fig. 3.1 bottom centre).

The correlation values (shown in Fig. 3.2) showed a negative correlation for thresholds 1,2 and 3 of BC (BC1, BC2, and BC3), thresholds 1, 2 and 3 of PC (PC1, PC2 and PC3), and thresholds 1 of IIC (IIC1). In contrast, a positive correlation was found for threshold 4 of BC (BC4), thresholds 4 of PC (PC4) and thresholds 2, 3 and 4 of IIC (IIC2, IIC3, and IIC4).

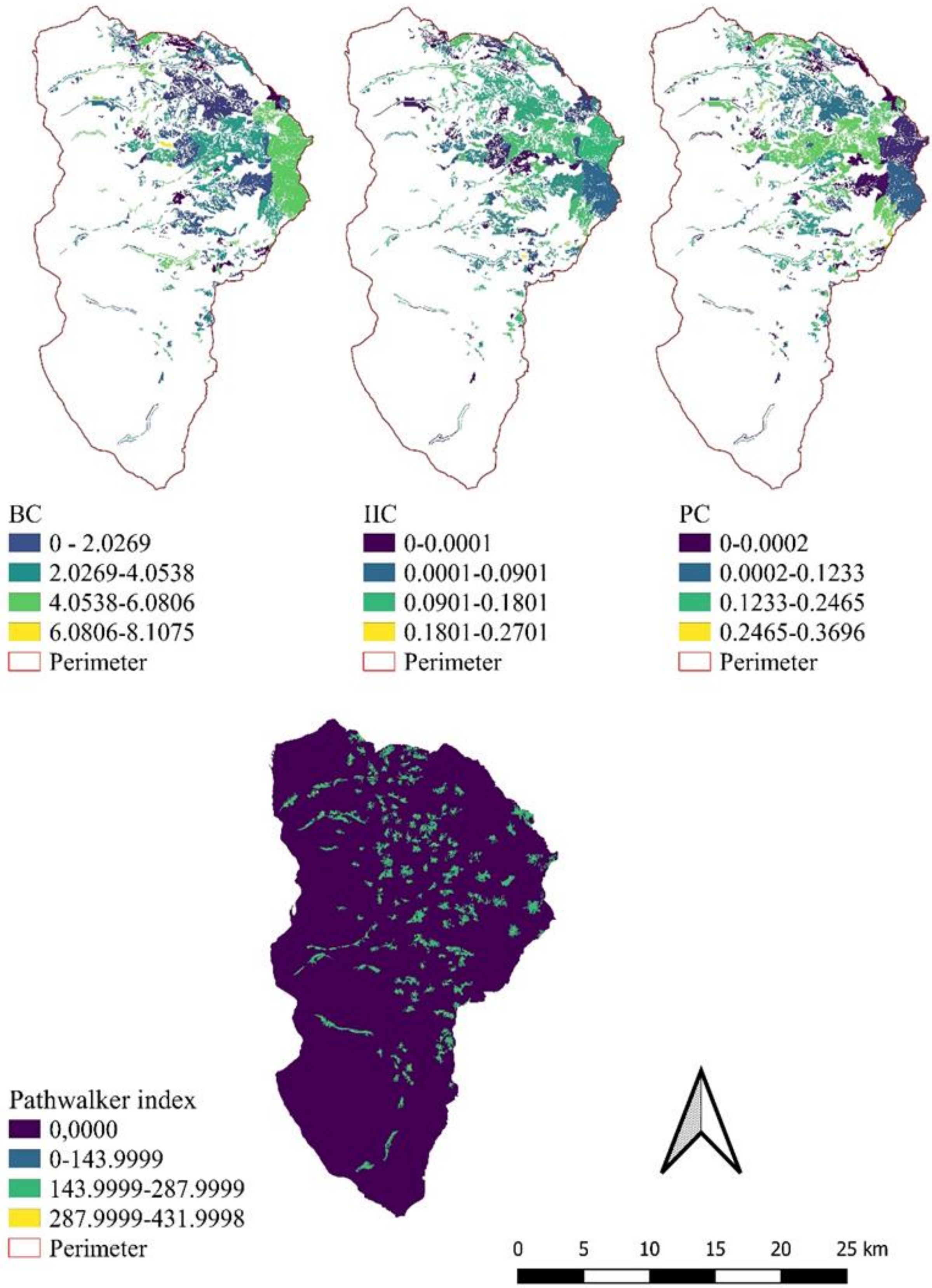

Figure 3.1- Pathwalker surface density (bottom left) and connectivity indices for Betweenness Centrality (top left), Integral Index of Connectivity (top centre) and Probability of Connectivity (top right) according to a 4-class division ranging from lower to higher values.

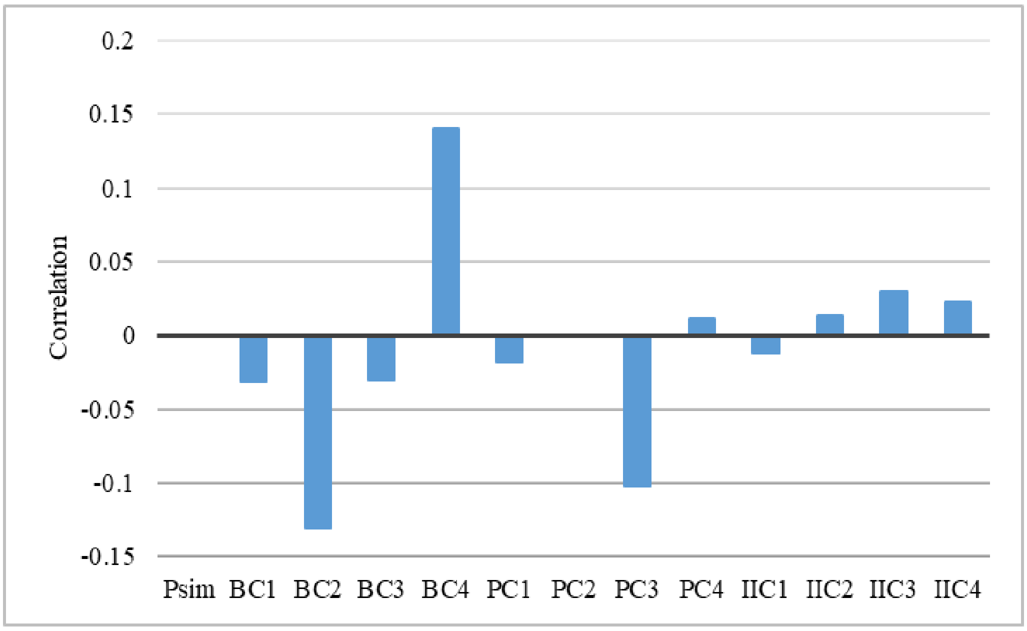

Figure 3.2 - Correlation values between Pathwalker simulation (Psim) and the 4 thresholds of Betweenness Centrality (BC1, BC2, BC3, BC4), IIC (IIC1, IIC2, IIC3, IIC4) and Probability of Connectivity (PC1, PC2, PC3, PC4).

3.3. Discussions

A greater number of high-area patches in mountainous areas is consistent, given the more natural feature of these areas. Indeed, the population centres and areas most occupied by infrastructure and agricultural activities are largely located in the low hill and coastal areas. The trend in the connectivity indices IIC, PC and BC values, which were higher near mountainous areas, underscores the greater importance to the network of these areas. Although these results suggest a correct representation of connectivity predictions, correlation analysis with Pathwalker simulations tended to show a negative or slightly positive trend for only a few indices. This was expected. The Graphab indexes we used are patch-based, and the individual index values refer to the centroids of the patches. In Pathwalker, on the other hand, the animal's movement is not related to the presence of patches but exploits the mechanism of resistant kernels for simulations. The mechanism of resistant kernels has been shown to be more accurate in predictive terms than the patch-based approach (Calabrò et al., 2021; Cushman et al., 2014b; Spatari et al., 2022). This is, thus, the reason for the generally low level of correlation between Graphab and Pathwalker indices. In addition, this phenomenon was expected, considering that Graphab does not consider attraction and risk factors. The Pathwalker energy mechanism, understood as an animal's energy budget that ends its movement when it exhausts it, is the parameter in common with Graphab. The attraction parameter evaluates which path is the lowest cost and tends to avoid paths with high resistance surrounding the walker. On the other hand, the risk parameter considers the possibility that an animal, during a gradually less favourable path, will suddenly stop its movement, with a gradually higher probability as the inhospitality of the area increases. The positively trending correlation values for all category 4 levels of the indices underscore the potential in predictive terms of the joint work of the attraction and risk mechanisms. Returning to the B4, PC4 and IIC4 values, the reason why the correlation levels are higher in these areas seems to be related to the presence of large areas with low levels of resistance that do not have a great effect on the risk and attraction mechanisms. A greater effect on the attraction and risk indices occurs instead, where patches become smaller and the distances between them increase. An underestimation by the IIC, PC and BC indices against the Pathwalker simulations emerges in these areas. We next analyse the effect on the simulation (and on the levels of correlation between Graphab and Pathwalker metrics) of using a parameter that indicates the tendency of a walker to continue along its direction or change path. This parameter is intended to make the animal's movement even more faithful to reality. In fact, in nature, animals exploring the territory may not always choose the path that offers the most resources (K. McGarigal et al., 2000; M. Wang et al., 2021; Wu et al., 2023). For this reason, the effect of taking non-ideal paths in highly fragmented areas is more pronounced. The fact that Pathwalker considers this variable as opposed to Graphab further lowers the correlation levels, especially in the level 1, 2 and 3 areas located in the most fragmented areas.

3.4. Conclusions

In this work, we compared connectivity indexes and movement simulations to identify network weaknesses and what factors affect the predictions under certain conditions. Specifically, the values of the IIC, BC and PC indexes were divided into 4 levels of consistency, and for each level, the level of correlation with Pathwalker simulations over the same area was analysed. It was found that Pathwalker's ability to consider factors such as energy, attraction and mortality risk allows it to provide a higher level of detail in predictive terms. Especially where the natural areas are found to be more fragmented, considering more behavioural factors allows for a more realistic representation of the animal's movements, which is consistent with what is in the literature (Kumar et al., n.d.-a; Unnithan Kumar & Cushman, 2022b). The land use resolution used is undoubtedly a limitation that can be overcome in future elaborations. In particular, for the same study area, a habitat map could be used instead of a simple land use map (the implementation of which was planned under the Natura 2000 context: https://www.isprambiente.gov.it/it/servizi/sistema-carta-della-natura - last access 20 February

2024). The use of other statistical analyses could also be considered in the future to highlight other network characteristics (Vizzari & Sigura, 2013). This work has given rise to new insights into the issues of connectivity prediction. We have shown how the reliability of predictions can vary within the same network in dependence on structural factors (of the network), behavioural factors (of the animal species) and the method used (graph theory and Pathwalker).

4 Comparison of two different strategies, centroid vs synoptic approach

Adapted from

Lumia G., Modica G., Praticò S., Cushman S.: Comparison of patch-based and synoptic connectivity algorithms with graph theory metrics. Under review.

Comparison of patch-based and synoptic connectivity algorithms with graph theory metrics. A case study in Reggio Calabria metropolitan area (south Italy)

Giovanni LUMIA[1[0000-0003-0745-4497]], Giuseppe MODICA[3[0000-0002-0388-0256]], Salvatore PRATICÒ[1*[0000-0003-1684-178X]], Samuel CUSHMAN[3,4],

[1]Dipartimento di Agraria, Università degli studi 'Mediterranea' di Reggio Calabria, 89122 - Reggio Calabria, Italy – E-mail: giovanni.lumia@unirc.it ; salvatore.pratico@unirc.it

[2] Dipartimento di Scienze Veterinarie, Università degli studi di Messina, 98168 - Messina, Italy – E-mail: giuseppe.modica@unime.it

[3] University of Oxford, Department of Biology, Wildlife Conservation Research Unit, 11a Mansfield Road, Oxford OX1 3SZ, England.

[4] US Forest Service, Rocky Mountain Research Station, 2500 S. Pine Koll Dr., Flagstaff, AZ 86001, United States – E-mail: sam.cushman@gmail.com; samuel.cushman@usda.gov

*Corresponding author: Giuseppe Modica – giuseppe.modica@unime.it

ABSTRACT

Predicting and mapping connectivity between habitats and populations is critical to addressing habitat loss and biodiversity issues. Several strategies in the literature exist to understand, restore, and preserve ecological connectivity. The main issue of the current research is to identify among the connectivity modelling strategies which are the most reliable for planning purposes.

Our goal in this work were to compare connectivity predictions using a wide variety of commonly used approaches to improve the understanding of the similarities and differences in the predictions of these methods. Specifically, we investigated the differences in connectivity predictions related to connectivity algorithm, the number and distribution of source points, and threshold distance at which connectivity is allowed between locations. First, we separately applied different strategies and methods commonly used in the literature to model connectivity in the same study area. Then, going through a series of hypotheses, we compared the different models to confirm or disprove the initial hypotheses. Particularly, the initial hypothesis was that what most influences the results of connectivity models are different dispersal distance thresholds; differences in connectivity algorithms, especially kernel, path, and graph theory-based approaches; differences in predictions produced by two different software tools, UNICOR and Graphab; use of source points derived from a synoptic or patch-based perspective.

We proposed 4 main hypotheses and 14 combinations of them, hypothesizing that what most influences the results of connectivity models are: different dispersal distance thresholds; differences in connectivity algorithms, especially kernel, path, and graph theory-based approaches; differences in predictions produced by two different software tools, UNICOR and Graphab; use of source points derived from a synoptic or patch-based perspective.

We found that the dominant pattern of differences in the predictions of different connectivity analyses was related to the method of analysis, with clear differences between kernel, path and graph-theory approaches, and relatively little effect due to the density and distribution of source points or the distance threshold used to define dispersal capability.

This work provides one of the first comparisons of spatial predictions of different methods, frameworks, and parameterizations of connectivity models. Our results support environmental planning by clarifying

what most influences predictions of movement patterns and how the predicted connectivity networks differ between different analytical frameworks.

Connectivity between populations and habitats is important for a wide range of ecological processes (Cushman, 2006; Huang et al., 2020; Rudnick et al., 2012). In Europe, these issues have been the impetus of the Natura2000 program, which aims to create a series of protected areas for the entire continent. To succeed in achieving a robust and effective connectivity network, it is necessary to use models and metrics that take into account numerous factors related to ecology and additional variables that make these indicators reliable (Kaszta et al., 2020; Macdonald et al., 2013; Rudnick et al., 2012).

To understand, preserve, and restore landscape connectivity, several methods have emerged to simulate movement and connectivity across the landscape. These different methods produce predictions of landscape connectivity (An et al., 2021; Cushman, 2006; Cushman & Lewis, 2010; Clauzel, et al., 2012; Kevin McGarigal, 2000.) from a functional perspective. This entails building ecological networks based on high-natured natural areas that, as such, can sustain ecological functionality (Natura 2000 project, link: https://environment.ec.europa.eu/topics/nature-and-biodiversity/natura-2000_en; last access 31 January 2024), reflecting the hypothesized movement of organisms across gradients of landscape resistance. However, few studies have compared the results from these different strategies and how they are related to each other, this is the reason why with our contribution we decided to provide further substantial knowledge on this topic. Studies have compared how connectivity is affected by different patch sizes, number of nodes, and topological variables (De Montis et al., 2019). Other approaches have compared the properties of connectivity metrics calculated at the level of individual landscape elements (e.g., nodes or patches) and those at the global level (Niquil et al., 2020). Although these studies compare indices or connectivity metrics belonging to a specific model, there is a lack of studies comparing metrics and indices from different models. In this respect, our work can make an important contribution to the literature.

In this study, we focus on how connectivity predictions were affected by three different factors: different analysis methods, different dispersal thresholds, and different spatial frameworks for delineating source points or nodes for analysis. For the last of those topics, we have distinguished between patch centroid based source points and spatially synoptic source points distributed across patches at a density proportional to habitat suitability. This topic is important, as little is known about the relative differences of methods or the influence of dispersal threshold and spatial analysis framework on the predictions of connectivity modelling.

A study done by Cushman et al. (2013), shown that dispersal distance and the distribution of source points across the landscape influence connectivity predictions, where a synoptic point distribution gives better results than a patch-based one, just as wider thresholds give better results than narrower ones. Additionally, several researchers have recently compared the performance of different connectivity methods (Cushman et al., 2014; de Jonge et al 2021; Fath et al. 2020; Unnithan Kumar & Cushman, 2022; Zeller et al., 2018). Cushman et al. (2014) found significant differences in prediction spatially between resistant kernel and factorial least cost path models and that for that analysis, the factorial least cost path had nominally better performance. However, the resistant kernel was more stable and generalizable. Zeller et al. (2018) found that cost distance approaches, like resistant kernels, were generally more robust and accurate than circuit theory approaches in explaining observed movement patterns. Most recently, Unnithan Kumar et al., (2022) simulated a large pool of dispersal processes and compared their congruence with the predictions of different connectivity models run on the same resistance surfaces and the same sets of source points. They found that resistant kernels were almost always the most accurate and robust predictor of functional connectivity, whereas factorial least cost paths were always the worst. They found circuit theory predictors were occasionally the best when there was a strong destination bias in animal movement and when those destinations were known to the observer and included in the analysis. However, none of these or other comparative studies of connectivity methods have formally compared the similarities and differences of connectivity predictions concerning the combination of the analysis method, dispersal threshold used, and spatial framework (patch-centroid based vs. synoptic).

We used different methods to calculate connectivity metrics to fill this knowledge gap. First, we used the Graphab software to obtain a network composed of patches and corridors. A node was assigned for each patch following graph theory (patch-based approach). Different connectivity indices were calculated for each node. Subsequently, we used UNICOR to calculate and map a series of corridors based on the resistant kernels system (https://github.com/ComputationalEcologyLab/UNICOR. Different - last access 10 February 2024) dispersal thresholds were used. In this system, nodes were not allocated to patches but generated probabilistically in a proportional suitability manner (synoptic approach).

Subsequently, several statistical analysis techniques were used to compare them. In particular, we proposed four main and several combination hypotheses. We hypothesized that differences in the results of connectivity analyses might be mainly related to different dispersal thresholds (H1); synoptic vs. patch-based source points (H2); differences in methods, specifically kernel, path, and graph metrics (H3); and UNICOR connectivity value vs. several graph-theoretical metrics calculated in Graphab environment (H4); To evaluate these hypotheses, we employed Principal Component Analysis (PCA), hierarchical agglomerative clustering analysis (McGarigal et al., 2000), and Mantel testing on model matrices (which is a multivariate distance-based analysis of variance testing categorical hypotheses, e.g., Legendre, 1998). The main objective of this work was to evaluate the relationships among different approaches used for calculating landscape connectivity.

4.1. Materials and methods

The study area is located in southern Italy (Fig. 4.1) and includes the territory of 12 municipalities, accounting for nearly 50,000 ha. The area includes plains along the coastal strip, mostly occupied by meadows and cultivated with temporary or permanent crops. In the inland belt, we find hilly areas, from 100 to 600 m above sea level, occupied by permanent crops or shrubs typical of the Mediterranean maquis.

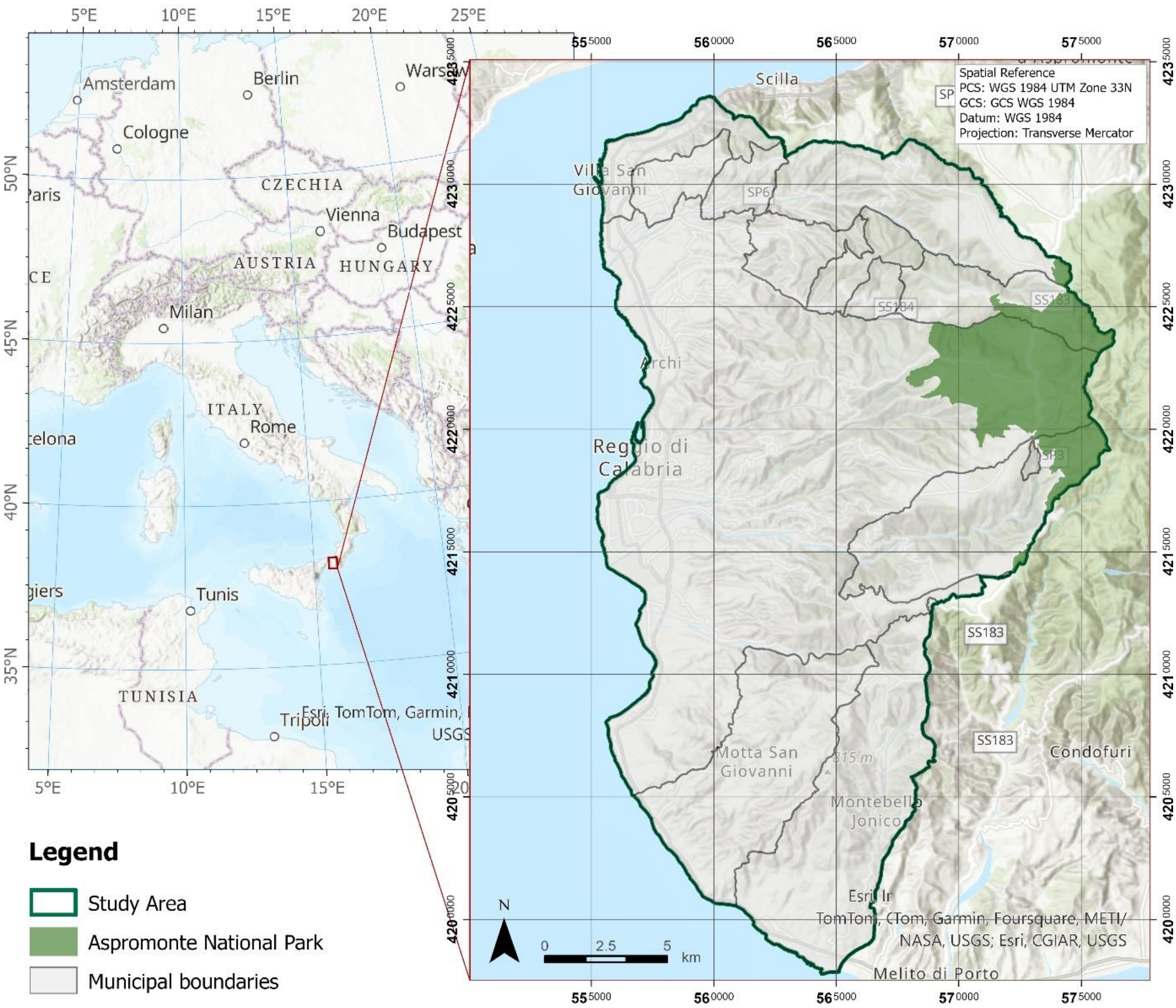

Figure 4.1: The study area (in red) located in southern Italy (within the Calabria region shown in green) includes the metropolitan area of Reggio Calabria and part of the Aspromonte National Park (in dashed yellow).

In the northeastern part of the study area, we find the mountainous zone, which ranges from 600 to 1700 m above sea level and includes deciduous, coniferous, and shrub forests. This area includes part of the Aspromonte National Park.

The analysis presented here was structured in three steps: (1) collection and organization and processing (through free and open source software) of datasets of both cartographic aspects of the study area and the autecological characteristics of focal species (habitat, home range dispersal distance, affinity level to land cover); (2) construction of an ecological network and calculation of connectivity metrics; (3) comparison and statistical analysis of networks and connectivity metrics.

4.1.1 Data collection and processing

Data referring to land cover provided by the European Copernicus program, Corine Land Cover (CLC) 2018, and Urban Atlas (UA) 2018 were used to define landscape patterns for our analysis (Copernicus, Land Monitoring Service, link: https://land.copernicus.eu/-last access 17/02/2022). CLC has a minimum mappable unit of 25 ha (where 25 ha is the area of the smallest polygon of the vectorial land cover map) and 25 different land cover classes; it was made with the aim of representing the natural areas of Europe according to 5 hierarchical class levels. With 27 land cover classes, UA has a minimum mappable unit of 0.25 ha for class 1 areas (urban centers, factories, human-made areas, etc.) and 1 ha for the remaining categories from 2 to 5. UA was made to represent the major Urban areas of Europe. It was therefore decided to integrate these two data since although CLC was designed to represent natural areas, it completely omits highly artificial areas such as roads, highways, buildings, etc., elements that were instead represented with a high level of detail by the UA. Therefore, the final dataset was composed of class 1 from UA and classes 2-5 from CLC.

In fig. 4.2, we reported the implemented dataset used in this study as previously described (CLC + UA, same as for chapter's two figure 2.4) and mapped using the official legend colors defined in the framework of the European Copernicus program.

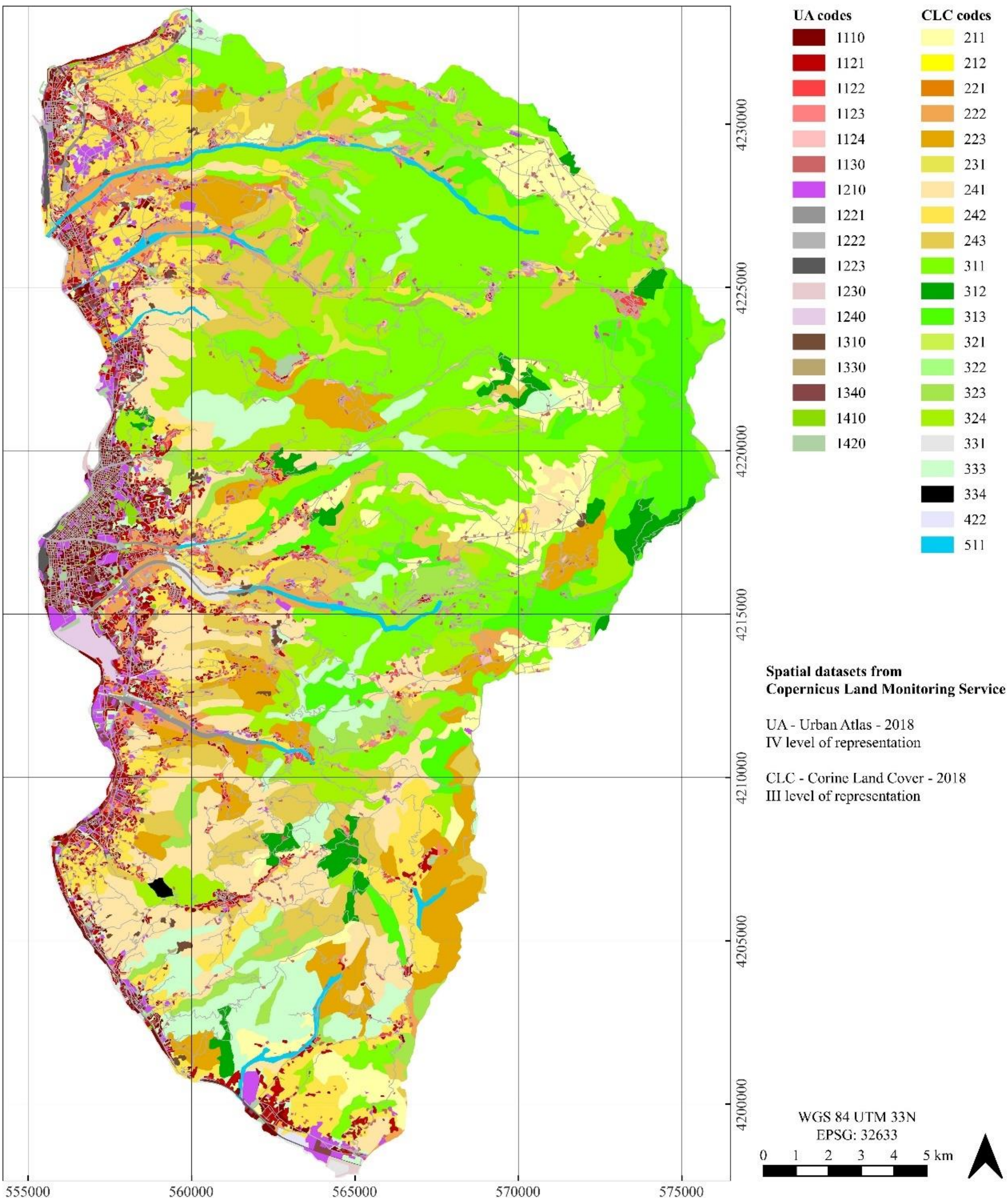

Figure 4.2: Map of the implemented dataset using Corine Land Cover (CLC) 2018 for classes 2 (Agricultural areas), 3 (Forest and seminatural areas), 4 (Wetlands) and 5 (Water bodies), and Urban Atlas (UA) 2018 for class 1 (Artificial Surfaces).

Drawing on the work of Boitani et al. (2002), our analysis represents the collective central tendency of connectivity of 10 mammal species in terms of their habitat associations and movement abilities (see Table 2.3). Considering that the goal of our work is not to create an ecological network but to test the differences between different approaches, we decided to identify this set of 10 species, which would serve solely as a model for the study area across life history space. We took the data from the 10 species to find a value in the middle, which gives a measure of the central tendency of connectivity. The decision to select only small and medium-sized mammals is related to their greater proximity in terms of the amount of resources they need, perception of their surroundings, ability to overcome obstacles (vertical walls, buildings, roads), and the distances they need to cross. In order to make reliable predictions, we relied on data collected by Boitani et al. (2002) on the behavioral and autecological properties of the selected species. This information gives values referring to each species' dispersal distance, home range and affinity level with a given environment. The choice of the species was based on work already done in the same area (Lumia et al., 2023; Modica et al., 2021), and selection was made by giving priority to species protected by national and international laws (https://www.mite.gov.it/pagina/repertorio-della-fauna-italiana-protetta - last accessed 16/02/2022).

The integration of UA and CLC was performed in the QGIS 2.8 environment. The geometries coded as class 1 (artificial areas) of UA were merged into CLC. The minimum mappable unit of the obtained data was UA being less than CLC. See Lumia et al. (2023) for more information about that process. The vector layer was converted to raster with a spatial resolution of 2.5 m x 2.5 m to allow subsequent processing. Then through a bilinear interpolation operation, the pixel size was increased to 10 m x 10 m. The data thus obtained were used in the subsequent analyses below. After carefully inspecting the 2.5 m datum, we evaluated the possibility of using bilinear interpolation to increase the pixel size while retaining the fundamental information of the base map. The choice of 10 m was considered a fair compromise, allowing us to reduce the estimated calculation time. This approach allowed us to have more detail than we would have had by starting the rasterization directly from 10 m.

4.1.2. Graphab Implementation

Graphab 2.6 was used to construct the multi-species ecological network of the entire study area (Clauzel & Godet, 2020; Clauzel et al., 2012; Ersoy et al., 2019; Foltête, 2019; Godet & Clauzel, 2021), it is compatible with GIS software, which makes it versatile and capable of providing significant support to those working in the field of cartography and planning (Clauzel & Godet, 2020). This software was designed for constructing and visualizing graphs, and it's capable of connectivity analysis and links to external data (https://sourcesup.renater.fr/www/graphab/en/home.html - last accessed 22/01/2023). Before launching operations in Graphab, we considered the characteristics of the 10 focal species. First, an affinity level between the species and each different land cover class was identified (Table

4.1). Different land cover types show different permeability depending on the mobility of the species passing through them (Cushman et al., 2012; Lechner & Lefroy, 2014).

Table 4.2: This table shows the characteristics of the 10 selected species, including land cover resistance values, dispersal ability, and home range. Land use codes from 11100 to 14200 refer to Urban Atlas 2018 while codes from 21000 to 51100 to Corine Land Cover 2018.

Urban Atlas + Corine Land Cover combined legend		*Martes foina*	*Martes martes*	*Felis silvestris*	*Hystrix cristata*	*Sciurus Vulgaris*	*Eliomys quercinus*	*Erinaceus europaeus*	*Glis glis*	*Mustela nivalis*	*Muscardinus avellanarius*
Animal home range (ha)		10	140	124	20	2	2	2	2	8	2
Animal dispersal threshold (m)		5000	10,000	150,000	2000	2000	2000	2000	2000	3400	2000
Land use code	**Land use description**	**Resistance values [1 = no resistance, 100 = very high resistance]**									
11100	Continuous Urban fabric (S.L. > 80%)	100	100	100	100	100	100	100	100	100	100
11210	Discontinuous Dense Urban Fabric (S.L. 50% - 80%)	100	100	100	100	100	100	100	100	100	100
11220	Discontinuous Medium Density Urban Fabric (S.L. 30% - 50%)	100	100	100	100	100	100	100	100	100	100
11230	Discontinuous Low-Density Urban Fabric (S.L. 10% - 30%)	100	100	100	100	100	100	100	100	100	100
11240	Discontinuous very Low-Density Urban Fabric (S.L. < 10%)	100	100	100	100	100	100	100	100	100	100
11300	Isolated Structures	100	100	100	100	100	50	50	50	100	100
12100	Industrial. Commercial, public, military and private units	100	100	100	100	100	100	100	100	100	100
12210	Fast transit roads and associated lands	100	100	100	100	100	100	100	100	100	100
12220	Other roads and associated lands	50	50	100	70	100	100	100	100	70	100
12230	Railways and associated lands	100	100	100	100	100	100	100	100	100	100
12300	Port areas	100	100	100	100	100	100	100	100	100	100
12400	Airports	100	100	100	100	100	100	100	100	100	100
13100	Mineral extraction and dumpsites	100	100	100	100	100	100	100	100	100	100
13300	Construction sites	100	100	100	100	100	100	100	100	100	100
13400	Land without current use	50	50	50	50	50	50	50	50	50	50
14100	Green urban areas	50	50	50	50	50	50	50	50	50	50
14200	Sport and leisure facilities	100	100	100	100	100	100	100	100	100	100
21000	Arable land	25	25	50	25	50	25	50	50	25	50
21100	Non-irrigated arable land	25	25	50	25	50	25	50	50	25	50
21200	Permanently irrigated land	25	25	50	25	50	25	50	50	25	50
22100	Vineyards	75	75	75	75	75	75	75	75	75	75
22200	Fruit trees and berry plantations	50	50	50	50	50	50	50	50	50	50
22300	Olive groves	50	50	50	50	50	50	50	50	50	50
23100	Pastures	25	25	50	25	50	25	50	50	25	50
24100	Annual crops associated with permanent crops	25	25	50	25	50	25	50	50	25	50

24200	Complex cultivation patterns	75	75	75	75	75	75	75	75	75	75
24300 *	Land principally occupied by agriculture, with significant areas of natural vegetation	1	1	1	1	1	1	1	1	1	1
31100 *	Broad-leaved forest	1	1	1	1	1	1	1	1	1	1
31200 *	Coniferous forest	1	1	1	1	1	1	1	1	1	1
31300 *	Mixed forest	1	1	1	1	1	1	1	1	1	1
32000 *	Scrub and/or herbaceous vegetation associations	1	1	1	1	1	1	1	1	1	1
32100 *	Natural grasslands	25	25	50	25	50	25	50	50	25	50
32200 *	Moors and heathlands	1	1	1	1	1	1	1	1	1	1
32300 *	Sclerophyllous vegetation	1	1	1	1	1	1	1	1	1	1
32400 *	Transitional woodland-shrub	1	1	1	1	1	1	1	1	1	1
33100	Beaches, dunes, sands	75	75	75	75	75	75	75	75	75	75
33300 *	Sparsely vegetated areas	25	25	50	25	50	25	50	50	25	50
33400	Burnt areas	50	50	50	50	50	50	50	50	50	50
42200	Salines	100	100	100	100	100	100	100	100	100	100
51100	Water courses	1	1	1	1	1	1	1	1	1	1

* Land use codes considered for patches.

As explained in Lumia et al. 2023, a slope factor was also considered in constructing the network. In particular, areas with a slope greater than 100% were excluded from being considered patches. In addition, the Graphab software allows through a function related to the following equation to consider slope when calculating corridors:

$$rfinal = r^*(1 + c \cdot p) \qquad [1]$$

In equation 1, p is the importance of slope, c is the weighting coefficient, r is the pixel resistance, and rfinal is the pixel resistance weighted by the slope (p). When c = 1, the resistance value is doubled for a slope of 10%, while if c = 10, the resistance is doubled for a slope of 100% (p = 1). Since in this work, we considered the value of the coefficient c to be 1, as the slope increases, the permeability decreases.

The input data processed in Graphab consisted of a categorized raster land cover map. The nodes of the graph (patches) correspond to land cover classes that we defined as optimal for the selected species. Next, we defined a threshold of 2000 m as the maximum according to two types of distance, Euclidean and minimum cost. In our case, we used the minimum-cost system, starting from the assignment of resistance values to each land-cover category ranging from 1, we used resistance values ranging from 1 (lowest impedance to movement) to 100 (barrier to movement). Subsequently, we identified 2000 meters as the valid dispersal distance to meet the minimum requirements of each of the species (Boitani et al. 2002, see also tab A1 as annex). Next, we defined a threshold of 2000 m as the maximum distance that each species can travel (Boitani et al., 2003; Santini et al., 2013; Jones et al., 2009). In fact, this is a distance that all ten species can walk (Tab. A1). At this point, the simulation will take place so that the animal can cross 2000 pixels still having resistance before stopping.

The simulation will take place so that the animal can cross 2000 pixels having resistance 1 before stopping. The software makes the animal move in such a way that starting from the first pixel, it always chooses the adjacent pixel with minimum cost. Its movement stops when the sum of the resistances of the crossed pixels equals the value of 2000 cost units. A species' maximum affinity (land cover with resistance = 1) to a particular land cover has been considered a possible habitat. The home range, defined here as the extent of land large enough to contain the resources necessary to complete the individual's life cycle (Boitani et al., 2003), was used to set a threshold of 2 ha for the inclusion of patches as nodes for the patch-based analyses since this value is suitable for all the selected species (Tab S1). That threshold was used for the inclusion of patches as nodes for the patch-based analyses. Only areas with a surface area greater than or equal to 2 ha were considered nodes in the graph network; remaining areas with an area less than 2 ha were only considered structural elements favorable to the passage of species.

For the identification of the dispersal distance, a crossing threshold was established for all focal species, understood as the maximum distance an animal is able to travel in a hostile environment to reach resources.

Starting from the 10 m x 10 m raster containing the land cover codes and minimum patch size, land cover resistance and maximum dispersal threshold, Graphab 2.6 was launched. It returns a series of nodes and arcs that are the graphic representation of patches and ecological corridors, respectively (Clauzel, et al., 2012a). We set up the software so that all the arcs between patches are potentially taken into account, even those that might intersect or partially overlap. This method was used, as it does not exclude any possible pathways and provides an initial linear representation of displacements, allowing for a realistic representation of ecological corridors (Godet & Clauzel, 2021).

Graphab was then used to calculate a number of graph-theoretical metrics at the node level. These indices characterize the network, quantifying its connectivity and identifying its elements of centrality (Céline Clauzel, et al., 2012b; Orjan Bodin & Santiago Saura, 2010; Pascual-Hortal

& Saura, 2006; Saura & Pascual-Hortal, 2007; Urban, J. D., Keitt, 2001). This was done by calculating the following metrics (Table 4.2): Integral Index of Connectivity (IIC), Betweenness Centrality (BC), Flux (F) and Probability of Connectivity (PC).

Table 4.2: Ecological, graph theory connectivity indices calculated in the present work.

Connectivity index	**Ecological meaning**	**Formula**	**Reference**
Integral Index of Connectivity (IIC)	The probability that individuals randomly located in the landscape within a patch can access each other. A higher value indicates greater connectivity	$\frac{\sum_{i=1}^{n}\sum_{j=1}^{n}\frac{a_i * a_j}{1+nl_{ij}}}{A_L^2}$	Freeman, (1977)
Betweenness Centrality (BC)	The sum of the shortest paths through the focal patch, each path being weighted by the product of the capacities of the connected patches and their probability of interaction.	$BC_i = \sum_i \sum_k a_j^\beta a_k^\beta e^{-ad_{jk}}$ $j,k \in \{1..n\}, k < j, i \in P_{jk}$	(Bodin & Saura, 2010)
Flux (F)	For the entire graph: sum of the potential dispersions of all patches.	$F = \sum_{i=1}^{n}\sum_{j=1}^{n} a_j^\beta e^{-ad_{ij}}$ j≠i	(Foltête, Clauzel, et al., 2012)
Probability of Connectivity (PC)	The probability that two random points in the landscape fall within interconnected habitat areas (i. e., reachable to each other). Values are between 0 and 1.	$PC = \frac{\sum_{j=1}^{n} a_i a_j p_{ij}^*}{A_L^2}$	(Saura & Pascual-Hortal, 2007)

4.1.3 UNICOR Implementation

Before launching UNICOR, following the same process used for Graphab, each pixel of the base map raster was assigned a resistance value to movement in a range from 1 (low resistance) to 100 (high resistance), with resistance values tending toward unity, indicating land cover with higher species affinity, lower resistance to species movement; values tending toward 100 indicate anthropogenically modified land-cover types, lower species affinity and higher resistance to movement.

UNICOR requires two input datasets for model implementation: a raster layer representing the landscape resistance surface containing the locations of source points of individuals. One of the major strengths of UNICOR connectivity modelling is the ability to specify biologically realistic dispersal thresholds, specified in cost units, at which the connectivity algorithms (factorial least cost path and resistant kernel) terminate their spread. It is essential for connectivity analyses to realistically reflect the functional dispersal capabilities of focal species, given that this, along with the density and distribution of source points, often dominates predictions of functional connectivity (e.g., Cushman et al., 2012). In our analyses, we evaluated a range of plausible biological capabilities (Diniz et al., 2020; Lechner et al., 2015; Savary et al., 2021).

Our UNICOR analyses considered both patch-based and synoptic frameworks. We better specify that the ‘‘Synoptic’’ word refers to a situation where the analysis framework compares a patch (or node) based approach in which connectivity is measured between the centroids of patches, and a synoptic approach in which connectivity is measured among a large number of source points that are distributed proportional to the extensiveness of highly suitable and low resistance habitat (e.g., many points in areas of low resistance, instead of a single point in the centroid of a patch of low resistance). The patch-based framework used the 320 centroids of patches used as nodes in the Graphab analysis. The number of 320 comes from the number of total patches obtained by applying our criteria, that is: land cover with maximum affinity for species (see tab A1); minimum area of polygons to be considered patches of 2 ah; slope lower than 100%. We ran factorial least cost path and resistant kernel analyses for these source points at three dispersal distances: 50k, 100k and 150k. For the synoptic approach, we used a network of 3243 source points that were probabilistically generated with density proportional to habitat suitability and used dispersal distances of 17k and 35k cost units for resistant kernel and factorial least cost path, respectively, reflecting the expected cost distance to traverse 2 km in geographic space (17k cost distance) or twice that for factorial least cost path analysis (it is common to use a larger threshold for factorial least cost path analysis as it is pairwise and requires twice the distance threshold for points to be linked by paths as points to be overlapping in resistant kernel analysis; e.g., Cushman et al., 2013, 2014). The value of 3243 was obtained by random assignment of a series of points but with a higher probability directly proportional to the suitability of the study area (inverted resistance values). The approach we used to obtain the points is based on a series of processes. We created a raster with the same extension as the land cover raster but with random pixel values between 0 and 0.75. Next, the resistance values we had attributed to land cover were converted to suitability and then rescaled, going from 1-100 to 0-1. Finally, we overlaid the two layers (the one with values from 0 to 0.75 and the one with values from 0 to 1) and performed a difference. Finally, one point was assigned for each pixel with a value greater than 0.

The values of 50k ,100k, 150k, 17k, and 35k (all expressed as meters) were taken to be applied to the two different approaches, synoptic and patch-based. Next lines we further specify in UNICOR, the simulation allows the movement simulation to be calculated based on an energy budget. Thus, there is a relationship between the residual energy of the animal (the hypothetical animal moving in the software simulation) and the number of steps remaining. However, the ability of the animal to move varies with the heterogeneity of the pixel matrix (land cover raster). Therefore, it is possible to obtain that the total energy value of the animal is the sum given by the formula step*cost. This is directly related to dispersal capacity, the expected dispersal distance in steps (mean cost of resistance surface * the number of steps in the path) = energy budget, or number of steps = energy budget / mean cost of resistance surface. So, given the mean resistance value of the matrix that is 85, the value of 2 km (the value we have identified in the literature as being reachable by all the considered species) is equivalent to an energy budget of 17k. This is due to the mean resistance of 85 and pixel size of 10. Then, a 2 km distance will equal 85 average cost units per pixel * 200 pixels in 2km = 17k cost units for 2km. We used this value twice for the factorial least cost path, so we have the 35k value. This is because it has been proved that twice the dispersal distance is needed to connect two points by factorial least cost path to have kernels overlapping in resistant kernel analysis (Cushman et al., 2013).

4.1.4. PCA, Hierarchical Agglomerative Clustering and Mantel testing of hypotheses

The analyses described above produced 12 scenarios of predicted connectivity for comparison. These included: patch-based approach for factorial least cost path and resistant kernel connectivity, using 50k, 100k and 150k dispersal thresholds (p50k, p100k, p150k, k50, k100 and k150 respectively), the connectivity metrics BC, F, PC and IIC produced on these same source point nodes; synoptic analyses using source points synoptically distributed across the study area proportionally to habitat suitability to seed factorial least cost path 35k (sp35k) and resistant kernel 17k (sk17).

We proposed 4 main hypotheses of relationship among the 12 different scenarios. These were: (1) thresh – that methods using a similar dispersal distance threshold would be more similar in their predicted connectivity than methods using different thresholds, (2) synoptic – that scenarios using a synoptic framework would be more similar to each other than to scenarios that used a patch-based framework, (3) kernel-path-graph – that kernel methods would be more similar to each other in predicted connectivity than to path methods or graph methods and the converse, (4) UNICOR-graph – that connectivity methods using UNICOR approaches would produce connectivity results more similar to each other than to graph metrics and the converse.

We used Mantel testing with model matrices (Legendre, 1998), which is a form of multivariate, distance-based analysis of variance. We tested the four main hypotheses above and the additive combination of the various model matrices to test for joint support of multiple hypotheses

simultaneously (e.g., Kyaw et al., 2021). Thus, we used the Mantel test to identify the correlation between the 4 hypotheses and 14 different combinations of them (Tab. 4.4).
In addition to the hypothesis testing with Mantel model matrix analysis, we used two well-known multivariate analysis methods to compare the 12 scenarios. Specifically, we used Principal Component Analysis (PCA) and hierarchical agglomerative clustering analysis on the 12 scenarios and visually compared the results in reference to the Mantel hypothesis testing. The PCA was conducted on the correlation matrix and the hierarchical clustering was conducted using the Ward's fusion distance method in the 'hclus' function in R.

4.2. Results

In table 4.3, we present the description of the 12 scenarios In table 4.4, we can see summarized the values for the standard deviation, proportion of variance and cumulative proportion of variance from the principal components analysis applied to the results from the 12 different scenarios. We present three sets of results in comparing these scenarios. First, we present the results of the principal components analysis, which describes the multivariate relationships among scenarios in an ordination framework (McGarigal et al., 2000). Second, we present results from agglomerative hierarchical clustering, which presents the multivariate relationships in a hierarchical relationship. Finally, we present the results of the hypothesis testing of the 14 a priori hypotheses of the expected relationship among the 12 scenarios using Mantel testing on model matrices (Legendre and Legendre, 1998).

Table 4.3: Description of the 12 connectivity scenarios compared in this analysis.

Scenario Acronym	**Scenario Description**
p50k	Patch-centroid-based factorial least cost path with 50,000 cost unit threshold
p100k	Patch-centroid-based factorial least cost path with 100,000 cost unit threshold
p150k	Patch-centroid-based factorial least cost path with 150,000 cost unit threshold
k50k	Patch-centroid based factorial resistant kernel with 50,000 cost unit threshold
k100k	Patch-centroid based factorial resistant kernel with 100,000 cost unit threshold
k150k	Patch-centroid based factorial resistant kernel with 150,000 cost unit threshold
sp35k	Synoptic factorial least cost path with 35,000 cost unit threshold
sp17k	Synoptic factorial least cost path with 17,000 cost unit threshold
IIC	Patch-centroid-based graph theory metric Integral Index of Connectivity
PC	Patch-centroid-based graph theory metric Probability of Connectivity

F	Patch-centroid-based graph theory metric Flux
BC	Patch-centroid-based graph theory metric Betweenness Centrality

The response variables being compared, presented in following paragraphs, were the surfaces of predicted connectivity for each of the different methods, scopes of analysis, etc. The analysis compares those surfaces based on how similar they are in their values of predicted connectivity and assesses how much that similarity is related to different attributes of the method and scope of analysis.

4.2.1. Principal Component Analysis

The principal component analysis revealed that variance among the connectivity scenarios was relatively well concentrated on a few independent orthogonal dimensions (Table 4.4). Specifically, about 38% of the variance among connectivity predictions was captured by the first PC and 63.5% by the first two.

Table 4.4: Values of standard deviation, proportion of variance and cumulative proportion for the 12 scenarios (PC1,...PC12).

Importance of components	**PC1**	**PC2**	**PC3**	**PC4**	**PC5**	**PC6**
Standard deviation	2,1235	1,7633	1,1445	1,01538	0,83504	0.69050
Proportion of Variance	0.3758	0.2591	0.1092	0.08592	0.05811	0.03973
Cumulative Proportion	0.3758	0.6349	0.7440	0.82995	0.88806	0.92779
//	**PC7**	**PC8**	**PC9**	**PC10**	**PC11**	**PC12**
Standard deviation	0.66373	0.54153	0.28398	0.21220	0.06356	0.05454
Proportion of Variance	0.03671	0.02444	0.00672	0.00375	0.00034	0.00025
Cumulative Proportion	0.96450	0.98894	0.99566	0.99942	0.99975	1.00000

The correlation matrix (Table 4.5) shows that the highest correlations were between the different dispersal distance thresholds among kernel and path analyses, with higher values of correlation found for correlations between p100k-p150k (0.99) and k100k-k150k (0.99). The next highest correlations were found between the patch-based path and the patch-based kernel (e.g., path with path and kernel with kernel) with values ranging from 0.92 to 0.99. The synoptic path is relatively highly correlated with the patch-based path (0.71, 0.65, 0.62). Likewise, the synoptic kernel is relatively highly correlated with the patch-based kernel (0.77, 0.59, 0.55). The metric IIC is not highly correlated with any path or kernel analyses (most correlated with the synoptic kernel, 0.28). The metric PC is not highly correlated with any of the kernel or path values except the synoptic kernel (0.41). The metric F is highly correlated with the synoptic kernel (0.62). The metric BC is also correlated with the synoptic kernel (0.45).

Table 4.5: Correlation matrix of the 12 different scenarios. In red values > 0.9, yellow 0.9>x>0.8, dark green 0.8>x>0.7 and light green 0.7>x>0.6.

	p50k	**p100k**	**p150k**	**k50k**	**k100k**	**k150k**	**sp35k**	**sk17k**	**IIC**	**PC**	**F**	**BC**
p50k	**1**	0.96	0.92	0.22	0.21	0.2	0.71	0.15	0.09	0.05	0.15	0.06
p100k	0.96	**1**	0.99	0.08	0.08	0.08	0.65	0.07	0.06	0.01	0.11	0.03
p150k	0.92	0.99	**1**	0.03	0.02	0.03	0.62	0.05	0.04	0	0.09	0.02
k50k	0.22	0.08	0.03	**1**	0.93	0.88	0.26	0.77	0.24	0.34	0.48	0.29
k100k	0.21	0.08	0.02	0.93	**1**	0.99	0.21	0.59	0.2	0.29	0.37	0.23
k150k	0.2	0.08	0.03	0.88	0.99	**1**	0.2	0.55	0.19	0.27	0.35	0.21
sp35k	0.71	0.65	0.62	0.26	0.21	0.2	**1**	0.28	0.12	0.11	0.22	0.13
sk17k	0.15	0.07	0.05	0.77	0.59	0.55	0.28	**1**	0.28	0.41	0.62	0.45
IIC	0.09	0.06	0.04	0.24	0.2	0.19	0.12	0.28	**1**	0.52	0.19	0.13
PC	0.05	0.01	0	0.34	0.29	0.27	0.11	0.41	0.52	**1**	0.23	0.21
F	0.15	0.11	0.09	0.48	0.37	0.35	0.22	0.62	0.19	0.23	**1**	0.29
BC	0.06	0.03	0.02	0.29	0.23	0.21	0.13	0.45	0.13	0.21	0.29	**1**

The PCA analysis show three things: (1) most importantly, the graph-theoretical metrics were all highly related to the resistant kernel metrics (in Fig. 4.3, the vectors in blue were relatively parallel for these), (2) the factorial least cost path metrics were all quite different from the kernel and the graph-theoretical metrics (blue vectors for those were almost perpendicular toward the top from the kernel and graph-theoretical metrics), (3) the synoptic models (sk17 and sp34; e.g., UNICOR with many sources points proportional to suitability across the landscape instead of the centroid of the patches) were highly correlated with the patch-centric approach (e.g., highly parallel to the vectors).

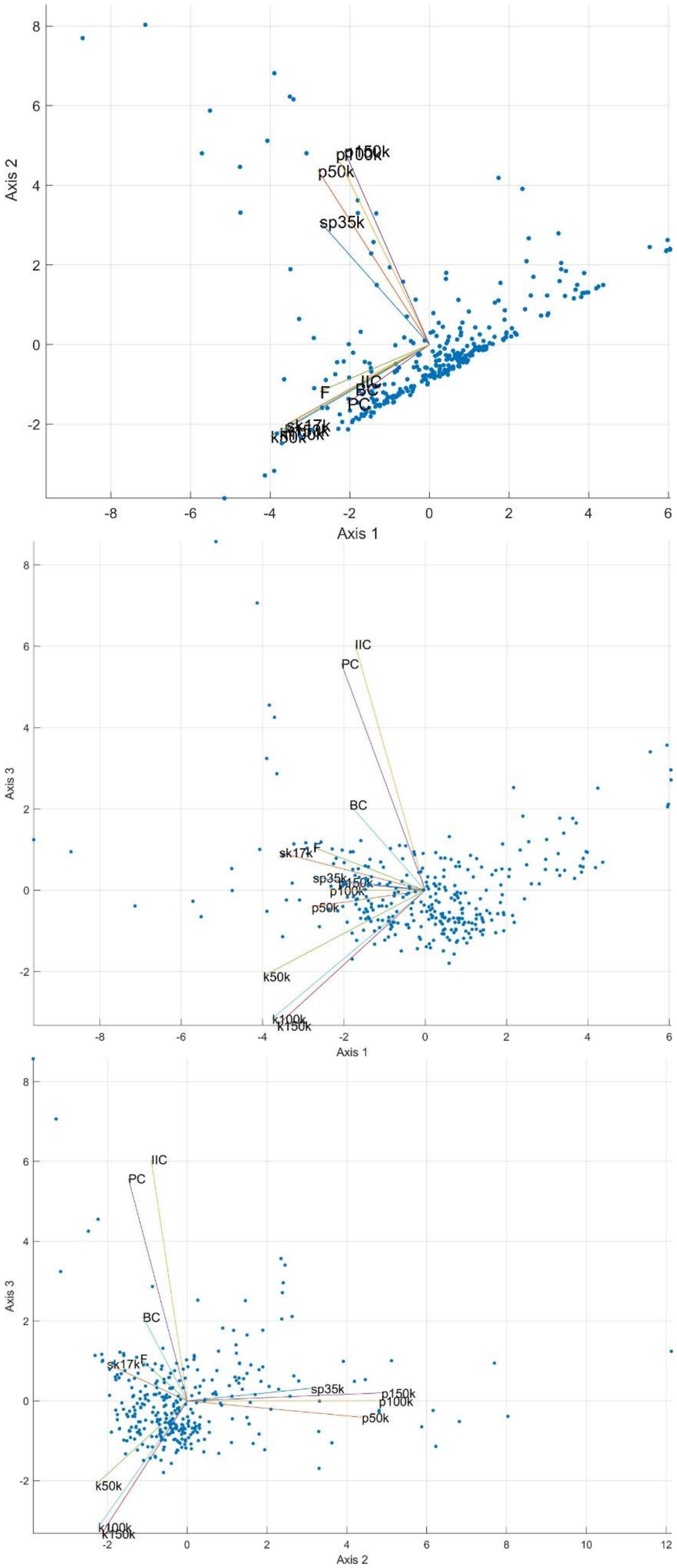

Figure 4.3: Biplot of the PCA analysis, a) Axis 1 vs Axis 2, b) Axis 1 vs Axis 3, c) Axis 2 vs Axis 3.

4.2.2. Hierarchical Agglomerative Clustering

The hierarchical clustering (Fig. 4.4) show the same general relationships as the PCA in a slightly different way. Specifically, the hierarchical clustering shows that: (1) the path analyses were all clustered separately (to the left of the diagram), (2) the kernel analyses were clustered together to the right, with the metric F most similar to the synoptic kernel. The other graph-theoretical metrics were clustered (IIC, PC, BC) and relatively similar to the kernel analyses.

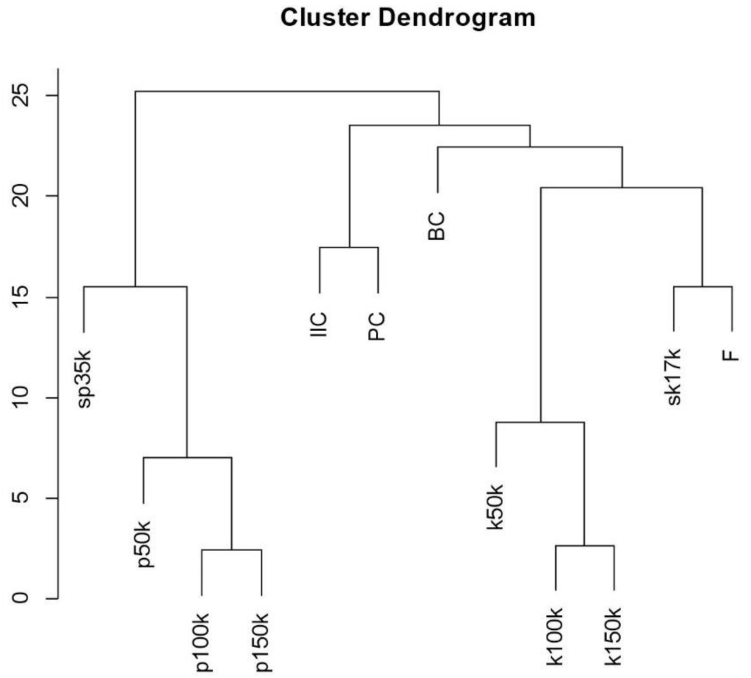

Figure 4.4: Clustering dendrogram of the 12 scenarios.

4.2.3. Mantel testing of hypotheses

Based on a significance level of 0.05 (p-value), 12 of the 14 hypotheses were supported. In Table 4.6, we order these hypotheses based on the strength of their Mantel r value. Hypothesis 3, which tests for differences among kernel, path, and graph theory methods, combining other factors (dispersal distance, patch-based vs. synoptic), has the strongest correlation value with an r of -0.711. The next highest support was for H6, which is a combination of kernel_path_graph and dispersal threshold effects. The fact that this combined hypothesis is less supported (r-value ~ 0.18 lower in magnitude) suggests that adding the effect of dispersal threshold to the effect of the analysis method reduces the ability to explain the differences in the connectivity results. Likewise, the next set of most supported hypotheses combines the method (kernel_path_graph) with other factors such as synoptic or the combination of synoptic and threshold. The reduced support of these combined hypotheses suggests that the method is the dominant driver of differences in predictions and threshold and synoptic vs. patch-based source points have relatively small influence. The least support of all hypotheses was for H2, synoptic vs patch-based source points. Furthermore, the 4 hypotheses with the lowest support in addition to H2 were composite hypotheses containing H2, suggesting that synoptic vs. patch-based analysis has the least influence on the difference in connectivity results.

Table 4.6: 14 different correlation hypotheses (in red the most interesting values).

Hypotheses n°			**r**	**P**
h3	kernel_path_graph	3	-0.71196	0.001
h6	thresh_kernel_path_graph	13	-0.57854	0.001
h10	kernel_path_graph_unicor_graph	34	-0.57773	0.002
h13	synoptic_kernel_path_graph_unicor_graph	234	-0.45688	0.005
h11	thresh_synoptic_kernel_path_graph	123	-0.43879	0.003
h14	thresh_synoptic_kernel_path_graph_synoptic_unicor_graph	1234	-0.43182	0.007
h8	synoptic_kernel_path_graph	23	-0.40205	0.002
h4	unicor_graph	4	-0.34138	0.006
h7	thresh_unicor_graph	14	-0.33068	0.019
h1	Thresh	1	-0.31747	0.021
h12	thresh_syoptic_unicor_graph	124	-0.24275	0.033
h9	synoptic_unicor_graph	24	-0.16499	0.082
h5	threst_synoptic	12	-0.11937	0.162
h2	Synoptic	2	0.141494	0.18

4.3. Discussion

The PCA, clustering and correlation analyses all generally supported the same conclusions. Namely, least cost path methods were different in their predictions and clustered and ordinated separately from other methods. Surprisingly, kernel and graph-theoretical metrics were generally closely aligned, particularly the synoptic kernel with the Flux parameter (F). Notably, dispersal threshold and synoptic vs. patch-based parameters did not appear to strongly separate results, which were highly aligned with the analysis method. This suggests that overall patterns of the connectivity prediction were relatively insensitive to changes in dispersal ability, at least across the range (50,000 to 150,000 cost units) evaluated in this study. Similarly, the multivariate results and correlation analysis show minimal relative effect of using patch-centric source points vs synoptic source points. The results suggest that resistant kernel predictions were highly consistent with the graph-theoretical metrics but were superior in that the resistant kernel produces predictions synoptically (for all locations) rather than just the centroid of the cells (Cushman et al., 2013; Unnithan Kumar & Cushman, 2022). The kernel analysis based on the centroids is similar to the synoptic kernel. However, the synoptic kernel is better since it considers biologically realistic dispersal ability and the correct distribution and density of source points (Cushman et al., 2013).

Analysing the results of Mantel testing of hypotheses, we found that the highest support was for H3, suggesting that the largest difference among connectivity predictions is related to the method of analysis, with kernel, path and graph theory approaches being different from each other.

The second most supported hypothesis was the H6, where we combined the kernel_path_graph hypothesis (H3) and the dispersal threshold hypothesis. The dispersal threshold hypothesis proposes that the dispersal distance used in the analysis is the main factor affecting the difference in results, whereas methods (kernel, path, graph theory) and framework (patch-based vs. synoptic) were not influential. The combination of these two hypotheses asks if the method (kernel, path, graph theory) and dispersal distance were both important. Observing substantially lower support for this joint hypothesis than for H3 confirms that the method of analysis is the dominant driver of differences and dispersal threshold is relatively less impactful.

The third most highly supported hypothesis was H10, where we combined H3 and H4. This gives relatively more similarity weight to UNICOR methods compared to graph theory methods but still discriminates between kernel and least cost path approaches. The lower Mantel r value for this hypothesis compared to H3 suggests that the dominant difference is between kernel, path and graph theory metrics and that adding additional similarity weight for path and kernel vs graph theory metrics did not improve the explanation of the differences in predictions.

The fourth most supported hypothesis was H13, similar to the third, except adding the additional factor of synoptic vs. patch-based source points. This resulted in a substantial decrease in the Mantel r value, suggesting adding the effect of synoptic vs. patch-based source points to the model matrix decreased the ability to explain differences in prediction. This, along with the observation that the pure synoptic vs patch-based hypothesis (H2) is the least supported of all hypotheses and is not statistically related to differences in connectivity predictions, suggests that synoptic vs. patch-based methods were relatively similar compared to the differences in results caused by other factors, particularly method (H3). Similarly, the fourth most supported hypothesis was the same as the first (H3), except including the additive model matrix effects of synoptic vs patch-based and dispersal threshold. The observation that this hypothesis was substantially less supported than the pure method hypothesis (H3) suggests that adding the influences of dispersal threshold and synoptic vs. patch-based analysis decreases the ability to statistically explain the differences among connectivity predictions. Considering the 7 most supported hypotheses were those in which H3 is present alone or in combination with other hypotheses, we have further confirmation that differences among connectivity results were dominated by the analysis method.

All four testing methods (correlation matrix, PCA, hierarchical clustering, model matrix, Mantel hypothesis testing) corroborate the same major interpretation. The analysis method (in our case, least cost path, resistant kernel and graph theory metrics) dominates differences in connectivity predictions. The least cost path methods produce a tight cluster or cloud in ordination space and were different in prediction than the other methods. Conversely, resistant kernel and graph theory metrics were generally highly congruent, notably the synoptic kernel and the Flux parameter (F) from graph theory.

Importantly, our results clearly show that the dispersal threshold and density and distribution of source points have much less relative influence than the analysis method. This is very interesting, given that other studies, e.g., Cushman et al. (2012), found large differences in predictions produced by a given method (e.g., resistant kernels) based on dispersal threshold and density and distribution of source points. The discrepancy in these results is likely because this previous study compared results for a particular method (such as least cost path or resistant kernel) while varying dispersal threshold and source point density and distribution. Thise previous papers showed substantial effects of dispersal ability and source point density but did not formally compare the relative effects of different methods. Our study is novel in combining evaluation of all these factors as main effects and in interaction. Our novel finding is that analysis methods, in particular least cost path, kernel and graph theory approaches, produce dramatically different predictions whose divergence dwarfs the effects caused by differences in dispersal threshold or the density and distribution of source points.

Given the predominant effect of the method and the observation that kernel and graph theory methods group together in clustering and ordination space, our results suggest that resistant kernel might be the preferred approach among those we evaluated. We conclude this partly based on the recent study by Unnithan Kumar et al. (2022), who showed, using a large simulation factorial experiment, that resistant kernel predictions had the highest similarity to movement patterns for a wide range of hypothetical organisms following a broad combination of movement rules. The similarity of the kernel and graph theory methods suggests that both approaches were likely robust. However, the resistant kernel is preferred in most cases as the graph theory approach generally produces predictions only for a smaller sample of nodes or centroids of patches. In contrast, the resistant kernel approach produces a fully synoptic prediction of movement density (incidence function, (Kaszta et al., 2020) across the full landscape. This provides a rich, spatially explicit mapping of movement patterns and density which allows the delineation of core areas, identification of barriers and prioritization of corridors (Cushman et al., 2016, 2018; Cushman & Landguth, 2012; Kaszta et al., 2018, 2021; Macdonald et al., 2019).

4.4. Conclusions

In this chapter of the PhD thesis was studied the relationships between several different methods, parameterizations and metrics by which assessments of landscape connectivity were commonly made in the literature. In particular, was studied how connectivity predictions were influenced by different analysis methods, dispersal thresholds and spatial frameworks for delineating source points. It was clarified that what most influences predictions is the method of analysis. Specifically, was found that resistant kernel-based analysis seems to be the most suitable to represent movement patterns. This study provided expanded knowledge regarding differences and similarities in the predictions of commonly used approaches in landscape connectivity by demonstrating through statistical analyses (PCA, clustering, Mantel test of hypotheses) how strong relationships exist between some of them and major differences between others. While highlighting which variables most influence connectivity predictions, our analysis did not indicate the best methods for predicting functional connectivity to delineate corridors or the ideal network configuration. In those cases, species-related factors such as energy (Movement simulation where the animal moves randomly until it runs out of energy), attraction (Movement simulation where the animal moves non-randomly and follows the path of least resistance) and risk (Movement simulation where the animal has an increasing probability of stopping its movement by crossing more and more pixels with resistance values) should be taken into account to identify what is the best configuration of the method, dispersal threshold and spatial framework so as to be able to provide a tool to the intervention planner. Future research should explore the functional performance of these and other connectivity methods in predicting functional connectivity.

5 Comparison of connectivity metrics and predictive models of movements

Adapted from

Lumia G., Modica G., Cushman S.: **Using simulation modelling to demonstrate the performance of graph theory metrics and connectivity algorithms.** https://doi.org/10.1016/j.jenvman.2024.120073.

Journal of Environmental Management 352 (2024) 120073

Contents lists available at ScienceDirect

Journal of Environmental Management

journal homepage: www.elsevier.com/locate/jenvman

ELSEVIER

Research article

Using simulation modeling to demonstrate the performance of graph theory metrics and connectivity algorithms

Giovanni Lumia [a], Giuseppe Modica [b,*], Samuel Cushman [c]

[a] *Dipartimento di Agraria, Università degli studi 'Mediterranea' di Reggio Calabria, 89122 - Reggio Calabria, Italy*
[b] *Dipartimento di Scienze Veterinarie, Università degli studi di Messina, 98168 - Messina, Italy*
[c] *Wildlife Conservation Research Unit, Department of Biology, University of Oxford, The Recanati-Kaplan Centre, Tubney House, Oxon, Tubney, OX13 5QL, United Kingdom*

A R T I C L E I N F O

Handling Editor: Jason Michael Evans

Keywords:
Ecological networks (EN)
Landscape connectivity
Animal dispersal
Patch or synoptic-based source point
Simulated and predicted movement density
Graph theory connectivity algorithms

A B S T R A C T

Models and metrics to measure ecological connectivity are now well-developed and widely used in research and applications to mitigate the ecological impacts of climate change and anthropogenic habitat loss. Despite the prevalent application of connectivity models, however, relatively little is known about the performance of these methods in predicting functional connectivity patterns and organism movement.

Our goal in this paper was to compare different connectivity models in their abilities to predict a wide range of simulated animal movement patterns. We used the Pathwalker software to evaluate the performance of several connectivity model predictions based on graph theory, resistant kernels, and factorial least-cost paths. In addition, we assessed the efficacy of synoptic and patch-based approaches to defining source points for analysis. In total, we produced 28 different simulations of animal movement.

As we expected, we found that the choice of connectivity model used was the variable that most influenced prediction accuracy. Moreover, we found that the resistant kernels approach consistently provided the strongest correlations to the simulated underlying movement processes. The results also suggested that the agent-based simulation approach itself can often be the best analytical framework to map functional connectivity for ecological research and conservation applications, given its biological realism and flexibility to implement combinations of movement mechanism, dispersal threshold, directional bias, destination bias and spatial composition of source locations for analysis. In doing so, we provide novel insights to guide future functional connectivity analyses. In future research, we could use the same model for several different species groups and see how this reliability depends on the species analyzed. This could bring to light other elements that play an essential role in predicting connectivity.

One of the topics receiving the most recent attention in the ecological networks research area is functional connectivity modelling (S. A. Cushman, Lewis, et al., 2013; A. Rudnick et al., 2012; Tischendorf & Fahrig, 2000), which is widely used to identify the most important areas for conservation planning. The scholarly literature has a long record of recruiting and evaluating different methods to predict, map, and assess population connectivity. The well-established methods in this field typically use algorithms like graph theory (Saura & Pascual-Hortal, 2007), resistant kernels (Compton et al., 2007), factorial least-cost paths (Cushman et al., 2009), and circuit theory (Foltête, Clauzel, et al., 2012; Kaszta et al., 2018a; Kumar et al., n.d.-a; McRae et al., 2008).

Using simulation modelling to produce the implications of different pattern-process relationships is a cornerstone of landscape ecology science (Turner, 1989). Simulation is widely used, for example, in landscape genetics to explore methodological and theoretical questions (e.g., CDPOP (S. A. Cushman et al., 2018; S. A. Cushman & Landguth, 2012; Landguth & Cushman, 2010; Shirk et al., 2018). However, there have been few simulation studies to explore and understand the factors that drive animal movement and the performance of different connectivity modelling approaches (see Unnithan Kumar et al., 2022).

Recently, Unnithan Kumar et al. (2022) developed a new agent-based movement simulation model that considers the landscape's local resistance, the energetic cost of movement, directional bias towards a destination, autocorrelation, scale effects, and mortality risk. This new model, called Pathwalker (Unnithan Kumar et al., 2021), has proven to be highly versatile; its ability to implement a broad range of different processes and their interactions in governing movement provides the opportunity to compare different models to gain important new information about their performance relative to known driving relationships. Pathwalker is designed to simulate movement paths across heterogeneous landscapes and offers predictions for movement density and landscape connectivity. It runs by a command line and requires Python 3, together with the basic NumPy and matplotlib packages.

Our goal was to apply the simulation paradigm to evaluate the performance of various widely used connectivity algorithms and different analytical frameworks (patch-based vs. synoptic). The synoptic connectivity modelling approach seeks to produce spatially explicit predictions of movement rates for every location across the landscape rather than for a few source or destination patches (as in the patch-based approach (Khosravi et al., 2018)). Were simulated seven different movement mechanisms in Pathwalker software: energy, attraction, risk, energy-attraction, energy-risk, attraction-risk, and energy-attraction-risk. Starting from these seven mechanisms, it was launched a series of 28 simulations combining different dispersal path lengths, path correlation, and source point configurations. Then, the predictions of the resistant kernels were compared, factorial least-cost paths, and graph theory connectivity modelling algorithms to these simulated movements. Considering the results of past research on related topics (Cushman et al., 2014, 2013, Unnithan Kumar & Cushman, 2022, Zeller et al., 2018), it we expected to find that, among the parameters varied in the simulation analysis, the choice of connectivity method would have the most significant impact on prediction accuracy, and that resistant kernel algorithms would have the highest correlation to simulated movement patterns (following Unnithan Kumar & Cushman, 2022).

5.1. Materials and Methods

An implementation of three major steps of analysis were carried out: (1) development of a resistance surface and landscape map for modelling the movement of species across space; (2) connectivity calculation according to three different model predictions and calculation of 28 simulation patterns of animal movement in Pathwalker software; (3) comparison of the connectivity metrics of the three models to the 28 simulated patterns of animal movement produced by the agent-based movement model Pathwalker (Github, last access 24/03/2023 - https://github.com/siddharth-unnithankumar/pathwalker).

5.1.2. Base data

The study area for these analyses was a region of 47,822.63 ha in Calabria (southern Italy, fig. 5.1). A datasets provided by the European Union were used (Urban Atlas and Corine Land Cover) as base data. In brief, CLC and UA for 2018 were merged (most recent data available on 03.03.2023 link: https: // land.copernicus.eu) to obtain the highest level of detail for both urban areas and natural and semi-natural areas. See Lumia et al. (2023a) for more details on the study area and the base data preparation.

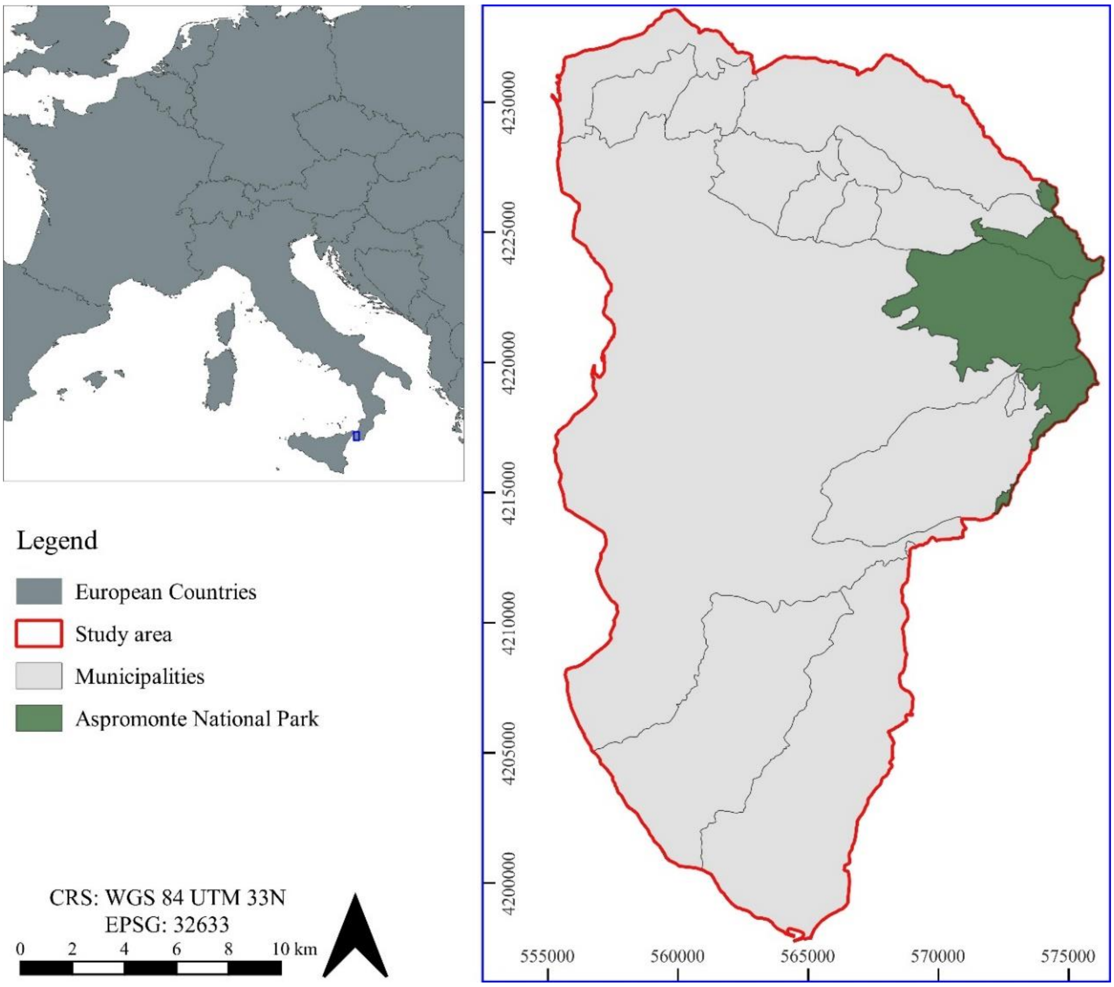

Figure 5.2: In red are the boundaries of the study area, in green is the border of the Aspromonte National Park, which partially falls within the study area.

For focal species, was selected a set of 10 small and medium-sized mammals that serve as umbrella species in a multispecies approach (Clauzel & Godet, 2020; Ersoy et al., 2019; Lechner & Lefroy, 2014; Opdam et al., 2006). The species were chosen considering past studies in the area (Modica et al., 2021; Lumia et al. 2023), paying particular attention to those protected by regional, national, and international laws (species list and laws protecting them, Tab. 2.1). However, there is a fundamental difference between these cited works, which aimed to identify a strategy to build a multi-species ecological network, and the work presented here. The construction of a multi-species ecological network is not the centre of gravity of this work. Therefore, it was not intended to use parameters that were directly referable to any particular species of the study area. What were done was to exploit the data on the 10 species to model one hypothetical species that had characteristics in the middle of the range of these 10 species, which provides a measure of the central tendency of connectivity across life history space. With this approach, the hypothetical specie was used as a model for all subsequent tests.

Data referring to the autecological characteristics of the species were obtained from the database produced by Boitani et al. (2002), which contains valuable information referring to: the maximum dispersal distance of each species moving in search of resources, the home range (minimum and maximum optimum values) and the level of affinity of the species with different land uses (Fichera et al., 2015; Modica et al., 2021; Lumia et al., 2023a; 2023b). Different weights were given to different infrastructures in terms of resistance to animal movement. Particularly, in the study area, the infrastructures are divided into: Fast transit roads and associated land (code 12210 Urban Athlas); Other roads and associated land (code 12220 Urban Athlas); Railways and associated land (code 12230 Urban Athlas).

5.1.3. Pathwalker simulations

It was applied a simulation framework to evaluate the predictions of the different analytical approaches and connectivity models against a range of known pattern-process relationships implemented in the Pathwalker agent-based model (Unnithan Kumar et al., 2022a). Pathwalker is designed to simulate animal movements using a relatively low number of inputs. It uses resistance surfaces in its calculations, as other models do (McRae et al. 2008; Landguth et al. 2011; Foltête et al. 2021; Unnithan Kumar et al. 2021a), but its algorithm takes into account parameters such as energy, attraction, risk, different autocorrelation thresholds, and movements directed to a destination (Unnithan Kumar et al., 2022a). In addition, Pathwalker takes into account the response of simulations at a multi-scale level on a given resistance surface. The algorithm calculates a set of paths by allowing the movement mechanisms to be functions of landscape resistance at different spatial extents around a focal point; density maps can obtained by aggregating these paths. In addition, Pathwalker was designed explicitly to operate in contexts similar to those in which models such as Circuitscape or models based on factorial least-cost paths and resistance kernels operate and thus be used to test the performance of these models, as was demonstrated in Unnithan Kumar et al., 2022b. Our analysis framework used the Pathwalker agent-based simulation model to produce a large number of instances of organism movement across the study area based on a range of parameters that then were compared to the predictions of graph theory, resistant kernel and factorial least cost path connectivity models. Various statistical analysis strategies were used such as analysis of variance and measured the levels of correlation between the models.

Using Pathwalker, were simulated movement patterns as a function of 7 different mechanisms (summarized in Table 5.1), which reflect different functional responses of movement to landscape resistance.

Table 5.1: Pathwalker's seven-movement simulation mechanisms summary.

Mechanism n°	Mechanism meaning
1	Energy: The random walk is unbiased, but the cumulative cost of movement across the resistance surface is measured, and the walk ends when a specified total cost has been reached.
2	Attraction: The walk responds probabilistically to the resistance surface values, with movement biased towards areas of lower resistance.
3	Risk: The random walk is unbiased but has a chance of ending at each tile, with a higher chance of ending at tiles with higher risk values (which are either derived from the resistance surface or provided by a separate risk surface).
4	Combination of energy + attraction
5	Combination of energy + risk
6	Combination of attraction + risk
7	Combination of energy + attraction + risk

As for the mechanism, 1 energy, it simulates the movement of an animal in an unfamiliar area, exploring.

When an animal is searching for resources, it is exploring a new area to find resources; therefore, it moves through the territory in a completely random manner. By choosing a path with little affinity, it will continue to expend energy until it runs out without achieving its goal. The mechanism simulates a probability based on the maximum dispersal distance an animal tends to reach during dispersal. Consider, for example, a dispersal distance of 2 km (as in our case) ascribed by wildlife expert (Boitani et al. 2003). The energy cap that was used is that which is required on average in our pixel matrix to travel 2 km (considering the distribution of resistances in the matrix). When the energy cap is reached, the animal's movement stops, indicating that, considering that the animal has expended energy and has not satisfied its needs (i.e., eating), it chooses to stop exploring and return to the area of origin.

Mechanism2, attraction, on the other hand, considers whether an animal can distinguish which way is more convenient and, therefore, has the capacity to perceive convenience or danger. In this case, the movement will still be random, but the walker's choice to continue in a less costly direction will be more likely.

The correlation factor, on the other hand, takes into account whether the animal tends to be more or less habituated, i.e., to follow the same path.

Mechanism 3 is risk; it takes into account the increasing danger of death that an animal has by walking through certain areas rather than others. The walker who walks, for example, 2 m along a road will have a low probability of stopping his movement and thus dying. The walker who instead follows the path of the road for kilometres will have an increasing road kill probability. Risk can be derived from the resistance surface or provided by a separate risk surface; in this analysis, were used the resistance surface to provide the risk values. In fact, the concept of using risk only for certain spatial elements was criticized in Kumar. et al. 2022. In particular, a limitation in the approach used by standard connectivity models such as Circuitscape, resistant kernels, and factorial least-cost paths was highlighted. These do not account for many key drivers of animal movement. In addition, they consider the mortality risk to remain unchanged through different regions of the landscape and movement choice to occur at a single spatial scale. Therefore, the decision to use resistance as a risk surface comes from the need to consider this factor in any region of our examination area The remaining four mechanisms implement different combinations of the first 3 to implement more complex kinds of movement resulting from multiple mechanisms acting simultaneously. Specifically, mechanism 4 is a combination of energy and attraction, mechanism 5 is a combination of energy and risk, mechanism 6 of attraction and risk, and mechanism 7 of energy, attraction and risk. The possibility of combining these mechanisms with each other is a major strength of this work, it allows simulation of movement based on resistance, energy (distance limited by cost but not direction) and risk (mortality risk is spatially explicit). All three are likely to affect real animal movement and being able to model each and in combination is a major advantage of the Pathwalker model and a strength of the simulation experiment presented here.

These seven mechanisms were used to conduct the simulations, but were considered three other factors before launching the process. The first is the distribution of source points. Were simulated all mechanisms using the 320 points identified by Graphab (patch-based approach) and the 3640 that were probabilistically generated with density proportional to habitat suitability (synoptic approach).

The second element were taken into account was directionality (Unnithan Kumar et al., 2022a). In particular, Pathwalker provides an autocorrelation parameter for determining the directional bias of the movement. This parameter ranges from 0 to 1 and is a factor that determines the tendency of the simulation's walker to continue along its present direction. The default value is 0, an uncorrelated random walk. Suppose we increase the value of the autocorrelation parameter. In that case, our walk becomes more correlated, with the extreme case of autocorrelation = 1 resulting in a straight line (a path in which the walker continues in the same direction). We used 0 and 0.25 as autocorrelation values for our simulations. In this case, since we have an autocorrelation value = 0.25, the nine movement probabilities are scaled to sum to 1 − 0.25 =0.75 instead of calculating to 1, and there will now be an added probability of 0.25 for continuing in the same direction as the previous step. Changing this parameter has an effect on the distance travelled, we bring as an example the results of the Pathwalker simulation launched on mechanism 1 with an energy value of 100,000 for both scenarios of 0 and 0.25 autocorrelation values. We obtained that in the simulation with a 0.25 autocorrelation value, the distance travelled is 3198.08 ha, superior to the simulation with a 0-autocorrelation value. This is expected considering that the higher the autocorrelation value, the greater the chance that the animal will cover a route that is not the shortest (the one with the lowest cost) in its movements. Were therefore concluded that increasing the autocorrelation factor affects the distance covered, leading to an increase.

The third element were considered was the energy factor, which refers to the total used energy accumulated from the walk in the simulation. Were used 100,000 and 1,000,000 as energy values. Energy is only for one of the mechanisms. This combination of mechanisms, directionality and energy parameters produced 14 different simulations for the patch-based approach and 14 simulations for the synoptic approach. In total, were obtained 28 different movement simulations in the same study area. Pathwalker's output is a density map of the entire study area. The simulation originates not from patches but from source points. In the patch-based approach, there is a source point within the patch for each patch. In the synoptic source, points are located across the landscape with a density and distribution proportional to suitability. The simulation will start independently of each individual source point and will be repeated a certain number of times (steps), 1000 in our case. Repeating the 1000 steps for each source point will give the density map. In total, we have a density map for each of the mechanisms 1 to 7. In fig. 5.2 we see as an example mechanism 7 density surface map produced by Pathwalker, this map indicates where the probability of species movements its more likely to happen, and where is less likely to.

A raster correlation analysis was then used to compute the pixel-wise correlation between each of the 28 simulations with the predictions of Graphab and UNICOR metrics (IIC, BC, PC, F, patch-based kernels 50km, 100km,150km threshold, path 50km, 100km, 150km threshold, synoptic kernels 17km threshold and synoptic path 35 km threshold). The decision to use these threshold values derives from a number of considerations which will be explained below.

In Pathwalker, energy is the budget of movement. It is related to the number of steps, but not all are equally costly given the heterogeneous resistance layer. The energy of the path is the sum (step*cost). This is directly linked to dispersal capacity, which is the expected dispersal distance in steps (mean cost of resistance surface * the number of steps in the path) = energy budget, or number of steps = energy budget / mean cost of resistance surface. The value of 2 km is equivalent to an energy budget of 17k given a mean resistance of 85. This is true since mean resistance is 85, and pixel size is 10, then a 2km distance will equal 85 cost units average per pixel * 200 pixels in 2km = 17k cost units for 2km. We used 2 times this amount, so 35k, for factorial least cost paths (fcp) given that it has been shown that twice the dispersal distance is needed to connect two points by fcp to have kernels overlapping in resistant kernel analysis.

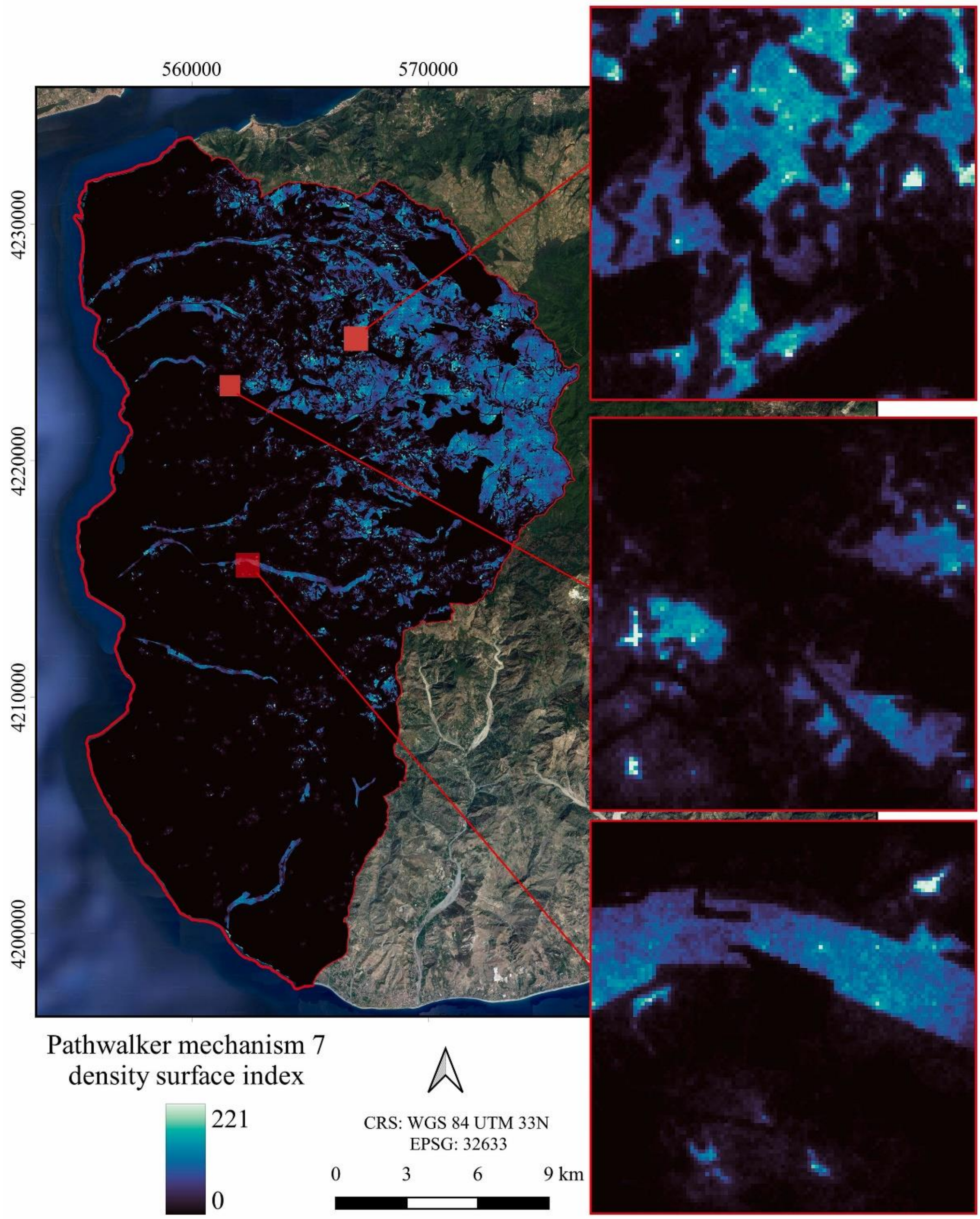

Figure 5.3: Representation of the Pathwalker density surface map for mechanism 7. Shades of light blue indicate areas where movement is more likely to occur, and dark blue shades areas where movement is less likely.

The 50, 100, and 150k thresholds were used for the centroid-based analyses, and not for synoptic analyses. For centroid-based analyses, a more significant movement threshold is needed to reflect that organisms are not limited to a single animal per patch that starts from the centre. A higher dispersal threshold reflects that connectivity is broader than movement limited to the biological dispersal limits from a centroid location (given realistically animals move from all the locations they exist in and not just from a centroid of a patch, this is one of the reasons why we strongly favour the synoptic approach, but given the centroid approach is widely used in applied conservation science we needed to evaluate and compare). We chose the three thresholds of 50, 100, and 150 to reflect a range of uncertainty in how movement from centroids would translate to patterns related to movement synoptically from occupied locations with the biologically based dispersal threshold.

5.1.4. Graphab analysis

The next model prediction we used was based on graph theory (Urban and Keitt 2001), implemented in the Graphab software (Foltête et al. 2021), which models the ecological system as a network constituting a series of nodes and arcs. Before the graph network modelling, we first developed a resistance model based on the10 focal species. Specifically, by referring to the data collected by Boitani et al. (2007), we assigned resistance values to each land use category, a dispersal distance, and a minimum patch size (see Lumia et al. 2023a). The resistance values were scaled to range from 1 (minimum resistance to movement) to 100 (maximum resistance) while the dispersal distance was specified as 2 km, taking into consideration the minimum dispersal distance of each of the 10 species. The minimum patch size of 2 ha was based on the concept of the home range (Boitani et al., 2002), defined as the minimum portion of territory needed for an animal to fully perform its vital functions (availability of resources, finding shelter, etc.). Areas with a surface area greater than or equal to 2 ha were considered nodes in the graph network; remaining areas with a surface less than 2 ha were only regarded as structural elements influencing the passage of species. We considered possible patches only as areas with maximum affinity (resistance level = 1) and an area equal to or greater than 2 ha (fig. 5.3). Areas with high affinity but less than 2 ha were not chosen as patches for the graph theory analysis but were considered stepping stones useful for species movement (Lynch, 2019; Saura et al., 2014). Then we calculated the connectivity metrics (table 2) Integral Index of Connectivity (IIC), Probability of Connectivity (PC), Flux (F), and Betweenness Centrality (BC) (Foltête et al., 2012; Freeman, 1977; Orjan Bodin & Santiago Saura, 2010; Saura & Pascual-Hortal, 2007). To enable comparisons in subsequent steps, we sampled the values of each graph theory index at the node level. In this manner, we constructed the multispecies ecological network of the entire study area among the nodes represented by these patches.

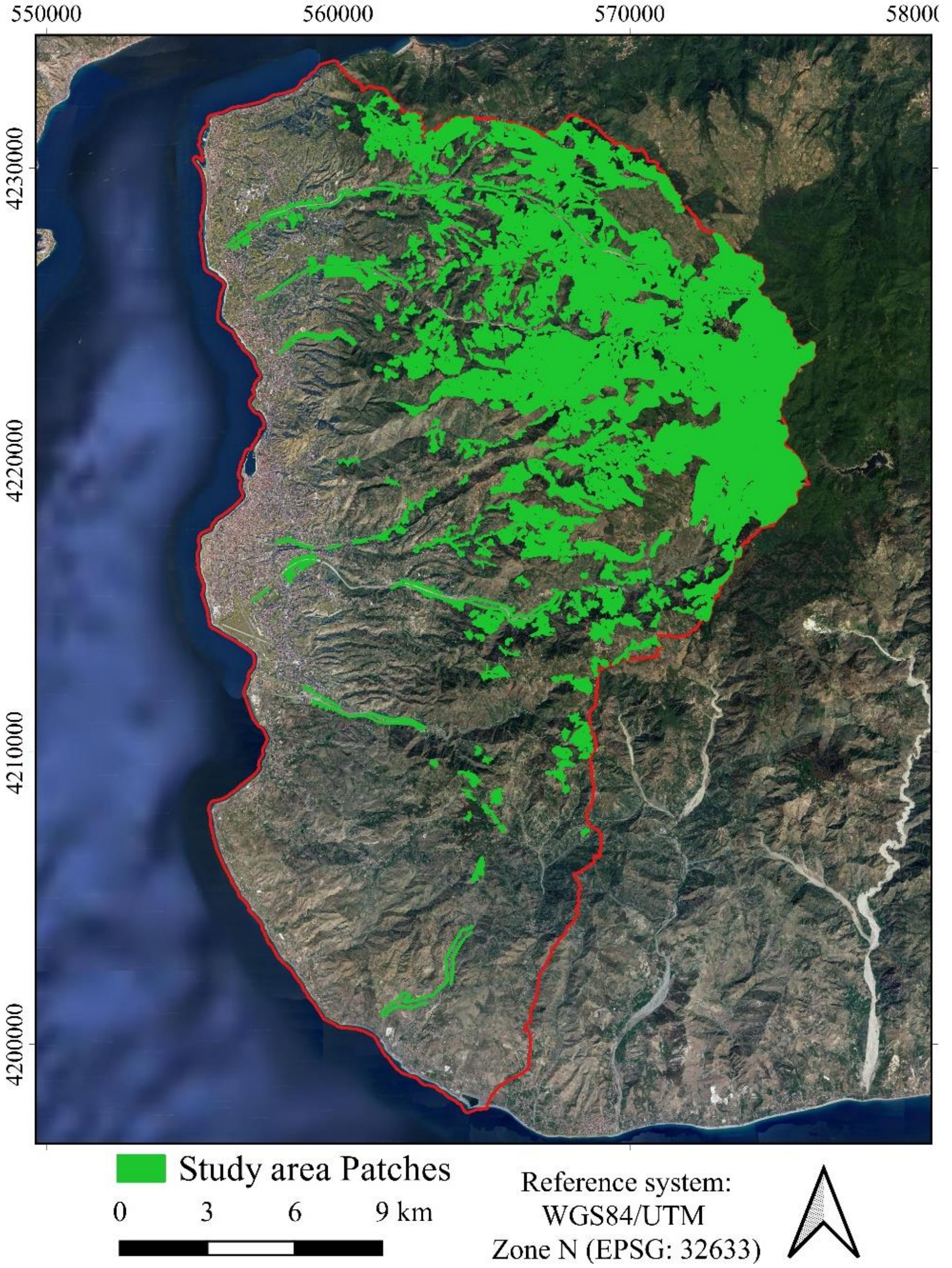

Figure 5.4: Patches within the study area, identified with a minimum area of 2 ha with the support of the Graphab software.

Table 5.2: Connectivity metrics calculated in this work.

Connectivity metrics	Ecological meaning	References
Integral Index of Connectivity	The probability that individuals randomly located in the landscape within a patch can access each other. A higher value indicates greater connectivity.	(Freeman, 1977)

Probability of Connectivity	The probability that two random points in the landscape fall within interconnected habitat areas (i. e., reachableto each other). Values are between 0 and 1.	(Saura & Pascual-Hortal, 2007)
Flux	For the focal patch i : sum of the capacity of patches other than i and weighted according to their minimum distance to the focal patch through the graph. This sum indicates the potential dispersion from the patch i or, conversely, to the patch i.	(Foltete et al., 2012a, Foltete et al., 2012b)
Betweenness Centrality	The sum of the shortest paths through the focal patch, each path being weighted by the product of the connected patches' capacities and their interaction probability.	(Bodin & Saura, 2010)

5.1.5. UNICOR analysis

We used UNICOR (Landguth et al. 2012) to implement factorial least-cost paths (Cushman et al. 2009) and resistant kernels (Compton et al. 2007) analyses of connectivity across the study area. For the operations in UNICOR, we used the same focal species data used in the previous computations. Therefore, we used the same resistance surface as in the Graphab analysis, with resistance values ranging from 1 to 100 (high landscape permeability and barrier to movement, respectively).

It was necessary to indicate source points for analysis, understood as the points at which animals initiated their movements. To explore the sensitivity of results to different paradigms of connectivity analysis, we defined two different sets of source points. In the first case (patch-based approach), we used as source points the same nodes that made up the network in Graphab, using these as source points to compute both the factorial least-cost paths and the resistant kernels analysis. For the patch-based factorial least cost path and resistant kernel analyses, we chose a range of dispersal distances (50 km, 100 km, and 150 km) to reflect the range of mobility in native species and the uncertainty in this mobility. In the second case (synoptic approach), we used a 10 times higher number of points (320 for patch-based, 3640 for synoptic) that were probabilistically generated with density proportional to habitat suitability. For the synoptic UNICOR analysis, we used two different dispersal thresholds. The first threshold was set at 17 km (cost units) for kernels analysis since this is the value expected considering the cost distance needed to traverse 2 km in geographic space (threshold consistent with that used in Graphab) based on median resistance in the landscape. The second threshold was 35 km (cost units) for the factorial least-cost paths. We used a wider threshold since, as Cushman et al. (2013b, 2014) demonstrated, the factorial least-cost paths calculation is pairwise and requires twice the distance threshold for points to be linked by paths as points to be overlapping in resistant kernels analysis.

5.2. Results

5.2.1 Analysis of Variance

In table 5.3 we present the analysis of variance for the different simulations approaches.

Table 5.3: Analysis of variance. For the different simulations approaches, in the table, we present the values of Degrees of Freedom (Df), Deviance (Sum Sq), Variance (Mean Sq), F-test for explained variance/residual variance (F value), F-test for statistical significance (Pr(>F)).

Simulations	Df	Sum Sq	Mean Sq	F value	Pr(>F)
Mechanism	1	0.386	0.386	60.171	3.56e-14 ***
Model	11	16.098	1.463	227.975	< 2e-16 ***
Synoptic	1	6.737	6.737	1049.463	< 2e-16 ***
Mechanism Model	11	0.726	0.066	10.283	< 2e-16 ***
Mechanism:Synoptic	1	0.004	0.004	0.618	0.432
Model:Synoptic	11	4.994	0.454	70.723	< 2e-16 ***
Mechanism:Model:Synoptic	11	0.035	0.003	0.502	0.903

As we can see the interactions between mechanism:model and model:synoptic are highly significant, while those between mechanism:synoptic and the three-way interaction of mechanism:model:synoptic are not statistically significant.

5.2.2 Main effect model boxplot

The boxplot for the choice of connectivity model across all levels of other factors (Fig. 5.5) shows that the resistant kernel analyses have the highest correlation with the simulated movement patterns, with the synoptic kernels and the kernel50 having the highest median correlation. The synoptic factorial least-cost paths have a modestly positive correlation.

The other path analyses have a median correlation close to zero. The connectivity metrics we calculated through Graphab environment all have median correlations less than zero, indicating these metrics' generally poor predictive ability in explaining simulated movement patterns. The graph theory flux metric (F) has a wide range of values, which indicates that some combinations of other parameters lead to this metric having a stronger positive correlation with simulated movement density.

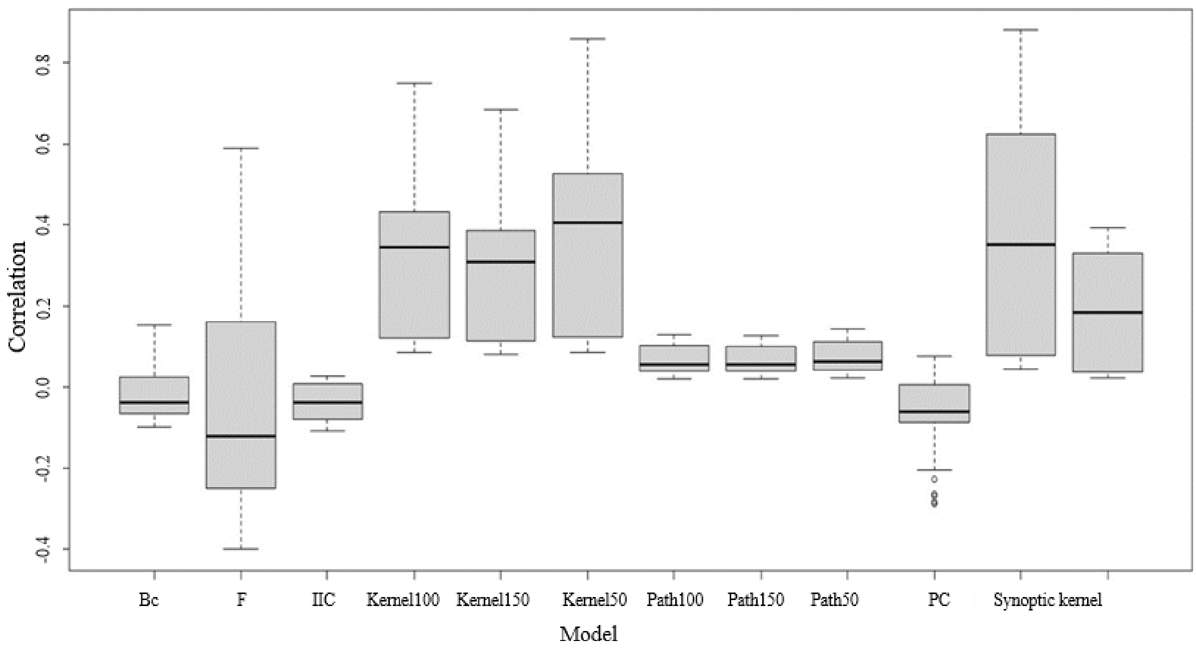

Figure 5.5: Boxplot for model across all levels of other factors

The boxplot for the synoptic main effect compares correlations between simulated and predicted connectivity, across patch-centroid source points and 3640 source points located synoptically across the landscape with a density and distribution proportional to suitability. It shows that the synoptic source point analysis produces a higher average correlation with simulated movement across the levels of the other factors than the patch-based approach. This suggests that a synoptic distribution of source points in connectivity analysis produces more accurate predictions relative to the simulated movement processes.

The boxplot of the main effect mechanism, which is the Pathwalker movement function parameter, shows little clear difference in the correlation strength with all medians in the same range. The upper quartile range of movement mechanism 1 (energy) is much higher than the other mechanisms, suggesting that some parameter combinations lead to higher correlations between Pathwalker simulations using movement mechanism 1 and predicted connectivity patterns.

The boxplot for the bivariate interaction between synoptic and model shows substantial differences in the strength of correlation between simulated and predicted connectivity among models, depending on whether source points are based on patch-centroids or are synoptically located with a distribution and density proportional to suitability. In all cases, the correlation for the synoptic analysis is higher than that for the patch-based analysis. In some cases, this difference is very large, such as for flux (F) metric (change from negative median correlation to a positive median correlation of ~0.2), and also for the resistant kernel analyses, which increase substantially, notably the synoptic kernels which uses the same large number of source points located synoptically proportional to suitability.

From the analysis of the bivariate interaction between mechanism and model we can ascertain differences in the strength of correlation between simulated and predicted connectivity across model types for each level of the Pathwalker movement type. The main result is that there is a strong difference in the performance of connectivity models, with resistant kernel analyses consistently producing higher correlations with the simulated movement patterns than other methods and with a much higher correlation between resistant kernel predictions and simulations produced using the Pathwalker movement mechanism 1 (Energy). Additionally, there is a substantially higher correlation for the flux metric for Pathwalker movement mechanisms 3 and 5 than the others.

The analyses produced five main patterns of results. First and most importantly, the strongest correlations between simulated movement and connectivity predictions are for predictions made by resistant kernel methods (Fig. 5.6).

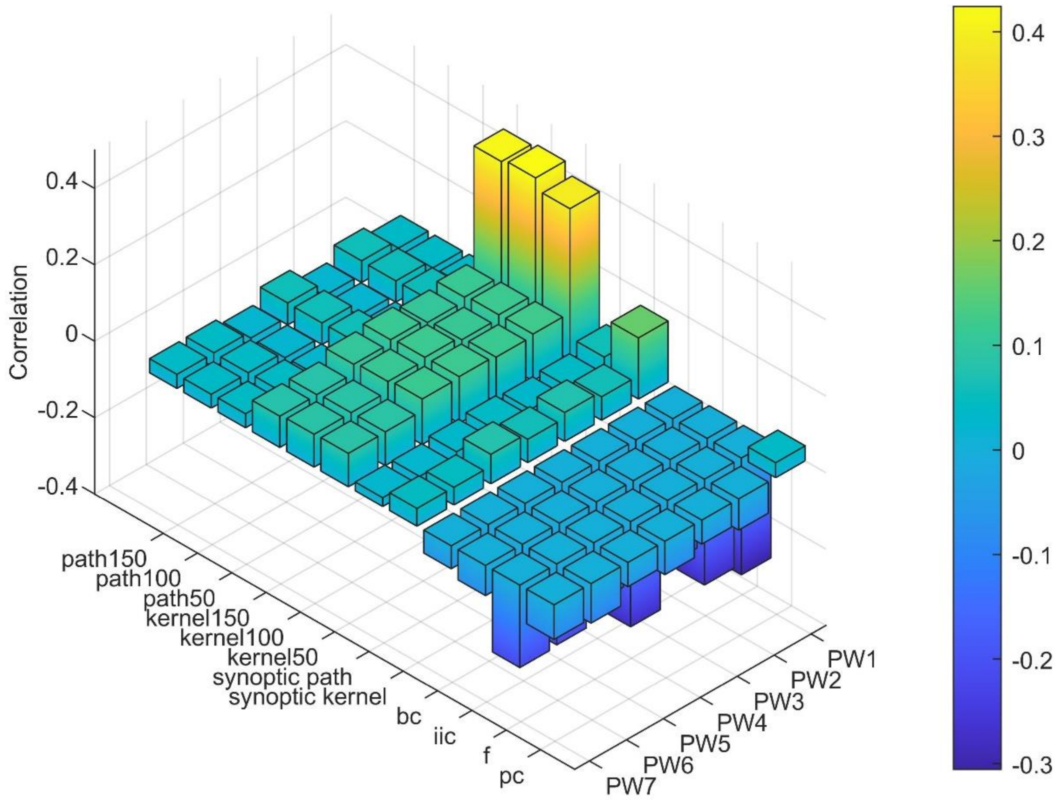

Figure 5.6. Correlation between simulated movement density from Pathwalker (PW1 – movement mechanism 1, PW2 - movement mechanism 2, PW3 - movement mechanism 3, PW4 - movement mechanism 4, PW5 - movement mechanism 5, PW6 - movement mechanism 5, PW7 - movement mechanism7) and predictions of different connectivity algorithms (PC – graph theory 3640, F – graph theory flux, IIC – graph theory 3640, BC – graph theory betweenness centrality, synoptic kernels – UNICOR resistant kernels with 3640 source points distributed proportionally to inverse of resistance with 17,000 cost distance threshold, synoptic path – UNICOR factorial least-cost paths with 3640 source points distributed proportionally to inverse of resistance with 34,000 cost distance threshold, kernel50 – UNICOR resistant kernels with 240 source points

at the centroid of patches used in the Graphab analyses with 50,000 cost unit dispersal threshold, kernel100 – same as kernel50 but with a 100,000 cost distance threshold, kernel150 – same as kernel50 but with 150,000 cost distance dispersal threshold, path50 – UNICOR factorial least-cost paths among 240 source points at the centroid of patches used in the Graphab analyses with 50,000 cost distance threshold, path100 – same as path50 but with 100,000 cost distance threshold, path150 – same as path50 but with a 150,000 cost distance dispersal threshold. These correlations are for Pathwalker settings 1 and 0 correlation of directionality.

Second, the resistant kernel results were much more strongly correlated to the Pathwalker results for Pathwalker movement mechanism 1 than the other six movement types (Fig. 5.6). The other Pathwalker mechanisms have lower correlations. Third, the resistant kernel analysis using the same source points used as origin locations for the Pathwalker simulations outperformed those based on the synoptic distribution of source points placed in a density proportional to the inverse of resistance (Figure 5.6). Conversely, the analysis using the synoptic source points (3640 source points located in distribution and density proportional to suitability) had much higher correlations with the synoptic kernels and much higher correlations with all the kernels analyses generally than the "patch-centric" analyses (Fig. 5.7).

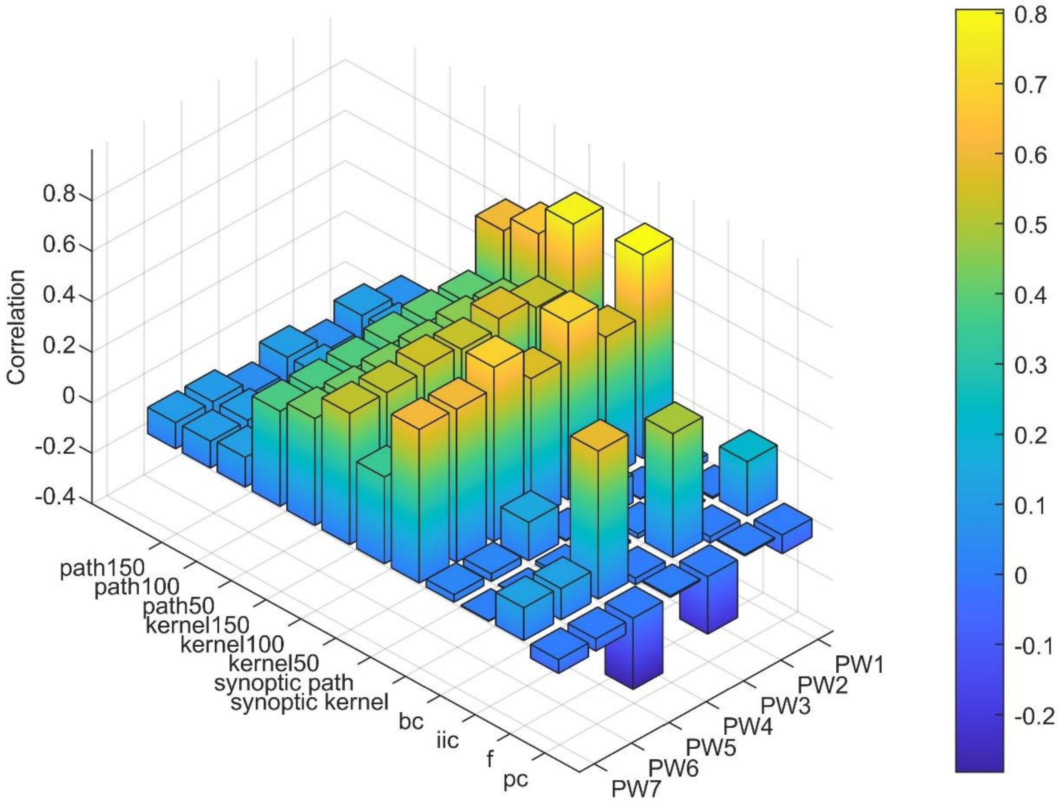

Figure 5.7. Correlation between simulated movement density from Pathwalker (PW1 – movement mechanism 1, PW2 - movement mechanism 2, PW3 - movement mechanism 3, PW4 - movement mechanism 4, PW5 - movement mechanism 5, PW6 - movement mechanism 5, PW7 - movement mechanism7) and predictions of different connectivity algorithms (PC – graph theory 3640, F – graph theory flux, IIC – graph theory, BC – graph theory betweenness centrality, synoptic kernels – UNICOR resistant kernels with 3640 source points distributed proportionally to inverse of resistance with 17,000 cost distance threshold, synoptic path – UNICOR factorial least-cost paths with 3640 source points distributed proportionally to inverse of resistance with 34,000 cost distance threshold, kernel50 – UNICOR resistant kernel with 3xxx source points distributed proportional to suitability with 50,000 cost unit dispersal threshold, kernel100 – same as kernel50 but with

a 100,000 cost distance threshold, kernel150 – same as kernel50 but with 150,000 cost distance dispersal threshold, path50 – UNICOR factorial least-cost paths among 240 source points at the centroid of patches used in the Graphab analyses with 50,000 cost distance threshold, path100 – same as path50 but with 100,000 cost distance threshold, path150 – same as path50 but with a 150,000 cost distance dispersal threshold. These correlations are for Pathwalker settings 100 and 0.25 correlation of directionality.

Fourth, the factorial least-cost path analyses produced correlations with the Pathwalker simulations that were much lower than any resistant kernels parameterizations. We found that the factorial least-cost path analyses have a low correlation with these simulated movement patterns. Finally, the results of our simulation study show that the graph theory metrics produced for patches using Graphab software had the lowest association with patterns of movement simulated with Pathwalker across all parameterizations tested in this study. Indeed, the correlations between graph theory metrics and simulated movement density were negative for nearly all graph metrics across almost all the combinations of parameterization. The synoptic Pathwalker analysis (3640 source points located in distribution and density proportional to suitability) changed somewhat with the Flux parameter from Graphab increasing to a significant positive correlation in many of the movement mechanisms (in particular, mechanisms 3 and 5).

5.3. Discussion

The most striking result of our simulation study is the consistently high performance of resistant kernel methods as predictors of patterns of simulated organism movements in comparison to the factorial least-cost paths and graph theory metrics. The kernel method was superior across all modelling mechanisms, correlations, and other parameters. It has the highest association for mechanism 1 which is an energy kernel, but the pattern is consistent across the other mechanisms which are not algorithmically similar to the resistant kernel approach. We expected this result because past empirical (Cushman et al., 2012; Zeller et al., 2018) and simulation (Unnithan Kumar et al., 2022) studies have found that resistant kernel methods are generally superior as predictors of organism movement patterns. This is likely because resistant kernel models are intended to represent the spatial incidence function (expected movement density) of movement rates and patterns for organisms starting the movement at the specified source points and moving up to a specified cost distance from that source point. This result suggests that studies that aim to predict the patterns of animal movement across the landscape as a function of landscape resistance should use resistant kernels analyses given their consistently higher performance than factorial least-cost paths (the present work and Unnithan Kumar et al. 2022) and graph theory (this work), and because they produce more accurate predictions of movement density than circuit theory in all cases except when movement is strongly directed toward known destinations (Unnithan Kumar et al. 2022).

The simulation approaches used in Unnithan Kumar et al. (2022) and in the present work provide a rigorous assessment of the performance of these various connectivity models across an extensive range of known movement relationships that collectively span much of the potential range of real organism movement. We believe the consistent superiority of resistant kernel predictions across this wide range of simulated movement characteristics should guide best practices in connectivity modelling work in the future.

The second important result we wish to highlight is that the resistant kernel results were much more strongly correlated to the Pathwalker results for Pathwalker movement mechanism 1. Positive correlation values towards Pathwalker mechanisms indicate good reliability in predictive terms of the analysed metrics, in contrast negative values indicate poor reliability. This is expected given that Pathwalker mechanism 1 is "energy," in which the walker moves randomly and ends its walk once it reaches a limit of a specified energy budget. This is algorithmically analogous to the movement mechanism implemented in resistant kernels, which describe the probability distribution of movement from source points as a function of cumulative cost, which is conceptually and algorithmically very similar to the energy budget mechanism in Pathwalker. All other mechanisms of movement simulated in Pathwalker have a lower correlation with the resistant kernel predictions because they implement movement types that respond to landscape features differently than resistant kernels do. For example, the "attraction" mechanism (Pathwalker mechanism 2) simulates movement biased toward areas of lower resistance and away from high resistance in the neighbourhood surrounding the walker. This is a realistic mechanism for actual animal movement but is different from resistant kernels, which are purely energy attenuation kernels as a function of cumulative cost.

Similarly, the risk mechanism (Pathwalker mechanism 3) correlates relatively less with resistant kernel predictions than the energy mechanism. This is expected since the risk mechanism is a spatially random walk with a stochastic termination as a function of the mortality risk (taken as the scaled inverse of resistance). One would imagine this would produce a movement-density surface similar to that produced by the energy mechanism. Still, the much weaker correlation suggests that this is not the case, likely because of the binary termination as a probabilistic function rather than a walker that continues until an energy budget is exhausted.

The third interesting insight that emerged from our results is that the simulation that was based on a synoptic distribution of source points placed across the landscape in a density proportional to overall suitability (reflected by the inverse of suitability in this model) produced much higher correlations with resistant kernel connectivity predictions than Pathwalker simulations that used the centroids of patches as source locations. Furthermore, the resistant kernel analyses using the synoptic source points had a much higher correlation with the Pathwalker simulations overall and with the simulations that used the same large pool of synoptic source points. This result tests the effect of the distribution and density of source points on connectivity analysis. Often past connectivity research has adopted a patch-based approach that has been criticized (e.g., Cushman et al., 2013b; Cushman & Landguth, 2012) as it does not reflect the functional connectivity of populations, which is driven by the combination of density and distribution of source points, the resistance of the landscape, and the dispersal ability of the species. Our results confirm this, showing a much stronger correlation between simulated movement and predicted connectivity in analyses that incorporated a "realistic" distribution of source points reflecting the gradients of habitat suitability (which are expected to be positively associated with occurrence probabilities and densities). This follows the observations of Cushman et al. (2012), who found that the location and density of source points have a strong influence on the predictions of connectivity models and suggested that analyses that intend to reflect the functional connectivity of organisms must consider biologically realistic patterns of source point distribution and density, as well as realistic dispersal abilities and well-parameterized landscape resistance models. Indeed, some recent papers have suggested that the density and distribution of source points and dispersal ability often have a much larger influence on connectivity predictions than variation in resistance surfaces themselves (e.g., Ash et al., 2022). Another interesting element emerging from the results is that the correlations created between the factorial least-cost path analyses and Pathwalker simulations are much lower than any of the resistant kernel parameterizations. This is consistent with Unnithan Kumar et al. (2022), who also found much lower correlations between simulated movement patterns and the predictions of factorial least-cost paths than those of resistant kernels. The factorial least-cost path analysis maps the density of optimal (least-cost) routes among the network of source points following least-cost routes. Thus, it is explicitly destination directed and limited to optimal routes connecting the network of destinations. The Pathwalker model simulates realistic movement patterns incorporating energy, attraction, risk, interactions, and directional and destination bias. This provides a realistic and rich variety of movement patterns. The low correlation of factorial least-cost path analyses with these simulated movement patterns suggests that they do not accurately describe actual movement patterns, at least as represented in our broad agent-based simulations. However, factorial least-cost path analyses may still be helpful in localizing or optimizing movement corridors for conservation prioritization (e.g., Kaszta et al., 2018; Zeller et al., 2018b) or for predicting the location of movement through narrowly constricted features such as locations where animal's cross highways (e.g., Cushman et al. 2013a; 2014).

Finally, the negative correlation values of Graphab calculated metrics found for almost all the combinations of parameters suggest that these metrics are very poor predictors of the actual movement density of organisms, at least when implemented in the patch centroid approach used here. Given the frequent and widespread use of graph theory metrics for connectivity and conservation planning, this is a significant result. Our results found that graph metrics calculated for patches across the landscape were poor predictors of the actual movement patterns across that landscape, simulated with an extensive range of realistic movement processes. This result should be confirmed and explored more fully with additional research to understand the full reasons for the observed poor performance of the graph theory metrics and conditions in which they may produce more accurate and robust results. We suspect that the main reason that the Graphab calculated metrics performed poorly in our analysis is that they are patch-based. At the same time, Pathwalker simulates functional patterns of movement across a landscape as a function of the density and distribution of source points, landscape resistance, and the dispersal ability of the organism. Thus, it produces a spatially varying prediction of functional connectivity through movement density in each pixel. The graph theory metrics are explicitly tied to a patch-centric perspective on landscape pattern and connectivity which is inconsistent with the gradient and scale-dependent processes that drive functional connectivity (Cushman & Lewis, 2010; McGarigal & Cushman, 2005).

From the results as a whole, correlations with resistant kernel analyses and simulations were consistently higher than other connectivity approaches. We compared these relatively. This result is already important in itself, as it shows that the resistance kernel is the best of those we evaluated, across a broad combination of simulated comparisons. Indeed, our results are in line with the work of others that have also found strong relationships of resistant kernel to genetic diversity (Atzeni et al., 2020; Macdonald et al., 2019), and patterns of animal movement (Cushman et al., 2014). However, in some cases the best method did not have exceptionally strong similarity to simulated movement. This suggests that other factors may need to be included that are not in any of the connectivity algorithms we tested. These factors likely are in part included in how Pathwalker simulates movement and therefore we suggest the agent-based modelling approach also as an alternative to the algorithmic methods commonly used.

However, the present work has some limitations, such as using simple land use maps. From a future perspective, we should start modelling connectivity using habitat maps since having information on land ecology that is as accurate as possible is crucial for the reliability of predictions.

5.4. Conclusions

In work, we studied the relationships between different methods, parameterizations and metrics commonly used to assess landscape connectivity. We used simulation modelling to evaluate the reliability of movement pattern predictions obtained from different landscape connectivity models and strategies. Specifically, we used Pathwalker to simulate movements as a function of spatially varying mortality risk, energy, attraction and their combinations across different dispersal thresholds, different path correlation values and different energetic cost of movement. Using an extensive agent-based simulation, we confirmed that what most influences prediction accuracy is the choice of connectivity model used. Specifically, we found that resistant kernel-based analysis using synoptic source point distributions is the most effective method tested in predicting simulated movement patterns, which is consistent with recent literature (Cushman et al. 2012; Zeller et al. 2018; Unnithan Kumar et al. 2022). Importantly, we found that graph theory metrics were poor predictors of the simulated patterns of organism movement. Another important implication of our study is that the agent-based simulation approach itself may often be the best analytical framework to map functional connectivity for ecological research and conservation applications, given its biological realism and flexibility to implement combinations of movement mechanism, dispersal threshold, directional bias, destination bias and spatial composition of source locations for analysis.

6 A proposal for a Multispecies Ecological Network for the Reggio Calabria metropolitan area

6.1. Introduction

This final chapter presents a method for implementing an ecological network of the study area based on fully exploiting the strengths of circuit theory, graph theory, resistant kernels, and Pathwalker simulations. In fact, from what has been pointed out in the previous chapters, each approach has strengths and weaknesses. For example, circuit theory, resistant kernels, and Pathwalker simulations explicate their effectiveness by providing maps that highlight in the form of higher or lower intensity of movement flow the tendency of animals to cross different areas of the landscape (Foltête, Clauzel, et al., 2012; McRae et al., 2008; Unnithan Kumar & Cushman, 2022b). On the other hand, graph theory, which lacks this potential, nevertheless provides the possibility of assigning weight to patches and corridors (assuming them as nodes and links), thanks to a whole range of connectivity indices, which is lacking in the previously described approaches.

Moreover, two additional aspects were analysed and put into practice to define an effective multispecies ecological network of the study area. In the first aspect, a detailed habitat map was defined and implemented based on direct surveys and spatial analyses. This approach made it possible to have an accurate and current view of biodiversity in the study area. This was done to overcome the limitations of using a land use map (e.g., CLC and UA) with insufficient geometry and thematic resolution. As stated by several studies, LULC maps are one of the common input data to build ecological networks (An et al., 2021c; Gurrutxaga et al., 2010; Mackovčin, 2000). However, using these maps is less effective than habitat maps in conserving biodiversity (Tomaselli et al., 2013). Since ecological networks are implemented with the primary purpose of biodiversity conservation (Tillmann, 2005; Žák et al., 2020; R. Zhang et al., 2021), the use of habitat maps improves our output and adds high value in achieving the purpose.

On the second aspect, an in-depth examination of the faunal species occurring in the study area and their autecological requirements was provided. The selection of the faunal species was carried out with the help of a local wildlife expert. A species-by-species analysis was carried out to determine each species' needs and then isolate a set of requirements that can meet the necessities of all the species in the group. More details on this aspect will be presented in section 6.2.2.

6.2. Materials and Methods

The study area analysed in this chapter, falling within the boundaries of UA 2018, includes 13 municipalities in the metropolitan city of Reggio Calabria, as described in previous chapters 2-5. The approach we used to implement the Multispecies Ecological Network, which we present here, was divided into 5 phases: 1) Habitat mapping through field trips and direct data collection organised as phytosociological and vegetational surveys. 2) Collection of information on the autecological characteristics of focal species (as discussed in Chapter 1) through the involvement of an expert of the local wildlife (direct surveys in the study area) and literature search (Boitani et al., 2002b, 2003; Ciofi & Chelazzi, 1991; Gent H., 1993; Glandt D., 1986; Griffiths R.A., 1995; Lelièvre et al., 2012; Schulte et al., 2007). 3) Implementation of the Multispecies Ecological Network and calculation of connectivity indices. 4) Improvement of the network according to a defragmentation scenario aimed at upgrading the connections between the different ecological network components to achieve a more robust network. 5) Analysis of the geometric and ecological characteristics of the implemented networks by comparing the indices calculated in the previous steps.

6.2.1. Habitat mapping

The habitat mapping has been implemented in the framework of a research project involving the Department of Environment and Territory of the Regione Calabria, the Department of Agriculture of the University of "Mediterranea" Reggio Calabria, and the Department of Biology, Ecology and Earth Sciences of the University of Calabria, as part of the Action Programme Axis 6 (Protection and Enhancement of the Cultural Environmental Heritage) of the Region of Calabria. The project has aimed to implement a "Nature Map System" for the entire territory of the Calabria region https://www.isprambiente.gov.it/it/servizi/sistema-carta-della-natura/cartografia/carta-della-natura-alla-scala-1-50.000/calabria). The "Nature Map System" project moves from a previously shared activity between the same entities aimed at monitoring species and habitats of the Natura 2000 Network of the Region of Calabria (https://www.eea.europa.eu/t hemes/biodiversity/natura-2000, last access 10 November 2023). Among its objectives is creating a Habitat Map, which Calabria currently lacks, as a critical knowledge tool to highlight the natural values and territorial vulnerability.

The goal of creating the habitat map was pursued ranging from strategic planning to the final construction of the habitat map in Calabria. The work was organised as follows:

1) Participation in practical field training with the research project group to identify a modus operandi unique to the entire work group.

2) Field trips and phytosociological, photographic, and vegetation surveys.
3) Creation of a database for each of the surveyed habitat areas.
4) Photointerpretation of satellite images, polygonisation, and habitat map code assignment (see annex 1). This phase made it possible to identify habitats by photo-interpretation where it was not possible to carry out a field survey.
5) Identify among the software tools available in the literature the best set to catalog, process, and organise data collected in the field. We chose to use Qgis and ArcGisPro to polygonise the new habitat map and assign a habitat code to each polygon. The attribution of habitat codes was based on a new legend, purposely created for this map. In this context, the EUNIS legend was of great help in the attribution of habitat codes, from which we took our cue, modifying it where necessary in order to truthfully represent the habitats of Calabria. Codes were assigned to polygons by reference to data collected in the field and those deduced by photointerpretation.

The minimum mapping unit (MMU) was assigned at 1 ha, in order to include small but important habitats in the analysed area.

A range of software was reviewed, including Google Earth Pro (GEp), Google Maps, Google Photo, QGIS, ArcGisPro, and Excel, to organise, visualise, and process the data necessary for the realisation of the habitat map. At first, by analysing satellite images in GEp environment, we attributed georeferenced points in KML format containing the habitat code according to the habitat map legend. The legend consists of 134 habitats (134 For the entire territory of the Calabria region, southern Italy) divided into 8 macro-categories; our study area contains 72 habitats that fall into 7 of these categories (see annex 1). To make the habitat identification process more effective, we performed a diachronic analysis on GEp satellite images through the Historical Imagery tool (https://support.google.com/ earth/answer/148094?hl=en - last access on 13 November 2023). This tool allows the user to go through a time series of satellite images that helped us to detect vegetation characteristics such as leaf fall or wildfire occurrence, enhancing the ability of habitat identification.

After this first step, a congruous number of field surveys (at least one for each detected habitat) were performed to validate the data and to check areas that highlighted criticism during the previous step. Phytosociological survey according to the Braun-Blanquet numbering system (Braun-Blanquet, 1921), collection of samples of dubious plant species for herbarium analysis, and photographic habitat survey by geo-referenced photos were performed during the field surveys (Figg. 6.1-6.2). Here, data were collected referring to each species present in the survey area, the area occupied as a percentage of each species, the primary habitat, elevation, slope, aspect, land cover, coordinates, survey number, survey surface area, height of the different layers (Trees, shrub and or herbaceous layers) (Fig. 6.3, see also annex 2). The photographic surveys were entered into the Google Photos library and later viewed on Google Maps to check for errors in the placement of GNSS coordinates (Fig. 6.2).

Figure 6.1- Topside, some moments of compiling phytosociological sheets on coastal habitats. At the bottom are some helpful detailed observations for species recognition in hilly (left) and mountain (right) environments.

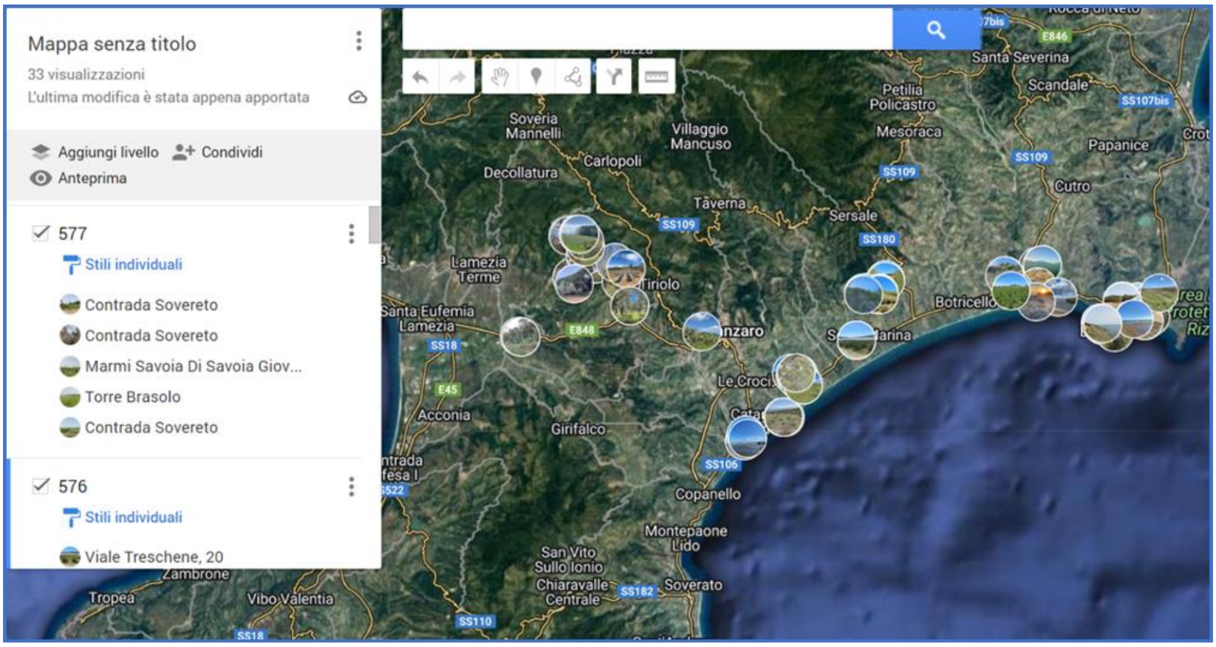

Figure 6.2 – Projection on Google Maps of geo-referenced photographic surveys to check the reliability of coordinates in frames 575, 576, and 577.

Polygonation of the territory falling in the study area was carried out, considering the points attributed through the photointerpretation and the field surveys. The processing phase was carried out in the QGIS and ArcGisPro environments. In addition, based on the ground truth obtained through field surveys, we organised the attribute table of the vector data, which contains primary habitat, secondary habitat, and percentage occupied by the latter concerning the former.

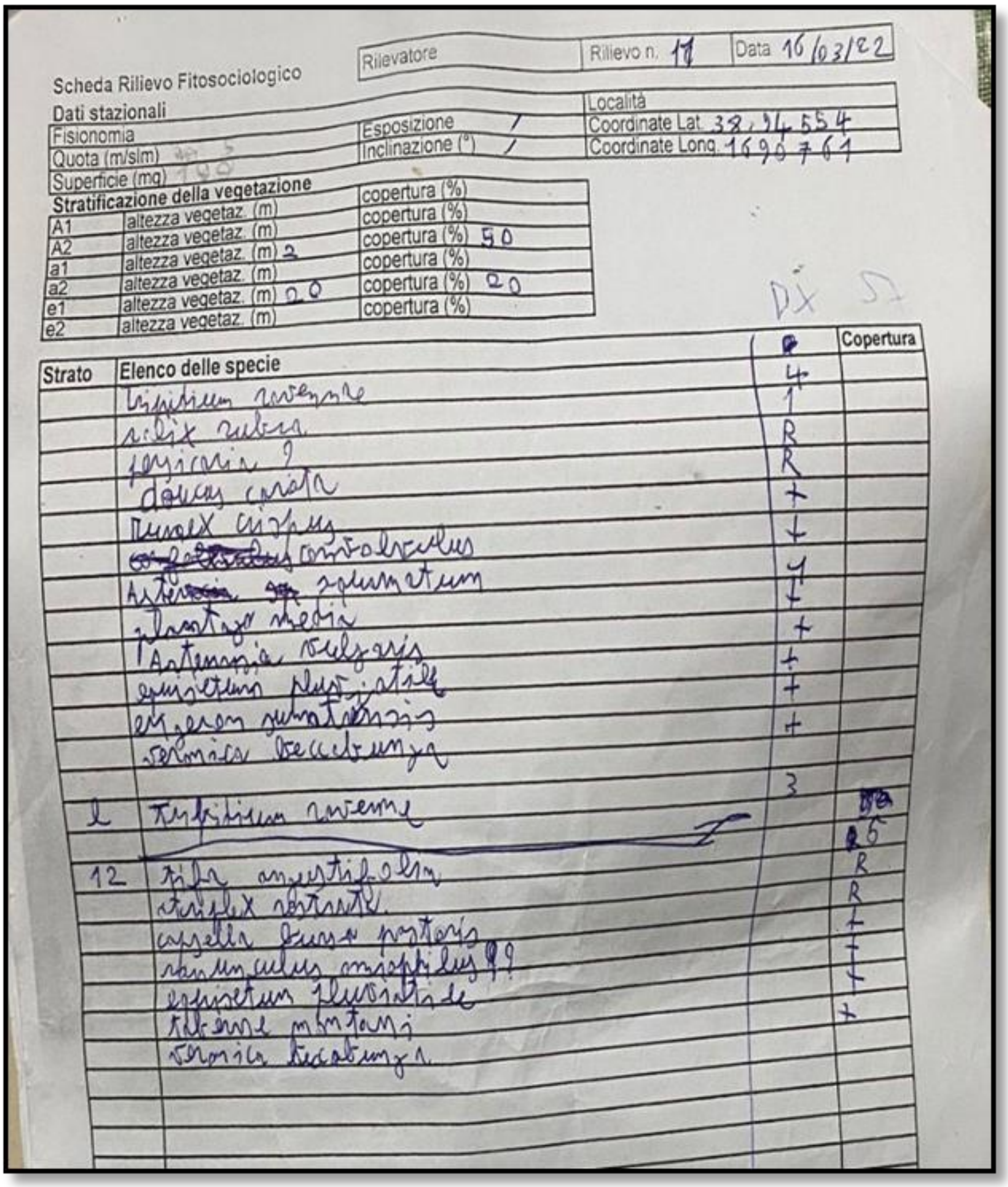
Scheda Rilievo Fitosociologico
Rilevatore
Rilievo n. 18
Data 16/03/22
Dati stazionali
Località
Coordinate Lat. 38,34554
Coordinate Long. 1690761
Fisionomia
Esposizione /
Quota (m/slm)
Inclinazione (°) /
Superficie (mq)
Stratificazione della vegetazione

A1	altezza vegetaz. (m)	copertura (%)	
A2	altezza vegetaz. (m)	copertura (%)	
a1	altezza vegetaz. (m) 2	copertura (%) 50	
a2	altezza vegetaz. (m)	copertura (%)	
e1	altezza vegetaz. (m) 20	copertura (%) 20	
e2	altezza vegetaz. (m)	copertura (%)	

Strato	Elenco delle specie		Copertura

Figure 6.3 – Example of a field sheet used to collect phytosociological survey data.

6.2.2. The Multispecies Ecological Network

In the following paragraphs, we present the work that led to the construction of the ecological network. This went through a series of three steps. The first step aimed to build a network by exploiting graph theory and thus obtain a set of connectivity indices and spatialisation into its canonical components of patches and corridors. In the second step, we used Pathwalker simulations to obtain a surface density map that spatialises different degrees of probability of species movements within the study area. This process allows to exploit the movement model of resistant kernels and, in addition, to consider further factors such as auto-correlation factor, energy, risk and attraction (see chapter 5 for more information on these factors). In the final step, we put together the strengths of the first two to obtain the final network, describing all the work that was done to make the predictions as realistic and accurate as possible. The ecological network that we present here has been implemented, bringing together the strengths of the models we studied in the previous chapters. The first major limitation we wanted to overcome was related to the use of land use maps. For this reason, as said in the previous paragraph, we decided to use a habitat map and take full advantage of its potential. In fact, building the network started from realising the habitat map, where the features would have been carefully considered. We, therefore, decided to produce the habitat map at the detail scale, with an MMU of 1ha. The choice to consider the above-mentioned MMU is due to the need to protect habitats that often occupy areas of about 1 ha and are of fundamental importance for the biodiversity of these places (Di Sabatino et al, 2013; Keijl et al., 1991). In fact, the field surveys carried out to create the habitat map enabled us to identify small habitats such as those included in code 22.4, freshwater lakes and ponds with vegetation (see annex 1). We have therefore observed that even very small habitats, such as ponds, have high importance for some species of amphibians (e.g., *Rana dalmatina*). This amphibian, which is one of those that spends less time in watercourses, only needs them in the phase of its life when it needs to reproduce, and for this purpose even pools of water smaller than 1 ha are sufficient (Sun life, *Rana dalmatina*: http://vnr.unipg.it/sunlife/specie_animale-dettagli.php?id=31). Other species, such as *Bombinia pachypus*, are often associated with watering holes found with high frequency in sub nitrophilous grassland or extensive crop habitats (habitat map codes 34.8m and 82.3, respectively), and spend entire generations in these places (Glandt et al., 1986; Steinfartz et al, 2007). The choice of parameters like dispersion, affinity, and home range is a step of extreme importance for the realisation of a robust ecological network. These were identified, evaluating each habitat on a case-by-case basis concerning each single species. For each habitat, one to two representative species have been chosen as focal species. A total of 18 species have been selected (see annex 3, values of resistance were assigned with a combination of literature and expert opinion; Ciofi & Chelazzi, 1991; Gent, 1993; Glandt, 1986; Lelièvre et al., 2012; Griffiths et al., 1995; Steinfartz et al., 2007), and their autecological characteristics have been used to build the EN. First of all, we consider the affinity of each selected species with all the habitats of the study area. A scale of 5 class values, ranging from a minimum of 0 and a maximum of 100, has been provided based on an expert opinion as follows:

I. 0 → no resistance;
II. 25→ low resistance;
III. 50 → medium resistance;
IV. 75 → high resistance;

V. 100 → maximum resistance (the barrier).

For the assignment of the resistance class ''0'' similarly to what we did in Chapter 2, we also considered a factor expressing vegetation vigour, the VFC index. This was obtained from multispectral Sentinel-2 images, data, which are constantly updated over time with intervals of 1-2 days. At this point, for each land use to which the expert had given resistance 0, and which also had a VFC value greater than 0.6, the resistance value of 0 was retained, where instead the VFC value is less than 0.6 a value of 25 was assigned. Each habitat with a value of 0 for at least one species has been selected as a patch.

The approach we used was based on a multi-species ecological network. What we did was to identify the needs of all species in the study area to create a network, weighted in such a way as to meet the needs or at least the minimum needs of all the selected species. We therefore did not create many networks for each individual species and then join them together, but rather created a single network from the beginning. Since the one proposed in this research is an effective multispecies approach, we assigned a resistance value for each habitat identified and with reference to all focal species considered. That means each habitat can assume one or all of the five provided R-values, comparing them to the focal species' requirements. To ensure that all potential species were considered for each habitat, the minimum resistance value was selected from among all the suggested R-values to build the EN's connection. Therefore, each identified habitat received the minimum R-value according to the matching requirements with all the considered focal species.

The approach we used can be better understood in the following example, taking Habitat 25.4 (see annex 3) as a reference. Following the species requirements, we have minimum resistance for *Bufo bufo* (R = 0), medium resistance for *Salamandrina terdigitata* (R=50), and maximum resistance for *Hierophis virdiflavus* (R=100). The resistance value we will select is the minimum, corresponding to 0 for *Bufo bufo*. With this approach, we ensure that all habitats that have maximum relevance for even one species are considered, none excluded. This approach was applied to each habitat we mapped in the study area until all resistance values were assigned.

To establish the maximum dispersion value, we went through a number of considerations. The maximum dispersion value was set at 1000m. According to what we have specified above, some species tend to spend their entire life cycle, and entire generations of individuals, without moving from the patch where they were born (Ciofi & Chelazzi, 1991; Gent, 1993; Glandt, 1986; Lelièvre et al., 2012). Of the species that we selected, all the amphibian and reptile species (e.g., *Hierophis virdiflavus*, *Ealphe quatuorlineata*, *Rana italica*) that have a maximum dispersal distance of 100 m, have this stationary behaviour within patches. On the other hand, the different species we considered (e.g., *Mustela putorius*, *Sciurus meridionalis*, *Martes martes*) have dispersal distances of 1000 m or more; therefore, using 1000 m will set a threshold that will be possible to cross for each species. All these considerations were of key importance in setting parameters and application graph theory and Pathwalker simulations that we will describe in the following steps.

6.2.2.1. Graph theory network analysis

Once we fixed the number of species, the minimum patch size, the maximum dispersal threshold, and the resistance to the movement of each habitat, we used Graphab 2.8 software to exploit the principles of graph theory and perform an analysis that will serve as the first step for the final network described in the following section (§ 6.2.2.3). In order to apply graph theory to landscape ecology, we had to make a number of evaluations on previously acquired data. First, the resistance values, identified as described in the previous paragraph, have been added to the attribute table of habitat map vector type data. Finally, a rasterization allowed us to obtain a resistance surface as raster-type data. This step was performed using a square pixel of 2.5m to maintain a high level of detail and not lose the information of smaller elements such as roads. Each pixel was assigned a resistance value, expressed on a scale of 5 resistance levels (see annex 3), as explained in the previous paragraph. This input was entered into Graphab, which simulates the possible movements of the selected animal by exploiting circuit theory (An et al., 2021; McRae et al., 2008). In order to run the simulation, we had to indicate the habitat considered as patches, the resistance to the movement of each habitat (see previous paragraph) and the energy budget (as explained in chapter 5) available for the walker. The simulation starts with the pixels we classified as patches. From there, the movement continues following the principle of the least coast path (Wang et al., 2022). This implies that the walker in the movement follows the adjacent pixels with the least resistance value. At each step from one pixel to another, depending on the resistance cost of the pixel itself, the walker consumes energy and the movement stops when the given energy cap is exhausted or when a patch is reached (Foltête et al., 2021a). A connection (as a poly-line type vector file) is identified using the least cost path technique in the latter case (Foltête, 2019). For the reasons we explained in the previous section, we considered a maximum dispersal distance of 1000m.

Obtained patches and least cos paths, we calculated a set of connectivity indices. This operation was performed within the Graphab 2.8 software environment, which exploits graph theory to assimilate node patches and least cost paths to graph links. We calculated the indices IIC, H, BC, F and PC, whose meaning and description we reported in Chapter 2 (Tab. 2.2).

6.2.2.2. Pathwalker simulations

In the second step, carried out during the period abroad in the U.S. with the collaboration of the School of Forestry Department of Northern Arizona University, we used the Pathwalker software (Kumar et al. 2022) to recreate a simulation of animal movements in the network. In this work, as outlined in Chapter 5, we have demonstrated the validity and versatility of this software when it comes to simulating movements by taking into account a large number of variables (Lumia et al., 2023; Unnithan Kumar & Cushman, 2022). Pathwalker, using the same input raster data that we used for Graphab, similarly allows us to simulate movements using the walker's energy mechanisms and the least cost path principle but, in addition, allows us to consider other variables such as attraction, risk, and autocorrelation factor (Kumar & Cushman, 2022b). The result of this operation produces a density surface map (Fig. 6.5) that expresses the probability of an animal crossing a specific portion of the territory (as explained in Chapter 4). As an example, considering only the energy mechanism, we will have a symmetrical movement probability between two adjacent pixels, so movement from an area of higher resistance to one of lower resistance or the opposite will be considered neglected. Instead, this variable is considered in the simulation by including the attraction mechanism, where a higher probability will be given for the animal to move from an area of higher resistance to one of lower resistance, as explained in Unnithan Kumar & Cushman (2022). In addition, by including the risk mechanism, we consider another variable, so with each additional step that the animal moves, the probability that its movement will stop increases relative to the risk surface crossed. In addition, considering risk in the calculation allows us to overcome a limitation present in most common energy-based simulation models; they assume the mortality risk to remain unchanged through different regions of the landscape and movement choice to occur at a single spatial scale.

Last, we considered an autocorrelation factor. This parameter expresses the tendency of the walker in the simulation to either proceed along a straight line or to change direction. This adds a realistic factor considering that animals in nature tend to follow the same path most conveniently, in a habitual manner, and to change direction to explore new areas (Dray et al., 2010; Gibbs, 1998; Zeller et al., 2014).

We then set the parameters for the simulation. The maximum dispersal distance was set at 1000 m for the reasons explained in the previous section. However, unlike Graphab, where the walker's movement starts from patches established a priori, the starting data for the movement is a vector file of points. We used a synoptic approach, using a number of points 10 times higher than the number of patches, which were probabilistically generated with density proportional to habitat suitability. This approach, as explained in Chapter 3, was used because it gives more realistic predictions of animal movement patterns. Following when found in studies (Dray et al., 2010; Gibbs, 1998; Zeller et al., 2014), the autocorrelation value, which can be set between 0 and 1, was set to 0.5, so the animal at each step will have a 50% chance of continuing along the same direction or changing. The density surface map obtained, showing the areas that are most likely to be travelled by the Pathwalker, will be used to obtain the corridors of the final ecological network, as we will explain in the following paragraph.

6.2.2.3. Ecological Network implementation

In the final step, we put together the strengths of the first two. First, we kept Graphab's network of nodes, LCPs and connectivity indexes. Next, we used the Pathwalker density surface map to identify corridors. In fact, as we showed in Chapter 4, Pathwalker is superior in producing maps that indicate the probability of species movements. However, this does not return a spatial distribution of network elements in its canonical components of patches and corridors. For this reason, the patches identified in the previous section (§ 6.2.2.1) via Graphab were retained. Conversely, to obtain corridors a 100m buffer was created around Graphab LCPs and used to crop the Pathwalker density surface map (Fig. 6.5). In this way we obtained a final network (Fig. 6.6) composed of patches on which it was possible to make quality considerations thanks to a series of connectivity indices (Fig. 6.7-6.8) and corridors that do not simply express the least-cost pathway but, thanks to Pathwalker simulations, it is possible to determine which of these are highly effective in promoting movement and which merely meet the minimum requirements to allow movement.

Once the network elements and connectivity indices were identified, all operations were repeated a second time within a defragmentation scenario in a way similar to what was done in the defragmentation scenario in Chapter 2. Here we analysed the first network obtained, and where connectivity problems were found, we assumed planning interventions through green bridges over roads, renaturation over areas altered by agricultural activities or abandoned, green tree lines in areas near urban parks or gardens, and green underpasses near elevated roads. These types of interventions are recognised in the literature for their ability to create connections where man-made areas meet natural ones (Carr, 1998; Clevenger & Wierzchowski, 2006; Gurrutxaga & Saura, 2014; Huck et al., 2010; Yu et al., 2012). This has the result of reducing the effects of fragmentation, increasing genetic and resource exchanges, and allowing animals to cross what may otherwise be barriers. The benefits of these interventions are in terms of protecting biodiversity and having long-term positive effects on the economy and safety of both animals and humans (Tarabon et al., 2022a). Indeed, interventions such as green bridges and green underpasses, for example, allow animals to cross roads safely, reducing roadkill and damage to people, infrastructures and vehicles.

6.3. Results

Here, we present the main results obtained from implementing the ecological network (EN1) and the same EN after the defragmentation interventions (EN2).

In both the scenarios (i.e., EN1 and EN2), a total number of 1909 patches were identified. This is expected since our defragmentation interventions aimed not to add new patches but to connect the existing ones. In Tab.6.1, we summarised the main properties of the patches.

These vary in extent from the selected minimum area of 1ha to a maximum of 437 ha, with a mean area of 10.36 ha and a standard deviation of 28.68. Overall, the area occupied by patches is 23,947 ha out of a total study area surface area of 48,082 ha. The habitat most represented by patches is Mediterranean oak forests with downy oak (22.3% of the total area), while those less present are Mediterranean riparian forests of willow trees and Larch pine forests (0.2% of the total area). In the second EN2 scenario, we have an increase in the most 101nthropized area in the number of corridors, which increased from 1291 to 1338. Connectivity index calculations on both scenarios also showed variations. The number of components (Fig. 6.4) in EN1 was 60, with a large number of small components near urban or cultivated areas. These were reduced to 20 in EN2, where many components were eliminated or merged with each other.

Table 6.1- Table with the main properties of habitats classified as patches in the network. The first two columns contain the habitat code of the original Habitat Map nomenclature, and the correspondence with the EUNIS code.

Habitat Map Code	Eunis code corrispondence	Number of Patches	Mean area (ha)	Standard Deviation	Min (ha)	Max (ha)
24.1_m	C3.5	1	4186.00			
24.225_m	C3.553	92	6.76	9.73	1	58.27
24.4	C2.3	4	1.75	1.75	1.45	2.17
34.8_m	E1.6	275	5.92	7.24	1.08	69.98
41.18	G1.67	43	59.02	97.73	1.29	428.54
41.732	G1.732	480	10.86	24.55	24.57	319.07
41.7511	G1.7511	2	12.94	6.30	8.48	17.40
41.9	G3.55	153	34.90	58.95	1.01	437.82
42.65	G3.55	1	5.20			
42.67	G3.57	12	21.10	20.06	2.41	69.58
44.12	G1.112	23	3.97	2.37	2.37	11.64
44.14	G1.1121	3	5.13	3.54	1.71	8.77
45.21	G2.11	3	91.89	75.81	8.90	157.49
45.31	G2.121A	27	20.55	16.74	1.86	57.14
45.32	G2.122	9	34.31	39.92	2.15	120.34

82.3	I1.3	25	5.59	4.41	1.03	15.28
84	I1.2	648	3.86	4.27	1	43.66
85	X11	108	2.39	1.38	1	7.31
Total		**1909**	**10.36**	**28.68**	**1**	**437.82**

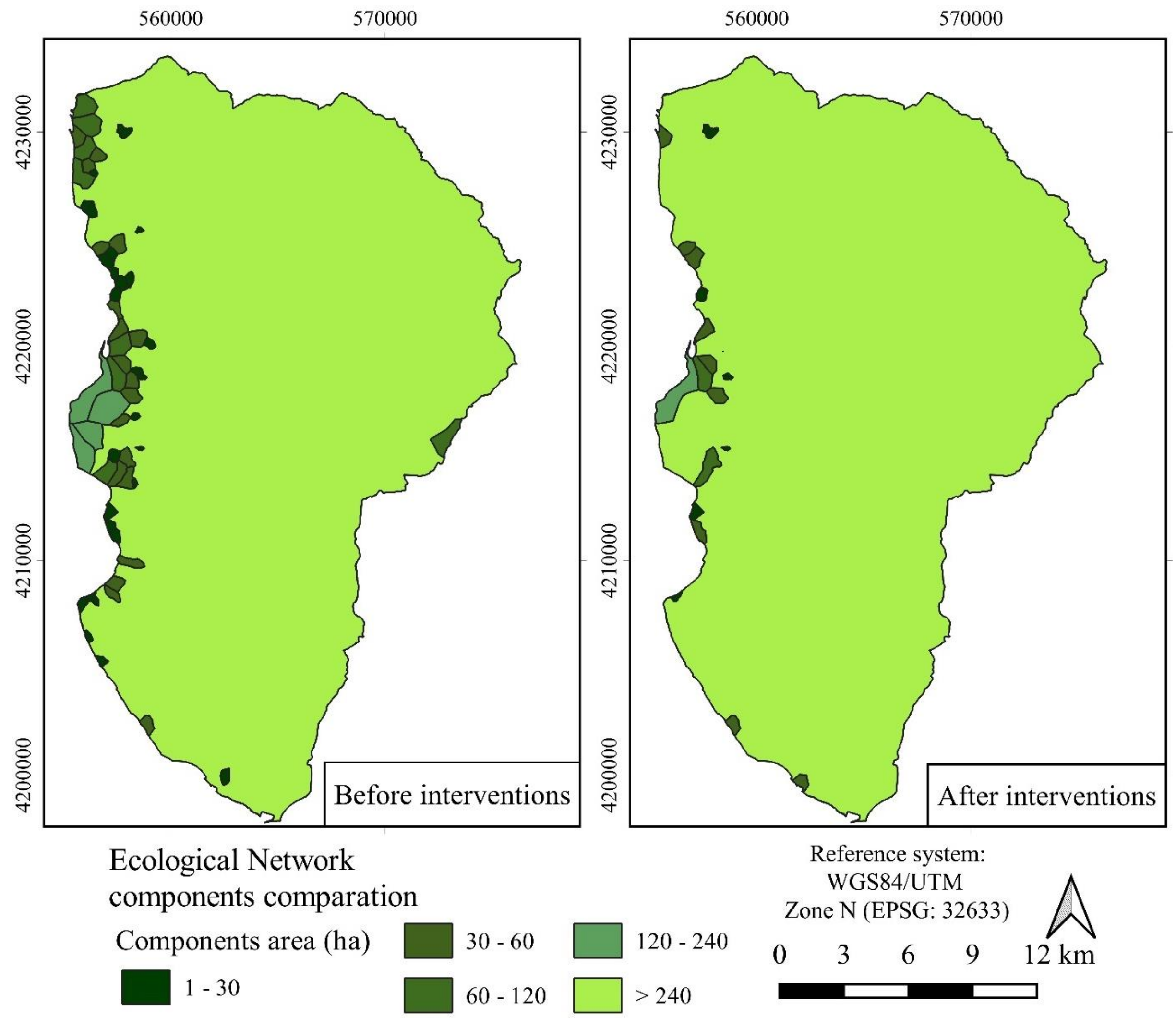

Figure 6.4 - Representation of network components before (left) and after (right) the defragmentation interventions.

The trend is also confirmed by the movement suitability map produced by Pathwalker (Fig. 6.5), showing that coastal areas have significantly lower suitability to species movement than hilly or mountainous areas. By categorising the Pathwalker suitability map into 5 different equal and continuous ranges of values, we have better emphasised which areas are ideal for corridors, i.e. high affinity areas and very high affinity areas (Fig. 6.6).

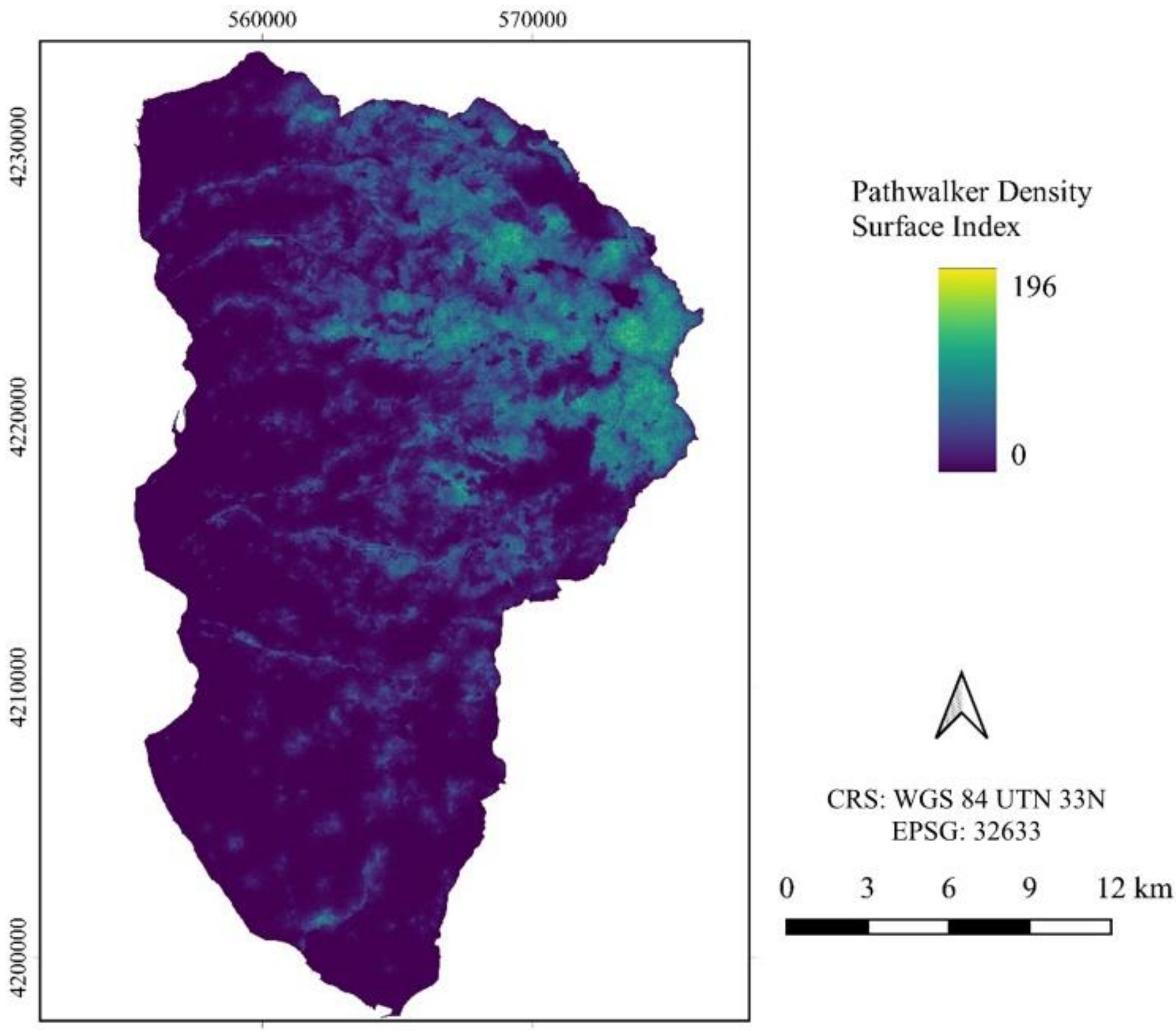

Figure 6.5 - Representation of the Pathwalker density surface map. Shades of yellow indicate areas where movement is more likely to occur, and blue shades areas where movement is less likely.

Interventions are mostly located in agricultural or urban areas; tab 6.2 summarises the main types of interventions carried out and their impact on the network. Renaturation interventions in agricultural areas benefitted the network the most, with 119.55 ha connected. In Figure 6.7, we can see the final network obtained because of the defragmentation interventions, it is represented according to the canonical components of patches and corridors. By comparing the area occupied by corridors in the network obtained in fig. 6.7. (corridors) occupying 705 ha, and the area suitable for corridors in fig. 6.6 (high and very high affinity areas, excluding areas that would fall within the boundaries of patches) occupying 3155 ah, we see that in the latter case there is a significantly higher value of potential corridor areas.

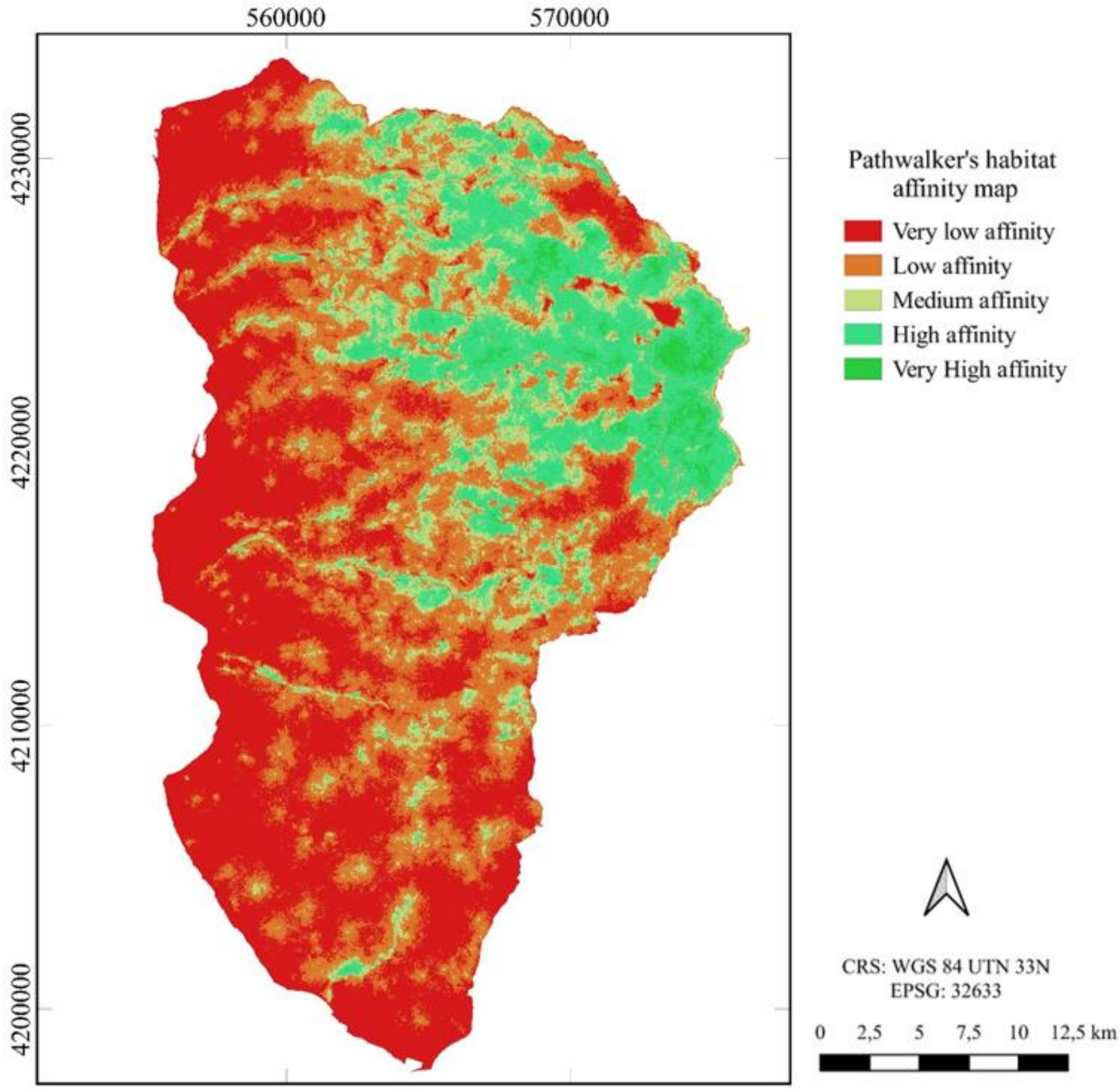

Figure 6.6: Pathwalker's habitat affinity map, The different colour gradations indicate a progressive increase from a very low affinity with the habitat (red, unsuitable to be a corridor) to a very high affinity with the habitat (darker shade of green, very suitable to be corridor).

Tab 6.2 - The table lists the different types of interventions and their respective impact in terms of area occupied and new links created.

Defragmentation intervention	**Interventions number**	**Total area covered by intervention [ha]**	**Surface of the new patches included in the network [ha]**
Greened bridges	51	4.34	19.33
Renaturalised areas	48	59.17	119.55
Tree-lined paths	15	4.25	18.60
Greened underpasses	2	0.20	5.33
Total	116	67.96	162.81

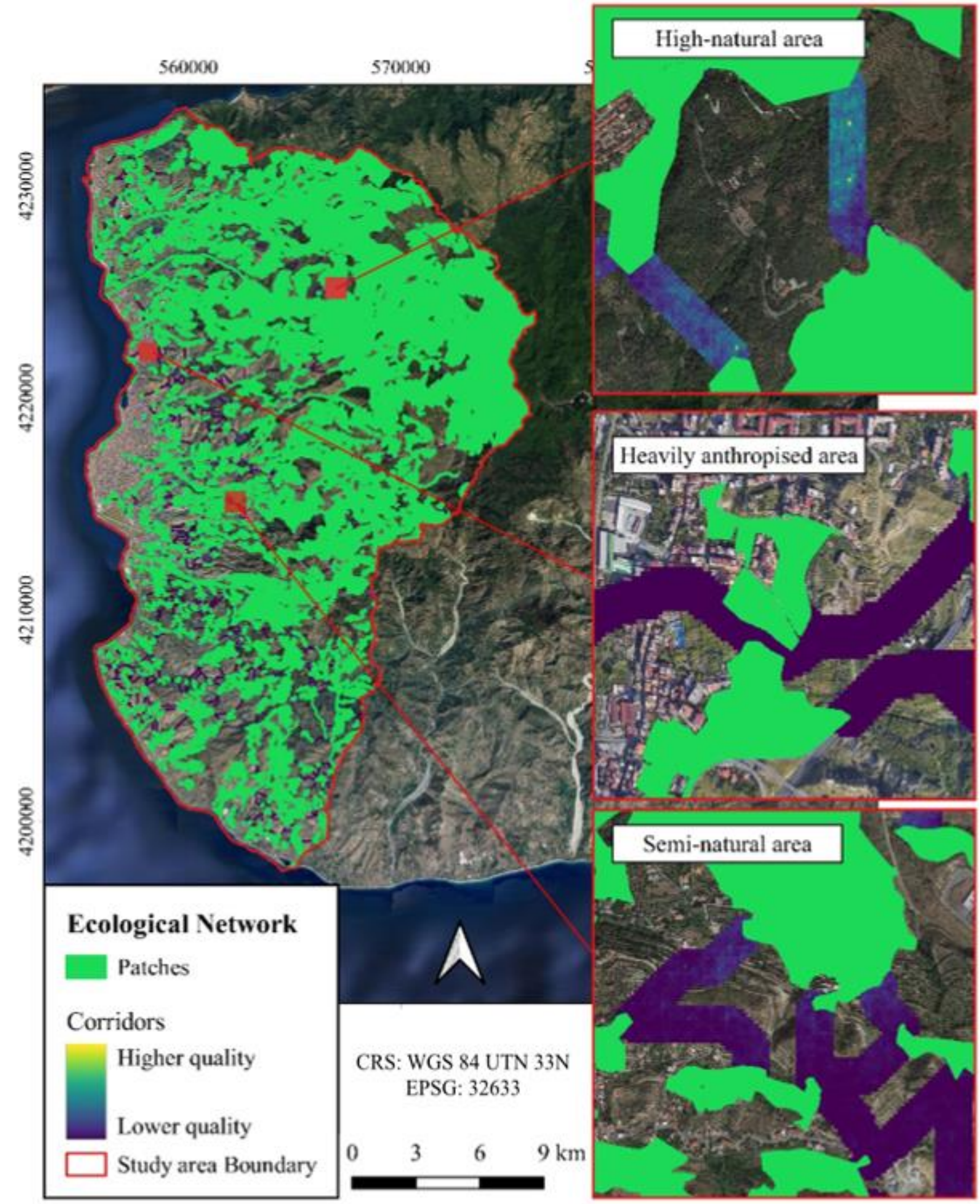

Figure 6.7 - Representation of ecological network obtained with patches (in green) and corridors (in colour shades as per fig. 6.5 according to Pathwalker density surface map). On the right, we see three network details in semi-natural (down), heavily anthropised (centre), and high-natural (top) areas.

The results regarding the connectivity indices (Summarised in tab 6.3) showed a positive change in the indices from EN1 to EN2. In the IIC and BC indices, which were calculated at the node level (Fig. 6.8-6.9) we found an increase in values in coastal areas as a result of the defragmentation interventions. Overall, the value of both indices was higher in inland areas distant from large urban centres.

Table 6.3 - Average values of connectivity indices calculated.

Connectivity Indices	***EN1***	***EN2***
Number of Components (NC)	60	20
Integral Index of Connectivity (IIC)	0.029	0.032
Probability of Connectivity (PC)	0.095	0.11
Flux (F)	1.88	2.55
Betweenness Centrality (BC)	0.098	0.21
Harary Index (H)	5075.28	7852.24

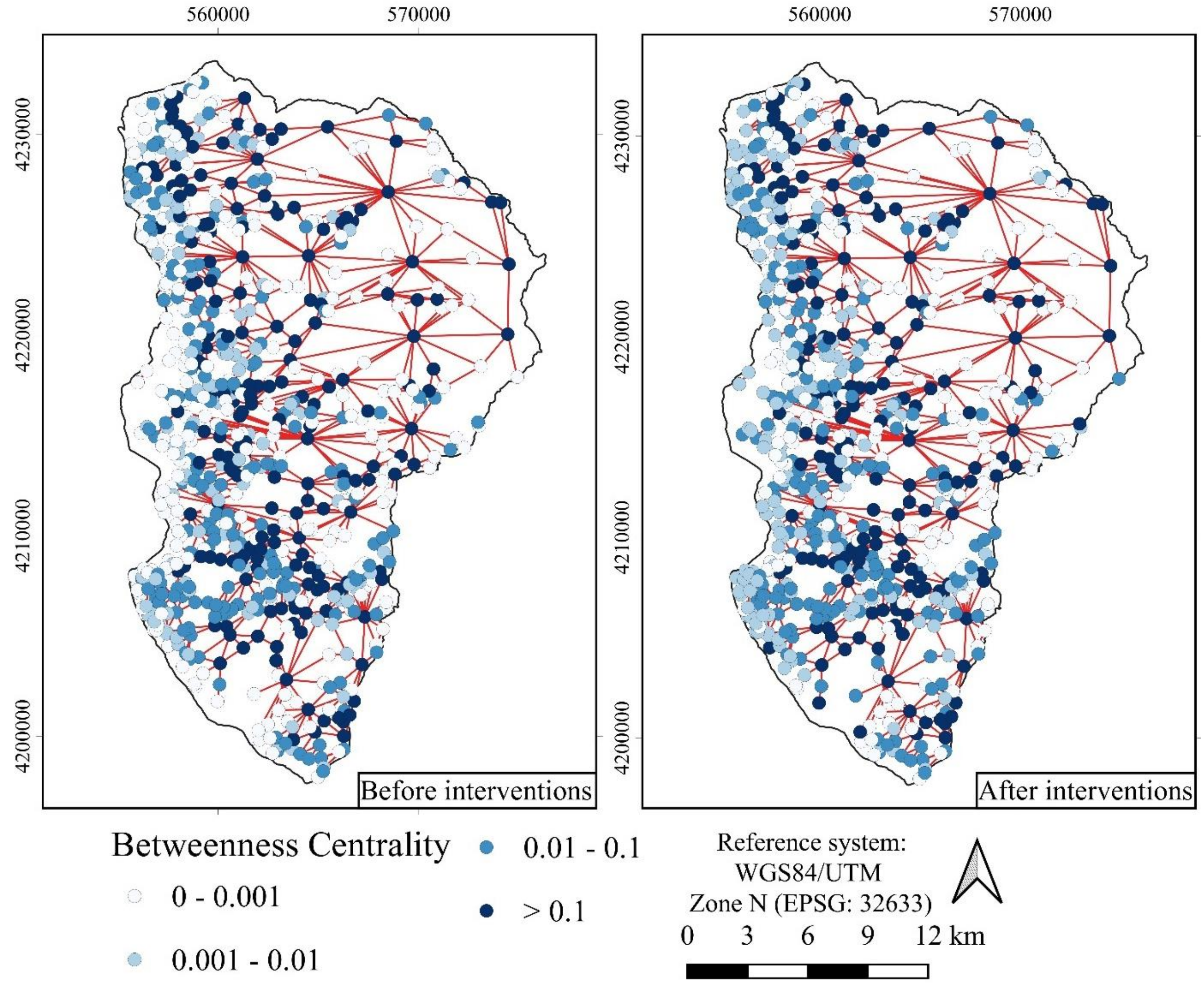

Figure 6.8 - Betweenness Centrality was calculated at the node level before (left) and after (right) defragmentation interventions. Lighter shades of blue indicate low connectivity and darker shades indicate high connectivity.

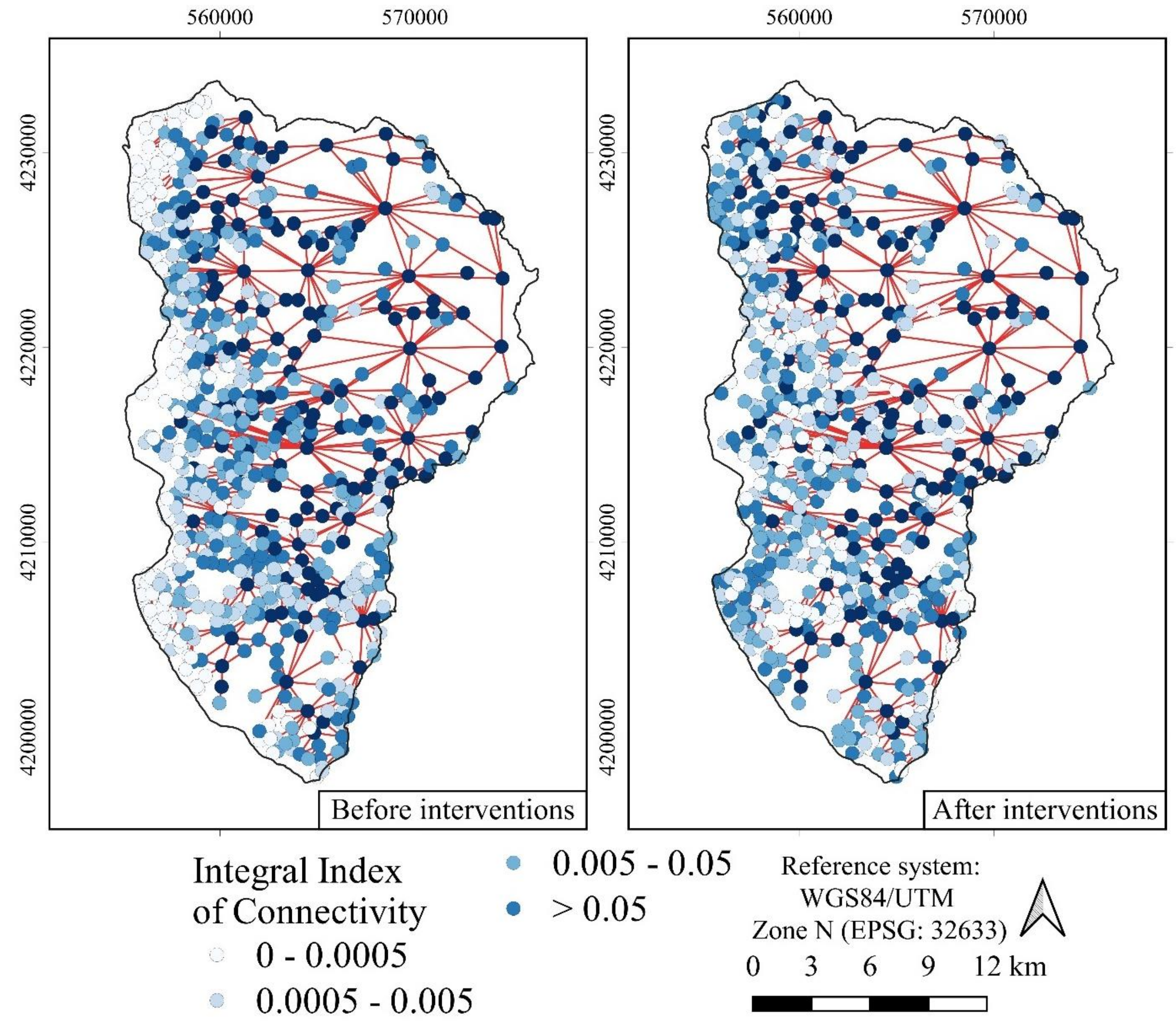

Figure 6.9 - Integral Index of Connectivity calculated at node level before (left) and after (right) defragmentation interventions. Lighter shades of blue indicate low connectivity and darker shades indicate high connectivity.

6.4. Discussion

Analysis of the results obtained on the Ecological Network and its defragmentation scenario showed in both cases that the best-connected areas those far from population centres. Coastal areas near Reggio Calabria show a high number of patches, especially of habitat code categories 84 and 85. Analysing the results in tab. 6.1, we see that these two habitats have a number of patches approaching half of the total for the entire network. The high number of patches with a small mean area, combined with low standard deviation values, confirms the high fragmentation character of these environments. In these patches, we will have a high content of edge habitats at the expense of core habitats, which is detrimental to the ecological qualities of these places (Gascon et al., 2000; Gignac & Dale, 2007). In contrast, we find high standard deviation values in habitats mostly located east of the study area. In hilly or mountainous areas, habitats such as 4.18, 45.21 and 41.9 are mostly forested in character. This leads us to observe that although these environments often possess large patches of good quality, some small patches are separated from the large patches due to anthropogenic activities.

The connectivity indices also confirm this trend. Fig. 6.5 shows us Pathwalker's density surface map, with high probability areas for the animal in mountainous areas, while the values drop in coastal areas. This result is expected, considering the work done by Unnithan Kumar & Cushman, 2022 and the results obtained in Chapter 4. Indeed, in urbanised areas, the ability to also consider factors such as risk and attraction plays a key role in the realistic nature of predictions. Network areas where there is a high concentration of roads result in increased roadkill mortalities (Coffin, 2007; Filius et al., 2020; Russo et al., 2020; Schwartz et al., 2020). For this reason, in the corridors (Fig. 6.7) obtained around the LCPs, we see a difference in the quality of corridors crossing heavily man-made areas (low quality) compared to those crossing natural areas (high quality). The greater number of suitable corridors found by the analysis on the Pathwalker affinity map (Fig. 6.6) compared to the corridors obtained in the final network (Fig. 6.7) is expected, considering that the corridors were constructed from a least-coast path. However, the presence of these corridors not included in the network may provide an important structural element of the network. These areas could be considered as stepping stones or as transition areas of the network.

The defragmentation interventions increased the connectivity of areas close to population centres, connecting 162 hectares of patches to the rest of the network. In particular, from Tab. 6.2 we see that the most remarkable results were obtained with the renaturation interventions. This is due to the type of areas that this intervention has reconnected, mostly agricultural areas or old cultivated areas now abandoned, on the edge of the city, of large extension (around 120 ha). In contrast, interventions such as green bridges and underpasses have connected smaller patch areas to the network (around 25ha). However, this does not denote a lower effectiveness of the latter, having a performance in terms of intervention occupied area/new patches occupied area of +445 % for green bridges, +437 % for green trees and +2265 % for green subways. The lower value of the total area reconnected to the ecological network is found in patches' nature. Urban green areas, gardens, urban parks, were found to be smaller in size, located in areas strongly influenced by anthropogenic elements, more suitable for this type of capillary intervention (Cameron et al., 2012; Cannas et al., 2018; Wu et al., 2023; Wuit Yee Kyaw et al., 2023).

The interventions had a positive effect on the network as confirmed by the connectivity indices (Tab. 6.3). The increase in the Harary index value in EN2 indicates a better-connected network (Harary, 1969), as well as the increase in BC calculated at the node level in areas that were disconnected in EN1 shows that they have become more important to the network in EN2, acting as stepping stones for other patches of the ecological network (Urban et al., 2009). This is in line with the increase in connections that have occurred in these areas with 47 new corridors, which, by increasing the likelihood of species moving between patches in this air, finds justification for the increase in the Flux index, which expresses precisely this likelihood (Saura & Pascual-Hortal, 2007). The increase in the number of corridors reduced the number of network components from 60 to 20, significantly reducing the number of isolated areas in the ecological network. The increase in the IIC index calculated at the node level underscores an increase in the spatial continuity of the ecological network, where defragmentation interventions have played a key role in enabling this (Pascual-Hortal & Saura, 2006, 2008). The VFC values are also in line with the rest of the indices, so we have higher values in the mountain area, mainly occupied by coniferous and broadleaf forests, while the lowest values are recorded in the coastal area. This is to be expected considering that the VFC index is able to identify the areas of highest vegetation vigour, which is lost as the land becomes more anthropised.

6.5. Conclusions

In this work were applied some of the most commonly used connectivity modelling strategies to create a multi-species ecological network, and a second network to create a defragmentation scenario in a Mediterranean climate metropolitan area. Specifically, we first used graph theory to identify some of the canonical network elements (patches, nodes and LCPs), studying their characteristics through different connectivity indices (IIC, F, PC, BC). We then used Pathwalker's movement simulations to identify a suitability map showing the places where animals are most likely to pass through and use it in conjunction with the LCPs to determine the corridors of the ecological network. The starting data for this work were a habitat map, specifically created for this purpose, data on the slopes of the study area, multispectral satellite images for calculating the VFC index, data on the autecological characteristics of the animal species in the study area. The use of a habitat map and species data provided by a local fauna expert made it possible to improve the value of this work. The study area before the defragmentation scenario were extremely fragmented, especially in the coastal area. This problem was considerably reduced as a result of the defragmentation measures (assumption of bridges, green subways, tree-lined avenues). The combined use of graph theory and movement simulations made it possible to exploit the strengths of the two models. In particular, the ability to give a precise spatialisation of the elements of graph theory (patches and LCP), and the greater accuracy in identifying animal passage areas (corridors) of Pathwalker (movement simulation software). The final network, following the defragmentation interventions, shows itself to be robust, greatly improved with respect to the starting situation and with good spatial continuity in the study area. This work has given new insights for research, being the first work to use a habitat map instead of a land use map, and to exploit two different connectivity modelling models to obtain a single network. In addition, the use of satellite data and indices such as the VFC are of great inspiration for the future, making it possible to overcome the limitation of land use maps or habitat maps that are updated in some cases every several years.

7. General Conclusions

All over the world, the emergence of large cities, villages, road networks, railways, and numerous other man-made interventions have resulted in fragmentation, isolation, and loss of natural habitats. These interferences between natural and artificial environments cause the reduction in the area of natural surfaces, the progressive spacing between residual fragments, and the consequent habitat loss. There is an increasing awareness of this issue among governments and the scientific community. In this scenario, for sustainable spatial planning, ecological networks are themselves the object of spatial planning. Their implementation can counteract landscape fragmentation, create and strengthen relationships, and promote exchanges between otherwise isolated elements.

In this Ph.D. thesis, the goal was to implement, through cartographic representation, an ecological network within a Mediterranean ecosystem in the Calabria region. We analysed different connectivity modelling strategies such as circuit theory, graph theory, resistant kernels, least-cost paths, and innovative movement simulation models to achieve our goal. In addition, in two separate steps, we first took advantage of the most up-to-date map data provided by the European Union through Copernicus, and in a second step, we produced new original map data as part of the international Natura 2000 project. Among the goals we set, many were achieved:

- ✓ Outline an ecological network considering the need for space for both sides, natural and anthropogenic, by capturing maximum detail from two Copernicus datasets created to represent the two sides, respectively.
- ✓ To identify which model is more reliable, compare different connectivity modelling strategies based on casual sub distribution of individuals in the network or stable position within patches.
- ✓ Compare different movement simulation models, movement strategies, source point assignments, dispersal distances, and connectivity indices to understand which variables most influence connectivity.
- ✓ Constructing a habitat map that allowed the levels of affinity with animal species to be captured in maximum detail.
- ✓ Implement an innovative method of ecological network construction based not on a land use map but on a habitat map. Implemented by exploiting the strengths of the most modern landscape connectivity simulation strategies.

The obtained results provided a useful contribution to the topic, emphasising the importance of the decision process not focusing on a single strategy, considering the complexity of ecological dynamics. In addition, ecological network production on a habitat map is currently lacking in the literature, and this work has contributed to this field.

We have also performed numerous simulations to show how the network responds differently to each variable change. The advantage of this approach is that it allows connectivity predictions to be made over areas where data on actual animal movements are not available, and it allows this to be done at a low cost and in a short time. On the other hand, this limitation does not allow the exact degree of reliability of the predictions to be assessed on actual data. This gives rise to insights into the possibility of applying these models to natural animal movement patterns data, used as a test to increasingly perfect these models.

8 Bibliography

An, Y., Liu, S., Sun, Y., Shi, F., & Beazley, R. (2021a). Construction and optimization of an ecological network based on morphological spatial pattern analysis and circuit theory. *Landscape Ecology*, *36*(7), 2059–2076. https://doi.org/10.1007/s10980-020-01027-3

An, Y., Liu, S., Sun, Y., Shi, F., & Beazley, R. (2021b). Construction and optimization of an ecological network based on morphological spatial pattern analysis and circuit theory. *Landscape Ecology*, *36*(7), 2059–2076. https://doi.org/10.1007/S10980-020-01027-3/FIGURES/8

An, Y., Liu, S., Sun, Y., Shi, F., & Beazley, R. (2021c). Construction and optimization of an ecological network based on morphological spatial pattern analysis and circuit theory. *Landscape Ecology*, *36*(7), 2059–2076. https://doi.org/10.1007/s10980-020-01027-3

Ash, E., Cushman, S. A., Redford, T., Macdonald, D. W., & Kaszta, Ż. (2022). Tigers on the edge: mortality and landscape change dominate individual-based spatially-explicit simulations of a small tiger population. *Landscape Ecology*, *37*(12), 3079–3102. https://doi.org/10.1007/s10980-022-01494-w

Balbi, M., Petit, E. J., Croci, S., Nabucet, J., Georges, R., Madec, L., & Ernoult, A. (2019a). Title : Ecological relevance of least cost path analysis : An easy implementation method for landscape urban planning. *Journal of Environmental Management*, *244*(January), 61–68. https://doi.org/10.1016/j.jenvman.2019.04.124

Balbi, M., Petit, E. J., Croci, S., Nabucet, J., Georges, R., Madec, L., & Ernoult, A. (2019b). Title: Ecological relevance of least cost path analysis: An easy implementation method for landscape urban planning. *Journal of Environmental Management*, *244*, 61–68. https://doi.org/10.1016/J.JENVMAN.2019.04.124

Battisti, C. (2004). *Frammentazione ambientale connettività reti ecologiche*. http://dau.ing.univaq.it/planeco/battisti.pdf

Beier, P., Spencer, W., Baldwin, R. F., & Mcrae, B. H. (2011). Toward Best Practices for Developing Regional Connectivity Maps. *Conservation Biology*, *25*(5), 879–892. https://doi.org/10.1111/j.1523-1739.2011.01716.x

Bender, D. J., Contreras, T. A., & Fahrig, L. (1998). Habitat Loss and Population Decline: A Meta-Analysis of the Patch Size Effect. *Ecology*, *79*(2), 517. https://doi.org/10.2307/176950

Bennet, G. (n.d.). *Bennett, G. (ed.), Towards a European Ecological Network. Insitute for European Environmental Policy/Ministry of Agriculture, Nature Manage- ment and Fisheries, the Netherlands, 1991, 80pp*.

Beyer, H. L., Gurarie, E., Börger, L., Panzacchi, M., Basille, M., Herfindal, I., Van Moorter, B., R. Lele, S., & Matthiopoulos, J. (2016). 'You shall not pass!': quantifying barrier permeability and proximity avoidance by animals. *Journal of Animal Ecology*, *85*(1), 43–53. https://doi.org/10.1111/1365-2656.12275

Bishop-Taylor, R., Tulbure, M. G., & Broich, M. (2015). Surface water network structure, landscape resistance to movement and flooding vital for maintaining ecological connectivity across Australia's largest river basin. *Landscape Ecology*, *30*(10), 2045–2065. https://doi.org/10.1007/s10980-015-0230-4

Boitani, L., Corsi, F., Falcucci, A., Marzetti, I., Masi, M., Montemaggiori, A., Ottaviani, D., Reggiani, G., & Rondinini, C. (2002a). *Rete Ecologica Nazionale. Un approccio alla conservazione dei vertebrati italiani*. . in. Università di Roma "La Sapienza", Dipartimento di Biologia Animale e dell'Uomo; Ministero dell'Ambiente, Direzione per la Conservazione della Natura; Istituto di Ecologia Applicata.

Boitani, L., Corsi, F., Falcucci, A., Marzetti, I., Masi, M., Montemaggiori, A., Ottaviani, D., Reggiani, G., & Rondinini, C. (2002b). *Rete Ecologica Nazionale. Un approccio alla conservazione dei vertebrati italiani*. in. Università di Roma "La Sapienza", Dipartimento di Biologia Animale e dell'Uomo; Ministero dell'Ambiente, Direzione per la Conservazione della Natura; Istituto di Ecologia Applicata.

Boitani, L., Falcucci, A., Maiorano, L., & Montemaggiori, A. (2003). *Italian Ecological Network: the Role of Protected Areas in the Conservation of Vertebrates* (I. of A. E. Animal and Human Biology Department, University of Rome "La Sapienza", Nature Conservation Directorate of the Italian Ministry of Environment, Ed.).

Boitani, L., FALCUCCI, A., MAIORANO, L., & RONDININI, C. (2007a). Ecological Networks as Conceptual Frameworks or Operational Tools in Conservation. *Conservation Biology*, *21*(6), 1414–1422. https://doi.org/10.1111/j.1523-1739.2007.00828.x

Boitani, L., FALCUCCI, A., MAIORANO, L., & RONDININI, C. (2007b). Ecological Networks as Conceptual Frameworks or Operational Tools in Conservation. *Conservation Biology*, *21*(6), 1414–1422. https://doi.org/10.1111/j.1523-1739.2007.00828.x

Bonnin, M. (2007). *Le Réseau écologique paneuropéen: état d'avancement, Strasbourg, Éditions du Conseil de l'Europe, Sauvegarde de la nature, no 146.*

Bourdouxhe, A., Duflot, R., Radoux, J., & Dufrêne, M. (2020). Comparison of methods to model species habitat networks for decision-making in nature conservation: The case of the wildcat in southern Belgium. *Journal for Nature Conservation*, *58*, 125901. https://doi.org/10.1016/j.jnc.2020.125901

Bourgeois, M., & Sahraoui, Y. (2020). Modelling in the Context of an Environmental Mobilisation: A Graph-Based Approach for Assessing the Landscape Ecological Impacts of a Highway Project. *Ekológia (Bratislava)*, *39*(1), 88–100. https://doi.org/10.2478/eko-2020-0007

Braun-Blanquet, J. (1921). *Prinzipien einer Systematik der Pflanzengesellschaften auf floristischer Grundlage.- Jahrb. St. Gallischen Naturwiss. Ges. 57(2): 305-351.*

Cafaro, P., Hansson, P., & Götmark, F. (2022). Overpopulation is a major cause of biodiversity loss and smaller human populations are necessary to preserve what is left. *Biological Conservation*, *272*, 109646. https://doi.org/10.1016/j.biocon.2022.109646

Calabrò, F., Iannone, L., & Pellicanò, R. (2021). *The Historical and Environmental Heritage for the Attractiveness of Cities. The Case of the Umbertine Forts of Pentimele in Reggio Calabria, Italy* (pp. 1990–2004). https://doi.org/10.1007/978-3-030-48279-4_188

Carr, M. H. , Z. P. D. , H. T. , H. W. , G. A. & B. B. (1998). *Using GIS for identifying the interfacebetween ecological greenways and roadway systems at the state andsub-state scales. In: Proceedings of the 1998 International Conferenceon Wildlife Ecology and Transportation, ed. G.L. Evink, P. Garrett,D. Zeigler & J. Berry, pp. 68–77, Tallahassee, USA: FloridaDepartment of Transportation*.

Casas, E., Fernandez, M., Gil, A., Yesson, C., Prestes, A., Moreu-Badia, I., Neto, A., & Arbelo, M. (2021). Macroalgae niche modelling: a two-step approach using remote sensing and in situ observations of a native and an invasive Asparagopsis. *Biological Invasions*, *23*(10). https://doi.org/10.1007/s10530-021-02554-z

Ciofi, C., & Chelazzi, G. (1991). Radiotracking of Coluber viridiflavus Using External Transmitters. *Journal of Herpetology*, *25*(1), 37. https://doi.org/10.2307/1564792

Clark, W. R. (2010). Principles of Landscape Ecology. In *Nature Education Knowledge* (Vol. 3, Issue 10). http://www.nature.com/scitable/knowledge/library/principles-of-...

Clauzel, C., & Godet, C. (2020). Combining spatial modeling tools and biological data for improved multispecies assessment in restoration areas. *Biological Conservation*, *250*, 108713. https://doi.org/10.1016/J.BIOCON.2020.108713

Clevenger, A. P., & Wierzchowski, J. (2006). Maintaining and restoring connectivity in landscapes fragmented by roads. In *Connectivity Conservation* (pp. 502–535). Cambridge University Press. https://doi.org/10.1017/CBO9780511754821.023

Coffin, A. W. (2007). From roadkill to road ecology: A review of the ecological effects of roads. *Journal of Transport Geography*, *15*(5), 396–406. https://doi.org/10.1016/j.jtrangeo.2006.11.006

COMPTON, B. W., McGARIGAL, K., CUSHMAN, S. A., & GAMBLE, L. R. (2007). A Resistant-Kernel Model of Connectivity for Amphibians that Breed in Vernal Pools. *Conservation Biology*, *21*(3), 788–799. https://doi.org/10.1111/j.1523-1739.2007.00674.x

Cushman, S. A. (2006). Effects of habitat loss and fragmentation on amphibians: A review and prospectus. *Biological Conservation*, *128*(2), 231–240. https://doi.org/10.1016/j.biocon.2005.09.031

Cushman, S. A., Elliot, N. B., Macdonald, D. W., & Loveridge, A. J. (2016). A multi-scale assessment of population connectivity in African lions (Panthera leo) in response to landscape change. *Landscape Ecology*, *31*(6), 1337–1353. https://doi.org/10.1007/s10980-015-0292-3

Cushman, S. A., & Landguth, E. L. (2012). Multi-taxa population connectivity in the Northern Rocky Mountains. *Ecological Modelling*, *231*, 101–112. https://doi.org/10.1016/j.ecolmodel.2012.02.011

Cushman, S. A., Landguth, E. L., & Flather, C. H. (2012a). Evaluating the sufficiency of protected lands for maintaining wildlife population connectivity in the U.S. northern Rocky Mountains. *Diversity and Distributions*, *18*(9), 873–884. https://doi.org/10.1111/j.1472-4642.2012.00895.x

Cushman, S. A., Landguth, E. L., & Flather, C. H. (2012b). Evaluating the sufficiency of protected lands for maintaining wildlife population connectivity in the U.S. northern Rocky Mountains. *Diversity and Distributions*, *18*(9), 873–884. https://doi.org/10.1111/j.1472-4642.2012.00895.x

Cushman, S. A., Landguth, E. L., & Flather, C. H. (2013). Evaluating population connectivity for species of conservation concern in the American Great Plains. *Biodiversity and Conservation*, *22*(11), 2583–2605. https://doi.org/10.1007/s10531-013-0541-1

Cushman, S. A., & Lewis, J. S. (2010). Movement behavior explains genetic differentiation in American black bears. *Landscape Ecology*, *25*(10), 1613–1625. https://doi.org/10.1007/s10980-010-9534-6

Cushman, S. A., Lewis, J. S., & Landguth, E. L. (2013). Evaluating the intersection of a regional wildlife connectivity network with highways. *Movement Ecology*, *1*(1), 12. https://doi.org/10.1186/2051-3933-1-12

Cushman, S. A., Macdonald, D. W., Willis, K. J., McRae, B., Adriaensen, F., Beier, P., Shirley, M., & Zeller, K. (2013). *Biological corridors and connectivity [Chapter 21]*.

Cushman, S. A., McKelvey, K. S., Hayden, J., & Schwartz, M. K. (2006). Gene Flow in Complex Landscapes: Testing Multiple Hypotheses with Causal Modeling. *The American Naturalist*, *168*(4), 486–499. https://doi.org/10.1086/506976

CUSHMAN, S. A., McKELVEY, K. S., & SCHWARTZ, M. K. (2009). Use of Empirically Derived Source-Destination Models to Map Regional Conservation Corridors. *Conservation Biology*, *23*(2), 368–376. https://doi.org/10.1111/j.1523-1739.2008.01111.x

Cushman, S. A., Shirk, A. J., Howe, G. T., Murphy, M. A., Dyer, R. J., & Joost, S. (2018). Editorial: The Least Cost Path From Landscape Genetics to Landscape Genomics: Challenges and Opportunities to Explore NGS Data in a Spatially Explicit Context. *Frontiers in Genetics*, *9*. https://doi.org/10.3389/fgene.2018.00215

Cushman, S., Lewis, J., & Landguth, E. (2014a). Why Did the Bear Cross the Road? Comparing the Performance of Multiple Resistance Surfaces and Connectivity Modeling Methods. *Diversity*, *6*(4), 844–854. https://doi.org/10.3390/d6040844

Cushman, S., Lewis, J., & Landguth, E. (2014b). Why Did the Bear Cross the Road? Comparing the Performance of Multiple Resistance Surfaces and Connectivity Modeling Methods. *Diversity*, *6*(4), 844–854. https://doi.org/10.3390/d6040844

De Montis, A., Caschili, S., Mulas, M., Modica, G., Ganciu, A., Bardi, A., Ledda, A., Dessena, L., Laudari, L., & Fichera, C. R. (2016). Urban–rural ecological networks for landscape planning. *Land Use Policy*, *50*, 312–327. https://doi.org/10.1016/j.landusepol.2015.10.004

Diaz, N., & Apostol, D. (1992). *No Title*. *“Forest la*.

Diniz, M. F., Cushman, S. A., Machado, R. B., & De Marco Júnior, P. (2020a). Landscape connectivity modeling from the perspective of animal dispersal. *Landscape Ecology*, *35*(1), 41–58. https://doi.org/10.1007/s10980-019-00935-3

Diniz, M. F., Cushman, S. A., Machado, R. B., & De Marco Júnior, P. (2020b). Landscape connectivity modeling from the perspective of animal dispersal. *Landscape Ecology*, *35*(1), 41–58. https://doi.org/10.1007/s10980-019-00935-3

Diniz, M. F., Machado, R. B., Bispo, A. A., & De M. Júnior, P. (2018). Can we face different types of storms under the same umbrella? Efficiency and consistency of connectivity umbrellas across different patchy landscape patterns. *Landscape Ecology*, *33*(11), 1911–1923. https://doi.org/10.1007/S10980-018-0720-2/FIGURES/2

Dong, J., Peng, J., Liu, Y., Qiu, S., & Han, Y. (2020). Integrating spatial continuous wavelet transform and kernel density estimation to identify ecological corridors in megacities. *Landscape and Urban Planning*, *199*, 103815. https://doi.org/10.1016/j.landurbplan.2020.103815

Dray, S., Royer-Carenzi, M., & Calenge, C. (2010). The exploratory analysis of autocorrelation in animal-movement studies. *Ecological Research*, *25*(3), 673–681. https://doi.org/10.1007/s11284-010-0701-7

Dugatkin, L. A. (2020). *Principles of animal behavior*.

Dunn, C. P., & Loehle, C. (1988). Species-Area Parameter Estimation: Testing the Null Model of Lack of Relationship. *Journal of Biogeography*, *15*(5/6), 721. https://doi.org/10.2307/2845335

Elsen, P. R., Monahan, W. B., & Merenlender, A. M. (2018). Global patterns of protection of elevational gradients in mountain ranges. *Proceedings of the National Academy of Sciences*, *115*(23), 6004–6009. https://doi.org/10.1073/pnas.1720141115

Ersoy, E., Jorgensen, A., & Warren, P. H. (2019a). Identifying multispecies connectivity corridors and the spatial pattern of the landscape. *Urban Forestry & Urban Greening*, *40*, 308–322. https://doi.org/10.1016/J.UFUG.2018.08.001

Ersoy, E., Jorgensen, A., & Warren, P. H. (2019b). Urban Forestry & Urban Greening Identifying multispecies connectivity corridors and the spatial pattern of the. *Urban Forestry & Urban Greening*, *40*(June 2018), 308–322. https://doi.org/10.1016/j.ufug.2018.08.001

Erwin, T. L. (2007). Applying Nature’s Design: Corridors as a Strategy for Biodiversity Conservation. Issues, Cases, and Methods in Biodiversity Conservation. By Anthony B Anderson and , Clinton N Jenkins. New York: Columbia University Press . $74.50 (hardcover); $34.50 (pape. *The Quarterly Review of Biology*, *82*(1), 72–72. https://doi.org/10.1086/513391

Ewers, R. M., Stephen, T., & Raphael, K. D. (2007). *No Title*. *“Synergist*.

Fichera, C. R., Laudari, L., & Modica, G. (2015). Application, validation and comparison in different geographical contexts of an integrated model for the design of ecological networks. *Journal of Agricultural Engineering*, *46*(2), 52. https://doi.org/10.4081/jae.2015.459

Filius, J., van der Hoek, Y., Jarrín-V, P., & van Hooft, P. (2020). Wildlife roadkill patterns in a fragmented landscape of the Western Amazon. *Ecology and Evolution*, *10*(13), 6623–6635. https://doi.org/10.1002/ece3.6394

Fletcher, Jr., R. J., Ries, L., Battin, J., & Chalfoun, A. D. (2007). The role of habitat area and edge in fragmented landscapes: definitively distinct or inevitably intertwined?This review is one of a series dealing with some aspects of the impact of habitat fragmentation on animals and plants. This series is one of severa. *Canadian Journal of Zoology*, *85*(10), 1017–1030. https://doi.org/10.1139/Z07-100

Foltête, J.-C. (2019). How ecological networks could benefit from landscape graphs: A response to the paper by Spartaco Gippoliti and Corrado Battisti. *Land Use Policy*, *80*(February 2018), 391–394. https://doi.org/10.1016/j.landusepol.2018.04.020

Foltête, J.-C., Céline Clauzel, Gilles Vuidel, & Pierline Tournant. (2012a). Integrating graph-based connectivity metrics into species distribution models. *Landscape Ecology*, *27*(4), 557–569.

Foltête, J.-C., Céline Clauzel, Gilles Vuidel, & Pierline Tournant. (2012b). Integrating graph-based connectivity metrics into species distribution models. *Landscape Ecology*, *27*(4), 557–569.

Foltête, J.-C., Clauzel, C., & Vuidel, G. (2012). A software tool dedicated to the modelling of landscape networks. *Environmental Modelling & Software*, *38*, 316–327. https://doi.org/10.1016/j.envsoft.2012.07.002

Foltête, J.-C., Girardet, X., & Clauzel, C. (2014). A methodological framework for the use of landscape graphs in land-use planning. *Landscape and Urban Planning*, *124*, 140–150. https://doi.org/10.1016/j.landurbplan.2013.12.012

Foltête, J.-C., Vuidel, G., Savary, P., Clauzel, C., Sahraoui, Y., Girardet, X., & Bourgeois, M. (2021a). Graphab: An application for modeling and managing ecological habitat networks. *Software Impacts, 8*, 100065. https://doi.org/10.1016/j.simpa.2021.100065

Foltête, J.-C., Vuidel, G., Savary, P., Clauzel, C., Sahraoui, Y., Girardet, X., & Bourgeois, M. (2021b). Graphab: An application for modeling and managing ecological habitat networks. *Software Impacts, 8*, 100065. https://doi.org/10.1016/j.simpa.2021.100065

Formica, V. A., Augat, M. E., Barnard, M. E., Butterfield, R. E., Wood, C. W., & Brodie, E. D. (2010). Using home range estimates to construct social networks for species with indirect behavioral interactions. *Behavioral Ecology and Sociobiology*, *64*(7), 1199–1208. https://doi.org/10.1007/s00265-010-0957-5

Franco, D. (2004). *No Title*. *Ecological*.

Freeman, L. C. (1977). A set of measures of centrality based on betweenness. *Sociometry*, *40*(1).

Freeman, L. C. (1978). Centrality in social networks conceptual clarification. *Social Networks*, *1*(3), 215–239. https://doi.org/10.1016/0378-8733(78)90021-7

Fricke, E. C., & Svenning, J.-C. (2020). Accelerating homogenization of the global plant–frugivore meta-network. *Nature*, *585*(7823), 74–78. https://doi.org/10.1038/s41586-020-2640-y

Gascon, C., Williamson, G. B., & da Fonseca, G. A. B. (2000). Receding Forest Edges and Vanishing Reserves. *Science*, *288*(5470), 1356–1358. https://doi.org/10.1126/science.288.5470.1356

Gent H., A. S. F. (1993). *MOVEMENT RATES OF THE SMOOTH SNAKE CORONELLA A USTRIACA (COLUBRIDAE) : A RADIO-TELEMETRIC STUDY. Herp. Jour. Vol. 3, pp. 140-146*.

Gibbs, J. P. (1998). Amphibian Movements in Response to Forest Edges, Roads, and Streambeds in Southern New England. *The Journal of Wildlife Management*, *62*(2), 584. https://doi.org/10.2307/3802333

Gignac, L. D., & Dale, M. R. T. (2007). Effects of size, shape, and edge on vegetation in remnants of the upland boreal mixed-wood forest in agro-environments of Alberta, Canada. *Canadian Journal of Botany*, *85*(3), 273–284. https://doi.org/10.1139/B07-018

Girardet, X., Conruyt-Rogeon, G., & Foltête, J.-C. (2015). Does regional landscape connectivity influence the location of roe deer roadkill hotspots? *European Journal of Wildlife Research*, *61*(5), 731–742. https://doi.org/10.1007/s10344-015-0950-4

Glandt D. (1986). *Die saisonalen Wanderungen der mittleuropäischen Amphibien. Bonner Zoologische Beiträge 37, 211-228*.

Godet, C., & Clauzel, C. (2021). Comparison of landscape graph modelling methods for analysing pond network connectivity. *Landscape Ecology*, *36*(3), 735–748. https://doi.org/10.1007/s10980-020-01164-9

Gorelick, N., Hancher, M., Dixon, M., Ilyushchenko, S., Thau, D., & Moore, R. (2017). Google Earth Engine: Planetary-scale geospatial analysis for everyone. *Remote Sensing of Environment*, *202*, 18–27. https://doi.org/10.1016/j.rse.2017.06.031

Griffiths R.A. (1995). *Newts and Salamanders of Europe. Poyser Natural History, London. - Schulte .*

Gross, J. L., & Yellen, J. (2005). *Graph Theory and Its Applications*. Chapman and Hall/CRC. https://doi.org/10.1201/9781420057140

Guimarães, P. R. (2020). The Structure of Ecological Networks Across Levels of Organization. *Annual Review of Ecology, Evolution, and Systematics*, *51*(1), 433–460. https://doi.org/10.1146/annurev-ecolsys-012220-120819

Guo, Y., & Liu, Y. (2017a). Connecting regional landscapes by ecological networks in the Greater Pearl River Delta. *Landscape and Ecological Engineering*, *13*(2), 265–278. https://doi.org/10.1007/S11355-016-0318-2/FIGURES/8

Guo, Y., & Liu, Y. (2017b). Connecting regional landscapes by ecological networks in the Greater Pearl River Delta. *Landscape and Ecological Engineering*, *13*(2), 265–278. https://doi.org/10.1007/S11355-016-0318-2/FIGURES/8

Gurrutxaga, M., Lozano, P. J., & del Barrio, G. (2010). GIS-based approach for incorporating the connectivity of ecological networks into regional planning. *Journal for Nature Conservation*, *18*(4), 318–326. https://doi.org/10.1016/j.jnc.2010.01.005

GURRUTXAGA, M., & SAURA, S. (2014). Prioritizing highway defragmentation locations for restoring landscape connectivity. *Environmental Conservation*, *41*(2), 157–164. https://doi.org/10.1017/S0376892913000325

Gustafson, E. J., & Gardner, R. H. (1996). The Effect of Landscape Heterogeneity on the Probability of Patch Colonization. *Ecology*, *77*(1), 94–107. https://doi.org/10.2307/2265659

Hanski, I. (1999). *Habitat Connectivity , Habitat Continuity , and Metapopulations in Dynamic Landscapes Author (s): Ilkka Hanski Published by : Wiley on behalf of Nordic Society Oikos Stable URL : https://www.jstor.org/stable/3546736 REFERENCES Linked references are avai*. *87*(2), 209–219.

Harary, F. (1969). *Graph Theory. CRC Press*. https://www.taylorfrancis.com/books/9780429493768.

Hardion, L., Pouvreau, M., Schwoertzig, E., Hoff, M., Nguefack, J., & Combroux, I. (2019). Performance, genetic and ecological insights for the conservation of the endangered large pink, Dianthus superbus L. (Caryophyllaceae) in semi-natural grassland. *Botany Letters*, *166*(1), 104–112. https://doi.org/10.1080/23818107.2018.1544506

Harper, K. A., MACDONALD, S. E., BURTON, P. J., CHEN, J., BROSOFSKE, K. D., SAUNDERS, S. C., EUSKIRCHEN, E. S., ROBERTS, D., JAITEH, M. S., & ESSEEN, P. (2005). Edge Influence on Forest Structure and Composition in Fragmented Landscapes. *Conservation Biology*, *19*(3), 768–782. https://doi.org/10.1111/j.1523-1739.2005.00045.x

Heller, N. E., & Zavaleta, E. S. (2009). Biodiversity management in the face of climate change: A review of 22 years of recommendations. *Biological Conservation*, *142*(1), 14–32. https://doi.org/10.1016/j.biocon.2008.10.006

Hilty, J., Worboys, G. L., Keeley, A., Woodley, S., Lausche, B. J., Locke, H., Carr, M., Pulsford, I., Pittock, J., White, J. W., Theobald, D. M., Levine, J., Reuling, M., Watson, J. E. M., Ament, R., & Tabor, G. M. (2020). *Guidelines for conserving connectivity through ecological networks and corridors* (C. Groves, Ed.). IUCN, International Union for Conservation of Nature. https://doi.org/10.2305/IUCN.CH.2020.PAG.30.en

Hu, J., Liu, Y., & Fang, J. (2021). Ecological Corridor Construction Based on Least-Cost Modeling Using Visible Infrared Imaging Radiometer Suite (VIIRS) Nighttime Light Data and Normalized Difference Vegetation Index. *Land*, *10*(8), 782. https://doi.org/10.3390/land10080782

Huck, M., Jędrzejewski, W., Borowik, T., Miłosz-Cielma, M., Schmidt, K., Jędrzejewska, B., Nowak, S., & Mysłajek, R. W. (2010). Habitat suitability, corridors and dispersal barriers for large carnivores in Poland. *Acta Theriologica*, *55*(2), 177–192. https://doi.org/10.4098/j.at.0001-7051.114.2009

Hudson, W. E. . (1991a). *Landscape Linkages and Biodiversity*. Island Press.

Hudson, W. E. . (1991b). *Landscape Linkages and Biodiversity*. Island Press.

Isaac, N. J. B., Brotherton, P. N. M., Bullock, J. M., Gregory, R. D., Boehning-Gaese, K., Connor, B., Crick, H. Q. P., Freckleton, R. P., Gill, J. A., Hails, R. S., Hartikainen, M., Hester, A. J., Milner-Gulland, E. J., Oliver, T. H., Pearson, R. G., Sutherland, W. J., Thomas, C. D., Travis, J. M. J., Turnbull, L. A., … Mace, G. M. (2018). Defining and delivering resilient ecological networks: Nature conservation in England. *Journal of Applied Ecology*, *55*(6), 2537–2543. https://doi.org/10.1111/1365-2664.13196

Jones, K. R., Venter, O., Fuller, R. A., Allan, J. R., Maxwell, S. L., Negret, P. J., & Watson, J. E. M. (2018). One-third of global protected land is under intense human pressure. *Science*, *360*(6390), 788–791. https://doi.org/10.1126/science.aap9565

Keijl, G. (1991). The network of wetlands for waterbird migration in the eastern Mediterranean. https://www.researchgate.net/publication/273595717

Kaszta, Ż., Cushman, S. A., & Macdonald, D. W. (2020). Prioritizing habitat core areas and corridors for a large carnivore across its range. Animal Conservation, 23(5), 607–616. https://doi.org/10.1111/acv.12575

Kaszta, Ż., Cushman, S. A., Sillero-Zubiri, C., Wolff, E., & Marino, J. (2018a). Where buffalo and cattle meet: modelling interspecific contact risk using cumulative resistant kernels. Ecography, 41(10), 1616–1626. https://doi.org/10.1111/ecog.03039

Kaszta, Ż., Cushman, S. A., Sillero-Zubiri, C., Wolff, E., & Marino, J. (2018b). Where buffalo and cattle meet: modelling interspecific contact risk using cumulative resistant kernels. Ecography, 41(10), 1616–1626. https://doi.org/10.1111/ecog.03039

Kaszta, Ż., Cushman, S. A., & Slotow, R. (2021). Temporal Non-stationarity of Path-Selection Movement Models and Connectivity: An Example of African Elephants in Kruger National Park. Frontiers in Ecology and Evolution, 9. https://doi.org/10.3389/fevo.2021.553263

Keeley, A. T. H., Beier, P., & Jenness, J. S. (2021). Connectivity metrics for conservation planning and monitoring. Biological Conservation, 255, 109008. https://doi.org/10.1016/J.BIOCON.2021.109008

Kevin McGarigal, S. A. C. S. S. (2000). Multivariate Statistics for Wildlife and Ecology Research. Springer-Verlag New York, Inc.

Kheirkhah Ghehi, N., MalekMohammadi, B., & Jafari, H. (2020). Integrating habitat risk assessment and connectivity analysis in ranking habitat patches for conservation in protected areas. Journal for Nature Conservation, 56, 125867. https://doi.org/10.1016/j.jnc.2020.125867

Khosravi, R., Hemami, M.-R., & Cushman, S. A. (2018). Multispecies assessment of core areas and connectivity of desert carnivores in central Iran. Diversity and Distributions, 24(2), 193–207. https://doi.org/10.1111/ddi.12672

Kumar, S. U., Kaszta, Ż., & Cushman, S. A. (n.d.-a). PATHWALKER: USER GUIDE. https://github.com/siddharth-unnithankumar/pathwalker.
Kumar, S. U., Kaszta, Ż., & Cushman, S. A. (n.d.-b). PATHWALKER: USER GUIDE. https://github.com/siddharth-unnithankumar/pathwalker.
Kyaw, P. P., Macdonald, D. W., Penjor, U., Htun, S., Naing, H., Burnham, D., Kaszta, Ż., & Cushman, S. A. (2021). Investigating Carnivore Guild Structure: Spatial and Temporal Relationships amongst Threatened Felids in Myanmar. ISPRS International Journal of Geo-Information, 10(12), 808. https://doi.org/10.3390/ijgi10120808
Lambeck, R. J. (2002). Focal Species and Restoration Ecology: Response to Lindenmayer et al. *Conservation Biology*, *16*(2), 549–551. https://doi.org/10.1046/j.1523-1739.2002.02007.x
LANDGUTH, E. L., & CUSHMAN, S. A. (2010). <scp>cdpop</scp> : A spatially explicit cost distance population genetics program. *Molecular Ecology Resources*, *10*(1), 156–161. https://doi.org/10.1111/j.1755-0998.2009.02719.x
Landguth, E. L., Hand, B. K., Glassy, J. M., Cushman, S. A., & Carlson, R. T. (2011). *UNICOR USER MANUAL 2011*.
Lechner, A. M., Doerr, V., Harris, R. M. B., Doerr, E., & Lefroy, E. C. (2015). A framework for incorporating fine-scale dispersal behaviour into biodiversity conservation planning. *Landscape and Urban Planning*, *141*, 11–23. https://doi.org/10.1016/j.landurbplan.2015.04.008
Lechner, A. M., & Lefroy, E. C. (2014a). *General Approach to Planning Connectivity from LOcal Scales to Regional (GAP CLoSR): combining multi-criteria analysis and connectivity science to enhance conservation outcomes at regional scale* (Issue March).
Lechner, A. M., & Lefroy, E. C. (2014b). *General Approach to Planning Connectivity from LOcal Scales to Regional (GAP CLoSR): combining multi-criteria analysis and connectivity science to enhance conservation outcomes at regional scale* (Issue March).
Legendre P., L. L. (1998). *Numerical ecology. Elsevier Science & Technology, 20, 853*.
Lelièvre, H., Moreau, C., Blouin-Demers, G., Bonnet, X., & Lourdais, O. (2012). Two Syntopic Colubrid Snakes Differ In Their Energetic Requirements and In Their Use of Space. *Herpetologica*, *68*(3), 358–364. https://doi.org/10.1655/HERPETOLOGICA-D-12-00007.1
Levins, R. (1969). *No Title*. *Some demog*.
Li, D., Yang, Y., Xia, F., Sun, W., Li, X., & Xie, Y. (2022). Exploring the influences of different processes of habitat fragmentation on ecosystem services. *Landscape and Urban Planning*, *227*, 104544. https://doi.org/10.1016/j.landurbplan.2022.104544
Liccari, F., Boscutti, F., Bacaro, G., & Sigura, M. (2022). Connectivity, landscape structure, and plant diversity across agricultural landscapes: novel insight into effective ecological network planning. *Journal of Environmental Management*, *317*, 115358. https://doi.org/10.1016/j.jenvman.2022.115358
Liu, J., Fan, J., Yang, C., Xu, F., & Zhang, X. (2022). Novel vegetation indices for estimating photosynthetic and non-photosynthetic fractional vegetation cover from Sentinel data. *International Journal of Applied Earth Observation and Geoinformation*, *109*, 102793. https://doi.org/10.1016/j.jag.2022.102793
Lumia G., M. G. , C. S. (2023). *Using simulation modeling to demonstrate the performance of graph theory metrics and connectivity algorithms*.
Luo, Y., Wu, J., Wang, X., & Peng, J. (2021a). Using stepping-stone theory to evaluate the maintenance of landscape connectivity under China's ecological control line policy. *Journal of Cleaner Production*, *296*, 126356. https://doi.org/10.1016/j.jclepro.2021.126356
Luo, Y., Wu, J., Wang, X., & Peng, J. (2021b). Using stepping-stone theory to evaluate the maintenance of landscape connectivity under China's ecological control line policy.

Journal of Cleaner Production, *296*, 126356. https://doi.org/10.1016/j.jclepro.2021.126356
MacArthur, R. H., & Wilson, E. O. (1963). AN EQUILIBRIUM THEORY OF INSULAR ZOOGEOGRAPHY. *Evolution*, *17*(4), 373–387. https://doi.org/10.1111/j.1558-5646.1963.tb03295.x
Macdonald, D. W., Bothwell, H. M., Kaszta, Ż., Ash, E., Bolongon, G., Burnham, D., Can, Ö. E., Campos-Arceiz, A., Channa, P., Clements, G. R., Hearn, A. J., Hedges, L., Htun, S., Kamler, J. F., Kawanishi, K., Macdonald, E. A., Mohamad, S. W., Moore, J., Naing, H., … Cushman, S. A. (2019). Multi-scale habitat modelling identifies spatial conservation priorities for mainland clouded leopards (*Neofelis nebulosa*). *Diversity and Distributions*, *25*(10), 1639–1654. https://doi.org/10.1111/ddi.12967
Mackovčin, P. (2000). A multi-level ecological network in the Czech Republic: Implementating the territorial system of ecological stability. *GeoJournal*, *51*(3), 211–220. https://doi.org/10.1023/A:1017518529210
Margules, C. R., & Pressey, R. L. (2000). Systematic conservation planning. *Nature*, *405*(6783), 243–253. https://doi.org/10.1038/35012251
Mateo-Sánchez, M. C., Balkenhol, N., Cushman, S., Pérez, T., Domínguez, A., & Saura, S. (2015a). Estimating effective landscape distances and movement corridors: comparison of habitat and genetic data. *Ecosphere*, *6*(4), 1–16. https://doi.org/10.1890/ES14-00387.1
Mateo-Sánchez, M. C., Balkenhol, N., Cushman, S., Pérez, T., Domínguez, A., & Saura, S. (2015b). Estimating effective landscape distances and movement corridors: comparison of habitat and genetic data. *Ecosphere*, *6*(4), 1–16. https://doi.org/10.1890/ES14-00387.1
Mateo-Sánchez, M. C., Cushman, S. A., & Saura, S. (2014). Connecting endangered brown bear subpopulations in the Cantabrian Range (north-western Spain). *Animal Conservation*, *17*(5), 430–440. https://doi.org/10.1111/acv.12109
May, R. (2006). "Connectivity" in urban rivers: Conflict and convergence between ecology and design. *Technology in Society*, *28*(4), 477–488. https://doi.org/10.1016/j.techsoc.2006.09.004
McCullough. (1996). *No Title*. *Metapopula*.
McGarigal, K., Stafford, S., & Cushman, S. (2000). *Multivariate Statistics for Wildlife and Ecology Research*. Springer New York. https://doi.org/10.1007/978-1-4612-1288-1
McGarigal, Kevin. , C. S. A. (2005). *The gradient concept of landscape structure. Issues and perspectives in landscape ecology*.
McRae, B. H., Dickson, B. G., Keitt, T. H., & Shah, V. B. (2008). USING CIRCUIT THEORY TO MODEL CONNECTIVITY IN ECOLOGY, EVOLUTION, AND CONSERVATION. *Ecology*, *89*(10), 2712–2724. https://doi.org/10.1890/07-1861.1
Meza-Joya, F. L., Ramos, E., & Cardona, D. (2019). SPATIO-TEMPORAL PATTERNS OF MAMMAL ROAD MORTALITY IN MIDDLE MAGDALENA VALLEY, COLOMBIA. *Oecologia Australis*, *23*(03), 575–588. https://doi.org/10.4257/oeco.2019.2303.15
Modica, G., Praticò, S., Laudari, L., Ledda, A., Di Fazio, S., & De Montis, A. (2021). Implementation of multispecies ecological networks at the regional scale: analysis and multi-temporal assessment. *Journal of Environmental Management*, *289*(April). https://doi.org/10.1016/j.jenvman.2021.112494
Mu, B., Liu, C., Tian, G., Xu, Y., Zhang, Y., Mayer, A. L., Lv, R., He, R., & Kim, G. (2020). Conceptual Planning of Urban–Rural Green Space from a Multidimensional Perspective: A Case Study of Zhengzhou, China. *Sustainability*, *12*(7), 2863. https://doi.org/10.3390/su12072863
Murcia, C. (1995). Edge effects in fragmented forests: implications for conservation. *Trends in Ecology & Evolution*, *10*(2), 58–62. https://doi.org/10.1016/S0169-5347(00)88977-6
Nevřelová, M., & Novota, M. (2020). Functionality of the Ecological Network Elements from the Point of View of Mammal Migrations in the Contact Zone of the Forest and

Agricultural Landscape. *Ekológia (Bratislava)*, *39*(1), 45–57. https://doi.org/10.2478/eko-2020-0004
Newman, M. E. J. (2004). Detecting community structure in networks. *The European Physical Journal B - Condensed Matter*, *38*(2), 321–330. https://doi.org/10.1140/epjb/e2004-00124-y
Newmark, W. D. (1995). Extinction of Mammal Populations in Western North American National Parks. *Conservation Biology*, *9*(3), 512–526. https://doi.org/10.1046/j.1523-1739.1995.09030512.x
Newmark, W. D. (2008). Isolation of African protected areas. *Frontiers in Ecology and the Environment*, *6*(6), 321–328. https://doi.org/10.1890/070003
Nie, W., Shi, Y., Siaw, M. J., Yang, F., Wu, R., Wu, X., Zheng, X., & Bao, Z. (2021). Constructing and optimizing ecological network at county and town Scale: The case of Anji County, China. *Ecological Indicators*, *132*, 108294. https://doi.org/10.1016/j.ecolind.2021.108294
Orjan Bodin, & Santiago Saura. (2010). Ranking individual habitat patches as connectivity providers: Integrating network analysis and patch removal experiments. *Ecological Modelling*, *221*(19), 2393–2405.
Pascual-Hortal, L., & Saura, S. (2006). Comparison and development of new graph-based landscape connectivity indices: towards the priorization of habitat patches and corridors for conservation. *Landscape Ecology*, *21*(7), 959–967. https://doi.org/10.1007/s10980-006-0013-z
Pascual-Hortal, L., & Saura, S. (2008). Integrating landscape connectivity in broad-scale forest planning through a new graph-based habitat availability methodology: application to capercaillie (Tetrao urogallus) in Catalonia (NE Spain). *European Journal of Forest Research*, *127*(1), 23–31. https://doi.org/10.1007/s10342-006-0165-z
Poisot, T., Bergeron, G., Cazelles, K., Dallas, T., Gravel, D., MacDonald, A., Mercier, B., Violet, C., & Vissault, S. (2021). Global knowledge gaps in species interaction networks data. *Journal of Biogeography*, *48*(7), 1552–1563. https://doi.org/10.1111/jbi.14127
Prăvălie, R., Sîrodoev, I., Nita, I.-A., Patriche, C., Dumitraşcu, M., Roşca, B., Tişcovschi, A., Bandoc, G., Săvulescu, I., Mănoiu, V., & Birsan, M.-V. (2022). NDVI-based ecological dynamics of forest vegetation and its relationship to climate change in Romania during 1987–2018. *Ecological Indicators*, *136*, 108629. https://doi.org/10.1016/j.ecolind.2022.108629
Prugh, L. R., Hodges, K. E., Sinclair, A. R. E., & Brashares, J. S. (2008). Effect of habitat area and isolation on fragmented animal populations. *Proceedings of the National Academy of Sciences*, *105*(52), 20770–20775. https://doi.org/10.1073/pnas.0806080105
Rayfield, B., Fortin, M.-J., & Fall, A. (2011). Connectivity for conservation: a framework to classify network measures. *Ecology*, *92*(4), 847–858. https://doi.org/10.1890/09-2190.1
Ribeiro, M. P., de Mello, K., & Valente, R. A. (2022). How can forest fragments support protected areas connectivity in an urban landscape in Brazil? *Urban Forestry & Urban Greening*, *74*, 127683. https://doi.org/10.1016/j.ufug.2022.127683
Ricketts, T. H. (2001). The Matrix Matters: Effective Isolation in Fragmented Landscapes. *The American Naturalist*, *158*(1), 87–99. https://doi.org/10.1086/320863
Ricotta, C. (2000). Quantifying the network connectivity of landscape mosaics: a graph-theoretical approach. *Community Ecol.*, *1*(1), 89–94. https://doi.org/10.1556/ComEc.1.2000.1.12
Ries, L., Fletcher, R. J., Battin, J., & Sisk, T. D. (2004). Ecological Responses to Habitat Edges: Mechanisms, Models, and Variability Explained. *Annual Review of Ecology, Evolution, and Systematics*, *35*(1), 491–522. https://doi.org/10.1146/annurev.ecolsys.35.112202.130148
Rudnick, A., Rudnick, D., A., E., Ryan, S. J., Beier, P., Cushman, S. A., Dieffenbach, F., Epps, C. W., Gerber, L. R., Hartter, J., Jenness, J. S., Kintsch, J., Merenlender, A. M.,

Perkl, R. M., Preziosi, D. V., & Trombulak, Stephen C.Rudnick, D. (2012). The role of landscape connectivity in planning and implementing conservation and restoration priorities. *Issues in Ecology*, *16*(16), 1–23.

Rudnick, D., A., E., Ryan, S. J., Beier, P., Cushman, S. A., Dieffenbach, F., Epps, C. W., Gerber, L. R., Hartter, J., Jenness, J. S., Kintsch, J., Merenlender, A. M., Perkl, R. M., Preziosi, D. V., Trombulak, Stephen C.Rudnick, D., & Rudnick, A. (2012). The role of landscape connectivity in planning and implementing conservation and restoration priorities. *Ecological Society of America*, *16*(16), 1–23.

Ruiz, L., Parikh, N., Heintzman, L. J., Collins, S. D., Starr, S. M., Wright, C. K., Henebry, G. M., van Gestel, N., & McIntyre, N. E. (2014). Dynamic connectivity of temporary wetlands in the southern Great Plains. *Landscape Ecology*, *29*(3), 507–516. https://doi.org/10.1007/s10980-013-9980-z

Russo, L. F., Barrientos, R., Fabrizio, M., Di Febbraro, M., & Loy, A. (2020). Prioritizing road-kill mitigation areas: A spatially explicit national-scale model for an elusive carnivore. *Diversity and Distributions*, *26*(9), 1093–1103. https://doi.org/10.1111/ddi.13064

Sáez, D., Spina, F., Margalida, A., Serra, L., Volponi, S., & Nadal, J. (2023). Reconstructing migratory network nodes to improve environmental management and conservation decisions: A case study of the common quail Coturnix coturnix as a biosensor. *Science of The Total Environment*, *893*, 164913. https://doi.org/10.1016/j.scitotenv.2023.164913

Samways, M. J., & Pryke, J. S. (2016). Large-scale ecological networks do work in an ecologically complex biodiversity hotspot. *Ambio*, *45*(2), 161–172. https://doi.org/10.1007/s13280-015-0697-x

Saura, S., & de la Fuente, B. (2017). Connectivity as the Amount of Reachable Habitat: Conservation Priorities and the Roles of Habitat Patches in Landscape Networks. In *Learning Landscape Ecology* (pp. 229–254). Springer New York. https://doi.org/10.1007/978-1-4939-6374-4_14

Saura, S., & Pascual-Hortal, L. (2007). A new habitat availability index to integrate connectivity in landscape conservation planning: Comparison with existing indices and application to a case study. *Landscape and Urban Planning*, *83*(2–3), 91–103. https://doi.org/10.1016/j.landurbplan.2007.03.005

Sauter, I., Kienast, F., Bolliger, J., Winter, B., & Pazúr, R. (2019). Changes in demand and supply of ecosystem services under scenarios of future land use in Vorarlberg, Austria. *Journal of Mountain Science*, *16*(12), 2793–2809. https://doi.org/10.1007/s11629-018-5124-x

Savary, P., Foltête, J., Moal, H., Vuidel, G., & Garnier, S. (2021). Analysing landscape effects on dispersal networks and gene flow with genetic graphs. *Molecular Ecology Resources*, *21*(4), 1167–1185. https://doi.org/10.1111/1755-0998.13333

Schulte, U., Küsters, D., & Steinfartz, S. (2007). A PIT tag based analysis of annual movement patterns of adult fire salamanders (Salamandra salamandra) in a Middle European habitat. *Amphibia-Reptilia*, *28*(4), 531–536. https://doi.org/10.1163/156853807782152543

Schwartz, A. L. W., Shilling, F. M., & Perkins, S. E. (2020). The value of monitoring wildlife roadkill. *European Journal of Wildlife Research*, *66*(1), 18. https://doi.org/10.1007/s10344-019-1357-4

Shirk, A. J., Landguth, E. L., & Cushman, S. A. (2018). A comparison of regression methods for model selection in individual-based landscape genetic analysis. *Molecular Ecology Resources*, *18*(1), 55–67. https://doi.org/10.1111/1755-0998.12709

Shobairi, S. O. R., Usoltsev, V. A., & Chasovskikh, V. P. (2018). Vegetation Fractional Coverage (VFC) Estimation of Planted and Natural Zones Based on Remote Sensing. *American Journal of Environmental Policy and Management*, *4*(1), 21–31.

Silverman, B. W. (2018). *Density Estimation for Statistics and Data Analysis*. Routledge. https://doi.org/10.1201/9781315140919

Spatari, G., Lorè, I., Viglianisi, A., & Calabrò, F. (2022). *Economic Feasibility of an Integrated Program for the Enhancement of the Byzantine Heritage in the Aspromonte National Park. The Case of Staiti* (pp. 313–323). https://doi.org/10.1007/978-3-031-06825-6_30

Tarabon, S., Calvet, C., Delbar, V., Dutoit, T., & Isselin-Nondedeu, F. (2020). Integrating a landscape connectivity approach into mitigation hierarchy planning by anticipating urban dynamics. *Landscape and Urban Planning*, *202*. https://doi.org/10.1016/j.landurbplan.2020.103871

Tarabon, S., Dutoit, T., & Isselin-Nondedeu, F. (2021). Pooling biodiversity offsets to improve habitat connectivity and species conservation. *Journal of Environmental Management*, *277*, 111425. https://doi.org/10.1016/j.jenvman.2020.111425

Tarabon, S., Godet, C., Coskun, T., & Clauzel, C. (2022a). Coupling spatial modeling with expert opinion approaches to restore multispecies connectivity of major transportation infrastructure. *Landscape and Urban Planning*, *221*, 104371. https://doi.org/10.1016/j.landurbplan.2022.104371

Tarabon, S., Godet, C., Coskun, T., & Clauzel, C. (2022b). Coupling spatial modeling with expert opinion approaches to restore multispecies connectivity of major transportation infrastructure. *Landscape and Urban Planning*, *221*, 104371. https://doi.org/10.1016/j.landurbplan.2022.104371

Theobald, D. M. (2006). *Exploring the functional connectivity of landscapes using landscape networks.* In: Crooks KR, Sanjayan M, eds. Connectivity Conservation. New York, NY: Cambridge University Press, 2006, Chapter 17, pp. 416-444.

Tiang, D. C. F., Morris, A., Bell, M., Gibbins, C. N., Azhar, B., & Lechner, A. M. (2021a). Ecological connectivity in fragmented agricultural landscapes and the importance of scattered trees and small patches. *Ecological Processes*, *10*(1), 20. https://doi.org/10.1186/s13717-021-00284-7

Tiang, D. C. F., Morris, A., Bell, M., Gibbins, C. N., Azhar, B., & Lechner, A. M. (2021b). Ecological connectivity in fragmented agricultural landscapes and the importance of scattered trees and small patches. *Ecological Processes*, *10*(1), 1–16. https://doi.org/10.1186/S13717-021-00284-7/FIGURES/9

Tiang, D. C. F., Morris, A., Bell, M., Gibbins, C. N., Azhar, B., & Lechner, A. M. (2021c). Ecological connectivity in fragmented agricultural landscapes and the importance of scattered trees and small patches. *Ecological Processes*, *10*(1), 20. https://doi.org/10.1186/s13717-021-00284-7

Tillmann, J. E. (2005). Habitat Fragmentation and Ecological Networks in Europe. *GAIA - Ecological Perspectives for Science and Society*, *14*(2), 119–123. https://doi.org/10.14512/gaia.14.2.11

Tischendorf, L., & Fahrig, L. (2000). On the usage and measurement of landscape connectivity. *Oikos*, *90*(1), 7–19. https://doi.org/10.1034/j.1600-0706.2000.900102.x

Tomaselli, V., Dimopoulos, P., Marangi, C., Kallimanis, A. S., Adamo, M., Tarantino, C., Panitsa, M., Terzi, M., Veronico, G., Lovergine, F., Nagendra, H., Lucas, R., Mairota, P., Mücher, C. A., & Blonda, P. (2013). Translating land cover/land use classifications to habitat taxonomies for landscape monitoring: a Mediterranean assessment. *Landscape Ecology*, *28*(5), 905–930. https://doi.org/10.1007/s10980-013-9863-3

Turner, M. G. (1989). Landscape Ecology: The Effect of Pattern on Process. *Annual Review of Ecology and Systematics*, *20*(1), 171–197. https://doi.org/10.1146/annurev.es.20.110189.001131

Unnithan Kumar, S., & Cushman, S. A. (2022a). Connectivity modelling in conservation science: a comparative evaluation. *Scientific Reports*, *12*(1), 16680. https://doi.org/10.1038/s41598-022-20370-w

Unnithan Kumar, S., & Cushman, S. A. (2022b). Connectivity modelling in conservation science: a comparative evaluation. *Scientific Reports*, *12*(1), 16680. https://doi.org/10.1038/s41598-022-20370-w

Urban, J. D., Keitt, T. (2001). Landscape Connectivity : A Graph-Theoretic Perspective. *Wiley on Behalf of the Ecological Society of America Stable*, *82*(5), 1205–1218.

Urban, J. D., Tachovsky, J. A., Haws, L. C., Wikoff Staskal, D., & Harris, M. A. (2009). Assessment of human health risks posed by consumption of fish from the Lower Passaic River, New Jersey. *Science of the Total Environment*, *408*(2), 209–224. https://doi.org/10.1016/j.scitotenv.2009.03.004

Venter, O., Magrach, A., Outram, N., Klein, C. J., Possingham, H. P., Di Marco, M., & Watson, J. E. M. (2018). Bias in protected-area location and its effects on long-term aspirations of biodiversity conventions. *Conservation Biology*, *32*(1), 127–134. https://doi.org/10.1111/cobi.12970

Vizzari, M., & Sigura, M. (2013). Urban-rural gradient detection using multivariate spatial analysis and landscape metrics. *Journal of Agricultural Engineering*, *44*(2s). https://doi.org/10.4081/jae.2013.333

Wang, G., Cushman, S. A., Wan, H. Y., Liu, M., & Jombach, S. (2022a). Comparison of Least-cost Path and UNICOR Cumulative Resistant Kernel Analyses in Mapping Ecological Connectivity Networks in Luohe Region, China. *Journal of Digital Landscape Architecture*, *2022*(7), 176–190. https://doi.org/10.14627/537724018

Wang, G., Cushman, S. A., Wan, H. Y., Liu, M., & Jombach, S. (2022b). Comparison of Least-cost Path and UNICOR Cumulative Resistant Kernel Analyses in Mapping Ecological Connectivity Networks in Luohe Region, China. *Journal of Digital Landscape Architecture*, *2022*(7), 176–190. https://doi.org/10.14627/537724018

Wang, M., Ma, Y., & You, X. (2021). An innovative approach to identify environmental variables with conservation priorities in habitat patches. *Journal of Environmental Management*, *292*, 112788. https://doi.org/10.1016/j.jenvman.2021.112788

Worton, B. J. (1989). Kernel Methods for Estimating the Utilization Distribution in Home-Range Studies. *Ecology*, *70*(1), 164–168. https://doi.org/10.2307/1938423

Wu, B., Bao, Y., Wang, Z., Chen, X., & Wei, W. (2023). Multi-temporal evaluation and optimization of ecological network in multi-mountainous city. *Ecological Indicators*, *146*, 109794. https://doi.org/10.1016/j.ecolind.2022.109794

Xing, S., & Fayle, T. M. (2021). The rise of ecological network meta-analyses: Problems and prospects. *Global Ecology and Conservation*, *30*, e01805. https://doi.org/10.1016/j.gecco.2021.e01805

Xu, M., Jia, X., Pickering, M., & Jia, S. (2019). Thin cloud removal from optical remote sensing images using the noise-adjusted principal components transform. *ISPRS Journal of Photogrammetry and Remote Sensing*, *149*, 215–225. https://doi.org/10.1016/j.isprsjprs.2019.01.025

Xu, W., Dejid, N., Herrmann, V., Sawyer, H., & Middleton, A. D. (2021). Barrier Behaviour Analysis (BaBA) reveals extensive effects of fencing on wide-ranging ungulates. *Journal of Applied Ecology*, *58*(4), 690–698. https://doi.org/10.1111/1365-2664.13806

Xu, Y., Si, Y., Wang, Y., Zhang, Y., Prins, H. H. T., Cao, L., & de Boer, W. F. (2019). Loss of functional connectivity in migration networks induces population decline in migratory birds. *Ecological Applications*, *29*(7). https://doi.org/10.1002/eap.1960

Yavartanoo, F., Song, Y., & Kang, J. (2023). Performance of wildlife fence systems under animal impact load. *Heliyon*, *9*(11), e21026. https://doi.org/10.1016/j.heliyon.2023.e21026

Yu, D., Xun, B., Shi, P., Shao, H., & Liu, Y. (2012). Ecological restoration planning based on connectivity in an urban area. *Ecological Engineering*, *46*, 24–33. https://doi.org/10.1016/j.ecoleng.2012.04.033

Žák, J., Kraus, M., Machová, P., & Plachý, J. (2020). Smart Green Bridge - Wildlife Crossing Bridges of New Generation. *IOP Conference Series: Materials Science and Engineering*, *728*(1), 012010. https://doi.org/10.1088/1757-899X/728/1/012010

Zeller, K. A., Jennings, M. K., Vickers, T. W., Ernest, H. B., Cushman, S. A., & Boyce, W. M. (2018a). Are all data types and connectivity models created equal? Validating common connectivity approaches with dispersal data. *Diversity and Distributions*, *24*(7), 868–879. https://doi.org/10.1111/ddi.12742

Zeller, K. A., Jennings, M. K., Vickers, T. W., Ernest, H. B., Cushman, S. A., & Boyce, W. M. (2018b). Are all data types and connectivity models created equal? Validating common connectivity approaches with dispersal data. *Diversity and Distributions*, *24*(7), 868–879. https://doi.org/10.1111/ddi.12742

Zeller, K. A., McGarigal, K., Beier, P., Cushman, S. A., Vickers, T. W., & Boyce, W. M. (2014). Sensitivity of landscape resistance estimates based on point selection functions to scale and behavioral state: pumas as a case study. *Landscape Ecology*, *29*(3), 541–557. https://doi.org/10.1007/s10980-014-9991-4

Zeller, K. A., McGarigal, K., & Whiteley, A. R. (2012). Estimating landscape resistance to movement: a review. *Landscape Ecology*, *27*(6), 777–797. https://doi.org/10.1007/s10980-012-9737-0

Zelený, J., Mercado-Bettín, D., & Müller, F. (2021). Towards the evaluation of regional ecosystem integrity using NDVI, brightness temperature and surface heterogeneity. *Science of The Total Environment*, *796*, 148994. https://doi.org/10.1016/j.scitotenv.2021.148994

Zhang, R., Zhang, L., Zhong, Q., Zhang, Q., Ji, Y., Song, P., & Wang, Q. (2021). An optimized evaluation method of an urban ecological network: The case of the Minhang District of Shanghai. *Urban Forestry & Urban Greening*, *62*, 127158. https://doi.org/10.1016/j.ufug.2021.127158

Zhang, S., Chen, H., Fu, Y., Niu, H., Yang, Y., & Zhang, B. (2019). Fractional vegetation cover estimation of different vegetation types in the Qaidam Basin. *Sustainability (Switzerland)*, *11*(3). https://doi.org/10.3390/su11030864

Zheng, R., Wu, G., Yan, C., Zhang, R., Luo, Z., & Yan, B. (2018). Exploration in Mapping Kernel-Based Home Range Models from Remote Sensing Imagery with Conditional Adversarial Networks. *Remote Sensing*, *10*(11), 1722. https://doi.org/10.3390/rs10111722

Zurita, G., Pe'er, G., Bellocq, M. I., & Hansbauer, M. M. (2012). Edge effects and their influence on habitat suitability calculations: a continuous approach applied to birds of the Atlantic forest. *Journal of Applied Ecology*, *49*(2), 503–512. https://doi.org/10.1111/j.1365-2664.2011.02104.x

9. Websites

- Istituto Superiore per la Protezione e la Ricerca Ambientale, ISPRA: https://www.isprambiente.gov.it/en/projects/biodiversity/ecological-network-and-terrritorial-planning. Last access on 10 November 2023
- European Commission website. last access 30 October 2023: https://environment.ec.europa.eu/topics/nature-and-biodiversity/habitats-directive_en
- Copernicus, Land Monitoring Service: Website: https://land.copernicus.eu/ -last access 11 November 2023
- Calabria Region Cartographic Centre (CCR). Website: http://geoportale.regione.calabria.it/opendata - last accessed 06 March 2023
- European Space Agency (ESA). Website: https://sentinel.esa.int/web/sentinel/user-guides/sentinel-2-msi/product-types/level-1c - last accessed 10 March 2023
- Italian Ministero dell'Ambiente e della Sicurezza Energetica. Website: https://www.mite.gov.it/pagina/repertorio-della-fauna–italiana-protetta- last accessed 16 February 2023
- QGIS.org (2023). QGIS Geographic Information System. Open Source Geospatial Foundation Project. Website: http://qgis.org
- Pathwalker software. Github, last access 24 March 2023 - https://github.com/siddharth-unnithankumar/pathwalker
- ISPRA. Carta della Natura Project. Website: https://www.isprambiente.gov.it/it/servizi/sistema-carta-della-natura - last access 17 May 2023
- European Environment Agency. Nature 2000 project. Website: https://www.eea.europa.eu/themes/biodiversity/natura-2000
- Sun life *Rana dalmatina*: http://vnr.unipg.it/sunlife/specie_animale-dettagli.php?id=31
- Google. Historical Imagery tool. Website: https://support.google.com/earth/answer/148094?hl=en - last access on 13 November 2023.

ANNEX 1: Habitat map codes included in 7 macro-categories and the corresponding EUNIS classification.

Habitat macro-categories	Habitat map code	EUNIS code	Habitat map code description	EUNIS Code description
COASTAL ENVIRONMENTS	15.6	A2.526	Mediterranean brackish environments with perennial woody halophilic vegetation	Mediterranean saltmarsh scrubs
	15.72	F6.8	Mediterranean alo-nitrophilous shrubs	Xero-halophile scrubs
	15.83		Clay areas with accelerated erosion	
	16.1	B1.21+B1.13	Sandy beaches	Unvegetated sand beaches above the driftline + Tethyan sand beach driftline communities
	16.21	B1.3	Mobile dunes	Shifting coastal dunes
	16.22	B1.4	Stable dunes with herbaceous vegetation	Coastal stable dune grassland (grey dunes)
	17.1	A2.1	Pebbly and pebbly beaches devoid of vegetation	Littoral coarse sediment
RIVER, LAKE AND LAGOON ENVIRONMENTS	22.4	C1.2	Freshwater lakes and ponds with vegetation	Permanent mesotrophic lakes, ponds and pools
	24.4	C2.3	Waterways with vegetation	Permanent non-tidal, smooth-flowing watercourses
	21_m	X02	Coastal lagoons and brackish lakes	Saline coastal lagoons
	24.1_m	C3.5	Watercourses with little or no vegetation	Periodically inundated shores with pioneer and ephemeral vegetation
	24.255_m	C3.553	Mediterranean river greens	Mediterranean river gravel habitats
MEADOW AND SHRUB ENVIRONMENTS	31.77	F7.4	Thorny shrub heathlands of the central and southern Apennines and Madonie Mountains	Hedgehog-heaths
	31.844	F3.2	Italian hill and mountain gorse thickets	Submediterranean deciduous thickets and brushes
	31.863	E5.3	Fields in Pteridium aquilinum	Pteridium aquilinum fields
	31.87		Areas recently cleared by fire, avalanche, or extreme weather events	
	32.12	F5.12	Matorral to olive tree and mastic tree	Olea europaea and Pistacia lentiscus matorral
	32.215	F5.515	Macchia a Cytisus laniger, Cytisus spinosus, Cytisus infestus	[Calicotome] brush
	32.22	F5.52	Euphorbia dendroides stain	Euphorbia dendroides formations
	32.23	F5.53	Heron to Ampelodesmos mauritanicus	Ampelodesmos mauritanica -dominated garrigues
	38.1*	E2.1	Grazed mesophyll grasslands	Permanent mesotrophic pastures and aftermath-grazed meadows
	31.863	E5.3	Fields in Ptiridium aquilinum	Pteridium aquilinum fields
	31.8A	F3.2	Brambles	F3.2: Submediterranean deciduous thickets and brushes
	32.A*	F5.4	Spartium Junceum Broom.	Spanish-broom ([Spartium junceum]) fields
	34.6_B	E1.422	Steppes of tall Mediterranean grasses in Hyparrhenia hirta	Central Mediterranean esparto steppes
	34.6A	E1.434	Steppes of tall Mediterranean grasses in Lygeum spartum	Andropogonid grass steppes
	34.8_m	E1.6	Subnitrophilous grasslands	Subnitrophilous annual grassland
	37.A_n	E1.44	Grasslands in Arundo plinii	Cane steppes
WOODLAND AND FOREST ENVIRONMENTS	41.18*	G1.67	Beech forests of southern Italy	Southern medio-European Fagus forests
	41.732	G1.732	Mediterranean oak forests with downy oak	Italo-Sicilian Quercus pubescens woods
	41.7511	G1.7511	Mediterranean turkey oak groves	Southern Italic Quercus cerris woods
	41.9	G1.7D	Castanea sativa forest	Castanea sativa woodland
	42.15	G3.15	Abetes of the central and southern Apennines	Southern Apennine Abies alba forests
	42.65	G3.55	Larch pine forests	Calabrian Pinus laricio forests
	42.67	G3.57	Pinus nigra reforestations	Pinus nigra reforestation
	42.83	G3.737	Natural and cultivated lodgepole pine (Pinus pinea) forests	Italic stone pine forests
	42.84	G3.747	Aleppo pine forests	Italic Pinus halepensis forests
	44.12	G1.112	Mediterranean riparian shrub willows	Mediterranean tall Salix galleries
	44.14	G1.1121	Mediterranean riparian forests of willow trees	Mediterranean white willow galleries
	44.61	G1.314	Riparian forests with poplars	Italic poplar galleries
	44.81	F9.31	Riparian thickets of tamarisk, oleander, agnocaste	Nerium oleander, Vitex agnus-castus and Tamarix galleries
	45.21	G2.11	Tyrrhenian cork oaks	Quercus suber woodland
	45.31	G2.121A	Thermo- and mesomediterranean ilexes	Southern Italian holm-oak forests
	45.32	G2.122	Supramediterranean ilexes	Supra-Mediterranean holm-oak forests
MARSHY ENVIRONMENTS, PEAT BOGS AND SPRINGS	53.1		Reed beds with Phragmites australis and other heliophytes	Water-fringing beds of tall canes Reedbeds normally without free-standing water
	53.62	C3.32	Formations in Arundo donax	Arundo donax beds
ROCKY, DETRITAL, GLACIAL AND VOLCANIC ENVIRONMENTS	62.11	H3.215	Reed beds with Phragmites australis and other heliophytes	Sicilo-Italic [Dianthus] cliffs
	62.7_n	H5.3	Terrigen slope in landslide	Sparsely- or un-vegetated habitats on mineral substrates not resulting from recent ice activity
ANTHROPIC ENVIRONMENTS	81	E2.6	Anthropogenic meadows	Agriculturally-improved, re-seeded and heavily fertilised grassland, including sports fields and grass lawns
	82.1	I1.1	Intensive crops	Intensive unmixed crops
	82.3	I1.3	Extensive crops	Arable land with unmixed crops grown by low-intensity agricultural methods
	83.11	G2.91	Olive groves	Olea europaea groves
	83.12	G1.D1	Chestnut groves for fruit	Castanea sativa plantations
	83.15_m	G1.D4	Orchards	Fruit orchards
	83.16	G2.92	Citrus groves	Citrus orchards
	83.21	FB.4	Vineyards	Vineyards
	83.325_m	G1.C4	Eucalyptus plantations	Other broadleaved deciduous plantations
	84	I1.2	Vegetable gardens and complex agricultural systems	Mixed crops of market gardens and horticulture
	85	X11	Parks, gardens and green areas	Large parks
	86.31	J3.2	Quarries, earthworks and landfills	Active opencast mineral extraction sites, including quarries
	86.32	J1.4	Manufacturing and commercial sites and major infrastructure nodes	Urban and suburban industrial and commercial sites still in active use
	86.6	X21	Archaeological sites and ruins	Archaeological sites
	89.2	J5	Freshwater canals and reservoirs	Highly artificial man-made waters and associated structures
	83.31_m	G3.F	Conifer plantations	Highly artificial coniferous plantations
	83.324_A	G1.C3	robinia's tree	Robinia plantations
	83.324_B		ailanthetes	
	83.324_C		Areas invaded by Opuntia sp. pl.	
	83.325_m	G1.C4	Broadleaf plantations	Other broadleaved deciduous plantations
	83.326_m		Hardwood and conifer plantations	
	86.1_m	J1	Population centers	Residential buildings of villages and urban peripheries
	86.1_s	J4	Road and rail infrastructure	Transport networks and other constructed hard-surfaced areas
	86.41_m	H3.1C H3.2F	Decommissioned quarries and waste debris deposits	Disused siliceous quarries,Disused chalk and limestone quarries

ANNEX 2:Phytosociological table containing vegetation and site information. The classification of the cover classes was done according to Braun Blanquet's numbering system.

	CALABRIA REGION - NATURE MAP SYSTEM - HABITAT SURVEY SHEET	
	Survey no.	17_o
	Date	27/07/2021
	Autor/s	Laface, Lumia, Mei, Spampinato
Station data	Habitat	32.4 Garrigue and mesomediterranean calcicolous scrubland
	Habitat Dir. CEE 43/92	-
	Physionomy	Garrigue
	Administrative Region	Calabria
	Province	Reggio Calabria
	Municipality	Reggio Calabria
	Location	Grado
	Inclusion in the Natura 2000 Network	-
	Coordinate N	38°5'21''
	Coordinate E	15°42'38''
	Quote (m)	224
	Exposure	S
	Slope (°)	50
	Geology	Sands with layers of soft sandstones
	Pedology (U.C.)	9.9
	Pedology (Classif. USDA)	Typic Hapludolls, coarse loamy, mixed, mesic
	Survey area (mq)	20
	Integrated area (in the case of fragmented areas)	-
Structure	Total coverage (%)	70
	Outcropping rock (%)	30
	Vegetation layer coverage A (%)	-
	Vegetation layer coverage a (%)	-
	Vegetation layer coverage e (%)	70
	Average height of the vegetation layer A (m)	-
	Average height of the vegetation layer a (m)	-
	Average height of the vegetation layer e (m)	0.7
Conservation	Pressure 1	H04 - Vandalism or arson
	Pressure importance 1	M
	Pressure 2	L01 - Abiotic natural processes (e.g. erosion, silting up, drying out, submersion, salinization)
	Pressure importance 2	H
	Pressure	M05 - Collapse of terrain, landslide
	Pressure importance 3	M
	Threat 1	A01 - Conversion into agricultural land (excluding drainage and burning)
	Threat significance 1	L
	Threat 2	F09 - Deposition and treatment of waste/garbage from household/recreational facilities
	Threat significance 2	L
	Conservation measure 1	CA01 - Prevent conversion of natural and semi-natural habitats, and habitats of species into agricultural land
	Target pressure of conservation measure 1	A01
	Conservation measure 2	CF02 - Habitat restoration of areas impacted by residential, commercial, industrial and recreational infrastructures, operations and activities
	Target pressure of conservation measure 2	F09
	Conservation measure 3	CH03 - Reduce impact of other specific human actions
	Target pressure of conservation measure 3	H04
	Conservation measure 4	CL01 - Management of habitats (others than agriculture and forest) to slow, stop or reverse natural processes
	Target pressure of conservation measure 4	L01
	Conservation measure 5	CL03 - Restore habitats following geological and natural catastrophes
	Target pressure of conservation measure 5	M05
Layer	**Specie**	**Coverage**
e	Thymbra capitata (L.) Cav.	4
e	Cistus creticus L. subsp. creticus	3
e	Cistus salviifolius L.	2a
e	Dianthus longicaulis Ten.	2a
e	Micromeria graeca (L.) Benth. ex Rchb. subsp. graeca	2a
e	Artemisia campestris L. subsp. variabilis (Ten.) Greuter	2a
e	Helichrysum italicum (Roth) G.Don subsp. italicum	1
e	Ampelodesmos mauritanicus (Poir.) T.Durand & Schinz	1
e	Fumana thymifolia (L.) Spach ex Webb	1
e	Euphorbia rigida M.Bieb.	1
e	Petrosedum sediforme (Jacq.) Grulich subsp. sediforme	1
e	Seseli tortuosum L. subsp. tortuosum	+
e	Allium sp.	+
e	Phagnalon rupestre (L.) DC. subsp. rupestre	+

ANNEX 3: In the table, dispersal threshold, home range and resistance values for each species are given for each habitat (resistence value goes from 0 to 100, in intervals of 25).
In red species with a dispersal threshold lower than 100m, in yellow species with not available data. * for habitats considered as patches

		Reptiles						Amphibians						Mammals						
	Specie's autoecological data in red species with a dispersal threshold lower than 100m in yellow species with not available data	Hierophis virdiflavus	Elaphe quatuorlineata	Coronella austriaca	Podarcis siculus	Lacerta bilineata	Zamenis lineatus	Rana dalmatina	Rana italica	Bufo bufo	Salamandra salamandra gliglioli	Salamandrina terdigitata	Bombina pachypus	Dryomys aspromontis	Felis silvestris	Canis lupus	Martes martes	Muscardinus avellanarius	Mustela putorius	Sciurus meridionalis
Habitat code (* for the habitat considered as patches)	Animal home range [ha]	0.05	N.A.	0.005	0.015	0.002	N.A.	0.002	0.002	N.A.	5	N.A.	N.A.	N.A.	124	8000	140	N.A.	8	2
	Animal dispersal threshold (m)	100	50	30	10	300	50	50	100	1000	100	100	50	N.A.	N.A.	38000	10000	1000	3400	1500
	Habitat description	**Resistance values** [0 = no resistance, 25 = low resistance, 50 = medium resistance, 75 = high resistance, 100 = very high resistance]																		
15.6	Mediterranean brackish environments with perennial woody halophilic vegetation	100	100	100	100	100	100	100	100	100	100	100	100	100	100	100	100	100	100	100
15.72	Mediterranean alo-nitrophilous shrubs	100	100	100	100	100	100	100	100	100	100	100	100	100	100	100	100	100	100	100
15.83	Clay areas with accelerated erosion	100	100	100	100	100	100	100	100	100	100	100	100	100	100	100	100	100	100	100
16.1	Sandy beaches	100	100	100	100	100	100	100	100	100	100	100	100	100	100	100	100	100	100	100
16.21	Mobile dunes	100	100	100	100	100	100	100	100	100	100	100	100	100	100	100	100	100	100	100
16.25	Stable dunes with herbaceous vegetation	100	100	100	100	100	100	100	100	100	100	100	100	100	100	100	100	100	100	100
17.1	Pebbly and pebbly beaches devoid of vegetation	100	100	100	100	100	100	100	100	100	100	100	100	100	100	100	100	100	100	100
25.4*	Freshwater lakes and ponds with vegetation	100	100	100	100	100	100	0	75	0	100	50	25	100	100	100	100	100	100	100
24.4*	Waterways with vegetation	100	100	100	100	100	100	75	0	0	0	0	100	100	100	100	100	100	25	100
31.77*	Thorny shrub heathlands of the central and southern Apennines and Madonie Mountains	50	100	25	100	75	100	100	100	100	100	100	100	100	75	75	100	100	100	100
31.844	Italian hill and mountain gorse thickets	25	25	25	25	25	25	25	25	25	25	25	25	25	25	25	25	25	25	25
31.863	Fields in Pteridium aquilinum	25	25	25	25	25	25	25	25	25	25	25	25	25	25	25	25	25	25	25
31.87	Areas recently cleared by fire, avalanche, or extreme weather events	25	25	25	25	25	25	25	25	25	25	25	25	25	25	25	25	25	25	25
32.12	Matorral to olive tree and mastic tree	25	25	25	25	25	25	25	25	25	25	25	25	25	25	25	25	25	25	25
32.215	Macchia a Cytisus laniger, Cytisus spinosus, Cytisus infestus	25	25	25	25	25	25	25	25	25	25	25	25	25	25	25	25	25	25	25
32.25	Euphorbia dendroides stain	25	25	25	25	25	25	25	25	25	25	25	25	25	25	25	25	25	25	25
32.23	Heron to Ampelodesmos mauritanicus	25	25	25	25	25	25	25	25	25	25	25	25	25	25	25	25	25	25	25
38.1*	Grazed mesophyll grasslands	75	75	75	75	50	75	100	100	75	100	75	75	100	100	50	100	100	100	100
38.16	Grazed mesophyll grasslands	25	25	25	25	25	25	25	25	25	25	25	25	25	25	25	25	25	25	25
41.18*	Beech forests of southern Italy	100	100	75	100	100	100	0	0	50	0	50	75	25	0	0	0	25	75	100
41.732*	Mediterranean oak forests with downy oak	75	50	75	100	100	0	0	75	75	100	50	75	100	25	25	25	75	75	100
41.7511*	Mediterranean turkey oak groves	75	50	75	100	100	25	0	75	75	100	75	100	100	50	25	50	75	75	100
41.9*	Castanea sativa forest	75	75	75	100	100	25	0	50	75	75	75	75	100	25	25	50	25	100	100
42.15*	Abetes of the central and southern Apennines	100	50	75	100	100	100	75	100	75	100	100	100	50	25	0	0	50	100	100
42.65*	Larch pine forests	75	75	50	100	75	75	75	75	75	75	75	75	75	25	25	0	75	100	0
42.67	Pinus nigra reforestations	50	50	50	50	50	50	50	50	50	50	50	50	50	50	50	50	50	50	50
42.83	Natural and cultivated lodgepole pine (Pinus pinea) forests	50	50	50	50	50	50	50	50	50	50	50	50	50	50	50	50	50	50	50
42.84	Aleppo pine forests	50	50	50	50	50	50	50	50	50	50	50	50	50	50	50	50	50	50	50
44.12*	Mediterranean riparian shrub willows	50	75	100	75	75	75	25	75	0	100	75	75	100	100	75	100	100	50	100
44.14*	Mediterranean riparian forests of willow trees	75	75	100	100	75	75	25	75	0	100	75	75	100	100	75	100	75	25	100
44.61	Riparian forests with poplars	25	25	25	25	25	25	25	25	25	25	25	25	25	25	25	25	25	25	25
44.81*	Riparian thickets of tamarisk, oleander, agnocaste	50	75	100	75	50	75	75	100	0	100	75	75	100	100	75	100	100	75	100
45.21*	Tyrrhenian cork oaks	75	25	75	100	100	0	0	50	75	100	50	75	100	50	25	25	25	50	100
45.31*	Thermo- and mesomediterranean ilexes	75	25	75	100	100	0	0	25	75	100	0	50	100	25	0	25	25	25	100
45.32*	Supramediterranean ilexes	75	75	75	100	100	75	0	25	75	100	25	50	100	25	0	25	25	25	100
53.1*	Reed beds with Phragmites australis and other heliophytes	50	75	100	75	100	75	75	100	0	100	100	100	100	100	100	100	100	100	100
62.11	Reed beds with Phragmites australis and other heliophytes	80	80	80	80	80	80	80	80	80	80	80	80	80	80	80	80	80	80	80
81	Anthropogenic meadows	25	25	25	25	25	25	25	25	25	25	25	25	25	25	25	25	25	25	25
31.863	Fields in Ptiridium aquilinum	25	25	25	25	25	25	25	25	25	25	25	25	25	25	25	25	25	25	25
82.1	Intensive crops	75	75	75	75	75	75	75	75	75	75	75	75	75	75	75	75	75	75	75
82.3*	Extensive crops	0	25	75	0	0	50	50	100	50	100	75	0	100	100	75	100	75	100	100
83.11	Olive groves	50	50	50	50	50	50	50	50	50	50	50	50	50	50	50	50	50	50	50
83.12	Chestnut groves for fruit	50	50	50	50	50	50	50	50	50	50	50	50	50	50	50	50	50	50	50
83.15	Orchards	50	50	50	50	50	50	50	50	50	50	50	50	50	50	50	50	50	50	50
83.16	Citrus groves	50	50	50	50	50	50	50	50	50	50	50	50	50	50	50	50	50	50	50
83.21	Vineyards	75	75	75	75	75	75	75	75	75	75	75	75	75	75	75	75	75	75	75
83.325	Eucalyptus plantations	25	25	25	25	25	25	25	25	25	25	25	25	25	25	25	25	25	25	25
84	Vegetable gardens and complex agricultural systems	25	25	25	25	25	25	25	25	25	25	25	25	25	25	25	25	25	25	25
85	Parks, gardens and green areas	50	50	50	50	50	50	50	50	50	50	50	50	50	50	50	50	50	50	50
86.31	Quarries, earthworks and landfills	50	50	50	50	50	50	50	50	50	50	50	50	50	50	50	50	50	50	50
86.32	Manufacturing and commercial sites and major infrastructure nodes	100	100	100	100	100	100	100	100	100	100	100	100	100	100	100	100	100	100	100
86.6	Archaeological sites and ruins	50	50	50	50	50	50	50	50	50	50	50	50	50	50	50	50	50	50	50
89.2	Freshwater canals and reservoirs	50	50	50	50	50	50	50	50	50	50	50	50	50	50	50	50	50	50	50
21_m	Coastal lagoons and brackish lakes	100	100	100	100	100	100	100	100	100	100	100	100	100	100	100	100	100	100	100
25.1_m	Freshwater lakes with little or no vegetation	100	100	100	100	100	100	100	100	100	100	100	100	100	100	100	100	100	100	100
24.1_m*	Watercourses with little or no vegetation	75	100	100	75	75	100	75	0	0	100	75	50	100	100	100	100	100	75	100
24.255_m*	Mediterranean river greens	50	75	75	25	50	75	75	25	0	100	75	50	100	100	100	100	100	75	100
31.8A	Brambles	25	25	25	25	25	25	25	25	25	25	25	25	25	25	25	25	25	25	25
32.A*	Spartium Junceum Broom.	50	50	50	75	25	75	100	100	100	100	100	100	100	75	75	100	75	100	100
34.6_B	Steppes of tall Mediterranean grasses in Hyparrhenia hirta	25	25	25	25	25	25	25	25	25	25	25	25	25	25	25	25	25	25	25
34.6A	Steppes of tall Mediterranean grasses in Lygeum spartum	25	25	25	25	25	25	25	25	25	25	25	25	25	25	25	25	25	25	25
34.8_m*	Subnitrophilous grasslands	25	0	50	25	25	50	100	100	100	100	100	0	100	100	100	100	100	100	100
37.A_n*	Grasslands in Arundo plinii	50	25	100	50	75	100	100	100	100	100	100	100	100	100	50	100	100	100	100
53.6B	Formations in Arundo donax	25	25	25	25	25	25	25	25	25	25	25	25	25	25	25	25	25	25	25
62.7_n	Terrigen slope in landslide	75	75	75	75	75	75	75	75	75	75	75	75	75	75	75	75	75	75	75
83.31_m	Conifer plantations	25	25	25	25	25	25	25	25	25	25	25	25	25	25	25	25	25	25	25
83.324_A	robinia's tree	25	25	25	25	25	25	25	25	25	25	25	25	25	25	25	25	25	25	25
83.324_B	ailanthetes	25	25	25	25	25	25	25	25	25	25	25	25	25	25	25	25	25	25	25
83.324_C	Areas invaded by Opuntia sp. pl.	25	25	25	25	25	25	25	25	25	25	25	25	25	25	25	25	25	25	25
83.325_m	Broadleaf plantations	25	25	25	25	25	25	25	25	25	25	25	25	25	25	25	25	25	25	25
83.326_m	Hardwood and conifer plantations	25	25	25	25	25	25	25	25	25	25	25	25	25	25	25	25	25	25	25
86.1_m	Population centers	100	100	100	100	100	100	100	100	100	100	100	100	100	100	100	100	100	100	100
86.1_s	Road and rail infrastructure	100	100	100	100	100	100	100	100	100	100	100	100	100	100	100	100	100	100	100
86.41_m	Decommissioned quarries and waste debris deposits	75	75	75	75	75	75	75	75	75	75	75	75	75	75	75	75	75	75	75